

Functional Analysis of Hydrothermal Vent Microbial Communities

I n a u g u r a l d i s s e r t a t i o n

zur

Erlangung des akademischen Grades eines
Doktors der Naturwissenschaften (Dr. rer. nat.)

der

Mathematisch-Naturwissenschaftlichen Fakultät

der

Universität Greifswald

vorgelegt von

Florian Götz

Greifswald, Januar 2021

Dekan: Prof. Dr. Gerald Kerth

1. Gutachter: Prof. Dr. Thomas Schweder
2. Gutachter: Prof. Dr. Costa Vetriani

Tag der Promotion: 21.05.2021

Table of Contents

Zusammenfassung	7
Summary	9
1 Introduction.....	11
1.1 Energy metabolism at hydrothermal vents	12
1.2 Questions and rationale of the thesis	16
1.2.1 Metaproteomics on Crab Spa diffuse-flow hydrothermal vent microbial community to determine the dominant metabolic pathways in situ	16
1.2.2 Cultivation experiments of <i>Sulfurimonas denitrificans</i> under limiting conditions in chemostats and elemental sulfur in batch culture to measure metabolic pathway changes in vitro	17
2 Material and Methods	18
2.1 Metaproteomics to identify the active chemoautotrophic community members inhabiting the seafloor at a deep-sea hydrothermal vent	18
2.1.1 Sampling.....	18
2.1.2 DNA extraction (performed by Dr. Lara Gulmann, Research Associate in the laboratory of Dr. Sievert).....	18
2.1.3 16S rRNA Sequencing and Analysis (performed by Clarissa Karthäuser, in the laboratory of Dr. Sievert).....	20
2.1.4 Metagenomic Sequencing and Analysis.....	20
2.1.5 Protein extraction from filter pieces	21
2.1.6 Proteomics and data analysis.....	22
2.2 Cultivation and proteomic analysis of <i>Sulfurimonas denitrificans</i> to assess adaptations to different growth conditions.....	24
2.2.1 Medium preparation and cultivation of <i>Sulfurimonas denitrificans</i>	24
2.2.1.1 Artificial seawater medium (Solution A).....	24
2.2.1.2 Sodium hydrogen carbonate stock solution (Solution C)	25
2.2.1.3 Iron(III) chloride stock solution (Solution D).....	25
2.2.1.4 Potassium phosphate stock solution (Solution E).....	25
2.2.1.5 Selenite-tungstate solution (Widdel and Bak, 1992)	25
2.2.1.6 Thiosulfate stock solution (Solution B).....	26
2.2.2 Batch culture experiments to study growth of <i>Sulfurimonas denitrificans</i> with either thiosulfate or octo-sulfur as electron donor. ..	26

2.2.3	Chemostat experiments to study the proteomic response of <i>Sulfurimonas denitrificans</i> to substrate limitation as well as the presence of oxygen and hydrogen.	27
2.2.4	Cell counts using 4,6 Diamidin-2-phenylindol (DAPI)	28
2.2.5	Analysis of ΣNH_3 , Nitrate, Nitrite, Sulfate, and Thiosulfate by Ion Chromatography	29
2.2.6	Proteomic analysis of <i>Sulfurimonas denitrificans</i>	29
2.2.6.1	Protein isolation	29
2.2.6.2	Protein digestion	30
2.2.6.3	Mass spectrometry and proteome analysis (Götz, Pjevac, et al., 2018)	30
2.2.6.4	RNA extraction, transcriptome sequencing and analysis (performed by Dr. Petra Pjevac, University of Vienna, Austria)	31
2.2.6.5	Statistical analysis.....	32
3	Results.....	33
3.1	MetaOmics analysis on Crab Spa diffuse-flow hydrothermal vent fluids	33
3.1.1	Taxonomic composition.....	33
3.1.2	Metagenome: Metabolic potential.....	34
3.1.3	Metaproteome: Active community members and their utilized pathways.....	36
3.1.4	Comparison of the metaproteomic profiles between the three dominant genera of Crab Spa	40
3.2	Chemostat experiments with <i>Sulfurimonas denitrificans</i> as a model organism for chemoautotrophy.	42
3.2.1	Growth and ion concentration in the chemostat of limitation experiments	42
3.2.2	Proteomics on <i>Sulfurimonas denitrificans</i> chemostat cultures	43
3.3	S ₈ metabolism in <i>Sulfurimonas denitrificans</i>	46
3.3.1	Growth characteristics.....	46
3.3.2	The transcriptome and proteome of thiosulfate- versus S ₈ -grown cells are largely similar	47
3.3.3	Flagella-related proteins and transcripts are differentially abundant	50
3.3.4	Genes and proteins of central biochemical pathways	51
3.3.5	Transcribed and translated genes involved in alternative energy metabolism	54
4	Discussion.....	56

4.1	Campylobacteria at Crab Spa	57
4.1.1	Metabolism of <i>Campylobacteria</i> in the environment	58
4.1.2	Difference in abundance of enzymes in relation to substrate concentration	59
4.2	Importance of sulfur oxidation for <i>Sulfurimonas denitrificans</i> and its implications for redox environments.....	62
4.2.1	The expression of genes and proteins involved in energy metabolism	63
4.2.2	Flagella likely facilitate attachment to S ₈	64
4.2.3	The mechanism of thiosulfate- and S ₈ -oxidation	65
4.2.4	An alternative model for sulfur oxidation in <i>Sulfurimonas denitrificans</i>	66
5	Conclusion and Outlook	69
6	References.....	71
7	Appendix.....	79
8	Appendix A: Eigenständigkeitserklärung	82
9	Appendix B: Curriculum Vitae	83
10	Appendix D: Acknowledgement.....	85

List of Figures

- Figure 1** Chemolithoautotrophic model of biochemical redox-reactions. Reduced sulfur compounds or hydrogen are oxidized and oxidized nitrate or oxygen is reduced. These redox reactions result in energy in form of ATP which is used to fix carbon dioxide into biomass (carbon compounds).14
- Figure 2** Schematic design of the used chemostat system. Incoming gas was filtered through cotton and sterile water before it was further directed into the 2 L medium tanks. Medium was pumped into the chemostat through a peristaltic pump. The gas was continuously redirected from the headspace of the medium tank into the chemostat and further to the waste container.....28
- Figure 3** Functional genes of the metagenomes and 16S rRNA diversity of the Crab Spa microbial community of samples LVP2 and LVP4 are shown. Over 90% of the microbial community of Crab Spa is dominated by Campylobacteria, which is also mirrored in functional genes of the metagenomes. The Sox system consists of the genes soxABCXYZ. CBB3 stands for the cbb₃ cytochrome oxidoreductase, NapA for nitrate reductase, NirS nitrite reductase, NorCB nitric oxide reductase and NosZ for the nitrous oxide reductase.35
- Figure 4** Bubble chart including the abundance and taxonomic differentiation of the most abundant pathways at Crab Spa. The black bubbles indicate the abundance with different radii, that represent the percentage of the normalized spectral abundance factor (%NSAF) for LVP2 and LVP4. Pie charts show the distribution of different taxa

	within these protein groups. The hypothetical proteins show the highest variability in taxa (turquoise) compared to all other abundant protein groups that are mainly dominated by Sulfurimonas (blue), Sulfurovum (orange), Arcobacter (grey) and other Camylobacteria (yellow- including e.g. Thioreductor, Nitratifractor, Nitratiruptor).	38
Figure 5	This bubble chart shows the abundance of enzymes involved in the energy metabolism of the Crab Spa most abundant community members. The most abundant enzymes presented are the ATP-synthase, ATP citrate lyase, Nitrate reductase and Nitrite reductase, all mostly dominated by Sulfurimonas and Sulfurovum species.....	39
Figure 6	Pie-Charts that show protein categories normalized to 100% to the three most abundant genera (Sulfurimonas, Sulfurovum and Arcobacter) with organism specific normalized spectral abundance factors (OrgNSAF). The protein category distribution in Sulfurimonas and Sulfurovum is similar but differs in comparison to Arcobacter. Thiosulfate reductase proteins are only found in Sulfurimonas species and not in Sulfurovum or Arcobacter. The rTCA cycle and denitrification pathway are over 10% more abundant in Sulfurimonas and Sulfurovum than in Arcobacter. The Cbb3 cytochrome c oxidoreductase is 3% more abundant as well as ribosomal proteins which are 20% more abundant in Arcobacter.....	40
Figure 7	Taxonomic distribution in identified Chemotaxis apparatus and Flagellar proteins (total chemotaxis proteins 2.35 % normalized spectral abundance factor in LVP2 and 1.95%NSAF in LVP4). Arcobacter species dominate flagellar proteins whereas Sulfurimonas and Sulfurovum dominate chemotaxis apparatus proteins.	41
Figure 8	Growth curves are indicated in blue and ion concentrations measured by ion-chromatography are indicated in red (Sulfate), grey (Nitrate) and yellow (Thiosulfate). A, B and C are indicative for three individual chemostats which were run simultaneously under thiosulfate limitation (TL) and D, E and F under nitrate limitation (NL). Steady state conditions were determined by the stable ion concentrations within the medium. Samples for proteomic analysis were taken on the last sampling point.....	43
Figure 9	Proteomic results for the expression of denitrification enzymes (A), sulfur oxidation enzymes (B), hydrogenases (C) and the cbb ₃ cytochrome oxidoreductase (D) in Sulfurimonas denitrificans under thiosulfate limitation (TL), nitrate limitation (NL), thiosulfate and oxygen (TO) and hydrogen and nitrate (HN). Protein expression is given as normalized spectral abundance factor (NSAF%).	45
Figure 10	Growth curves (dotted lines) of <i>S. denitrificans</i> cultures grown on thiosulfate (upper panel) or cyclooctasulfur (lower panel), as determined via cell counts after DAPI staining. Arrows indicate the time of sampling of the biological replicates. Published in (Götz, Pjevac, et al., 2018).....	46
Figure 11	Distribution of COG categories in the <i>S. denitrificans</i> proteome (%NSAF = Normalized Spectral Abundance Factor) and transcriptome (TPM = Transcripts Per Million) on cyclooctasulfur (S ₈) or thiosulfate (S ₂ O ₃ ²⁻). Published in (Götz, Pjevac, et al., 2018). 48	
Figure 12	Distribution of the proteomic (left) and transcriptomic (right) expression of <i>S. denitrificans</i> cultures grown on cyclooctasulfur (x-axis) versus thiosulfate (y-axis). Proteins and ORFs with statistically significant differences in expression are depicted in red. Published in (Götz, Pjevac, et al., 2018).....	49
Figure 13	The relative abundance of transcripts (TPM = Transcripts Per Million) and proteins (%NSAF = Normalized Spectral Abundance Factor) related to flagellar biosynthesis and motility. Light bars show the average values of <i>S. denitrificans</i> grown on cyclooctasulfur (S ₈) and dark bars show the average of cultures grown on thiosulfate.	

Statistically-significant differences are denoted with one ($p < 0.05$) or two ($p < 0.01$) asterisks. Genes indicated in bold were also identified in the proteomic dataset. Sudeen_0030: Flagellar hook capping protein = WP_011371666.1; Sudeen_0031: Flagellar hook protein = WP_011371667.1; FlgE: Flagellar hook = WP_011371668.1, Sudeen_0032; Sudeen_0172: Flagellin-like = WP_011371808.1; Sudeen_0173: Flagellin-like = WP_011371809.1; Sudeen_0202: Flagellar hook-associated protein 2-like = WP_011371838.1; FliS: Flagellar protein = WP_041672386.1, Sudeen_0203; FliE: Flagellar hook-basal body complex protein = WP_011371998.1, Sudeen_0363; FlgC: Flagellar basal-body rod protein = WP_011371999.1, Sudeen_0364; FlgB: Flagellar basal-body rod protein = WP_011372000.1, Sudeen_0365; FliF: Flagellar M-ring protein = WP_011372107.1, Sudeen_0472; FliG: Flagellar motor switch protein = WP_011372108.1, Sudeen_0473; Sudeen_0474: putative flagellar assembly protein = WP_011372109.1; Sudeen_0562: Flagellar P-ring protein = WP_011372195.1; Sudeen_0733: Flagellar L-ring protein = WP_011372366.1; FliL: Flagellar basal body-associated protein = WP_011372470.1, Sudeen_0840; Sudeen_1037: putative flagellin = WP_011372667.1; FlgG: Flagellar basal-body rod = WP_011372733.1, Sudeen_1103; Sudeen_1104: Flagellar basal body rod protein = WP_011372734.1. Published in (Götz, Pjevac, et al., 2018).....50

Figure 14 Expression of *S. denitrificans* transcripts (upper panel; TPM = Transcripts Per Million) and proteins (lower panel; %NSAF = Normalized Spectral Abundance Factor) involved in denitrification. Light bars show the average values of *S. denitrificans* grown on cyclooctasulfur (S8) and dark bars show the average of cultures grown on thiosulfate. napAGHBFLD = Nitrate reductase (napA = WP_011373143.1, Sudeen_1514; napB = WP_011373146.1, Sudeen_1517; napG = WP_041672542.1, Sudeen_1515; napH = WP_041672543.1, Sudeen_1516; napF = WP_011373147.1, Sudeen_1518; napL = WP_011373148.1, Sudeen_1519; napD = WP_011373150.1, Sudeen_1521); nirSF = nitrite reductase (nirS = WP_011373599.1, Sudeen_1985; nirF = WP_011373602.1, Sudeen_1988); norCB = nitric oxide reductase (norC = WP_011373597.1, Sudeen_1983; norB = WP_011373598.1, Sudeen_1984); nosZ1,2 = nitrous oxide reductase (nosZ1 = WP_011372928.1, Sudeen_1298; nosZ2 = WP_011373385.1, Sudeen_1770). Published in (Götz, Pjevac, et al., 2018).....52

Figure 15 The relative abundance of expressed SOX (sulfur oxidation multienzyme complex) and SQR (sulfide quinone reductase) proteins (%NSAF = Normalized Spectral Abundance Factor) and transcripts (TPM = Transcripts Per Million). Light bars show the average values of *S. denitrificans* grown on cyclooctasulfur (S8) and dark bars show the average of cultures grown on thiosulfate. Statistically significant differences ($p < 0.05$) are denoted with an asterisk. OMP (outer membrane protein) = WP_011373531.1, Sudeen_1917; soxH-like = WP_011373670.1, Sudeen_2056; SOX (sulfur oxidation multienzyme complex): soxZ2Y2DC: soxZ2 = WP_011373671.1, Sudeen_2057; soxY2 = WP_011373672.1, Sudeen_2058; soxD = WP_011373673.1, Sudeen_2059; soxC = WP_011373674.1, Sudeen_2060 ; soxXY1Z1AB: soxX = WP_011371896.1, Sudeen_0260; soxY1 = WP_011371897.1, Sudeen_0261; soxZ1 = WP_011371898.1, Sudeen_0262; soxA = WP_011371899.1, Sudeen_0263; soxB = WP_011371900.1, Sudeen_0264) and SQR (sulfide quinone reductase = WP_011372252.1, Sudeen_0619). B) The relative abundance of transcripts (upper panel; TPM = Transcripts Per Million) and proteins (lower panel; %NSAF = Normalized Spectral Abundance Factor) of the proposed polysulfide reductase

	(Suden_0498-Suden_0450: WP_011372132.1- WP_011372134.1). Published in (Götz, Pjevac, et al., 2018).....	54
Figure 16	Gene expression (TPM = Transcripts Per Million) of the cbb3-type cytochrome c oxidase (fixNOQP, fixN = WP_011371717.1, Suden_0081; fixO = WP_011371718.1, Suden_0082; fixQ = WP_011371719.1, Suden_0083; fixP = WP_011371720.1, Suden_0084), the membrane bound [Ni,Fe]-uptake hydrogenase (hydCBA, hydC = WP_041672535.1, Suden_1434; hydB = WP_011373064.1, Suden_1435; hydA = WP_011373065.1, Suden_1436) and the membrane bound formate dehydrogenase (fdhDCBAA, fdhD = WP_011372449.1, Suden_0817; fdhC = WP_011372450.1, Suden_0818; fdhB = WP_011372451.1, Suden_0819; fdhA = WP_011372452.1, Suden_0820; fdhA = WP_041672204.1, Suden_0821; fdx = WP_011372455.1, Suden_0824). Light bars show the average values of <i>S. denitrificans</i> grown on cyclooctasulfur (S8) and dark bars show the average of cultures grown on thiosulfate. Published in (Götz, Pjevac, et al., 2018).....	55
Figure 17	Model for the oxidation of elemental sulfur chains in <i>S. denitrificans</i> . The activation mechanism of cyclooctasulfur and the hydrolysis step resulting in the liberation of SO_4^{2-} from the outer sulfonate group (indicated with a '?') are currently unknown. The 'x7' indicates that the sulfur chain attached to SoxY2 might be oxidized completely (or in part) before accepting a new sulfur chain. Sulfur is indicated as black dot, whereas oxygen is indicated as small white circles on sulfur. Published in (Götz, Pjevac, et al., 2018).....	67

List of Tables

Table 1	Artificial seawater medium used as basis for the completion of the well-defined <i>S. denitrificans</i> medium.	24
Table 2	Sodium hydrogen carbonate is used in the medium to buffer the pH of the medium.....	25
Table 3	Iron(III) chloride in the medium serves as iron source needed for some enzymes.....	25
Table 4	Potassium phosphate in the medium serves as phosphate source.	25
Table 5	Selenite-tungstate solution as supplements (Widdel and Bak, 1992)	26
Table 6	Sodium thiosulfate in the medium serves as electron donor for <i>S. denitrificans</i>	26
Table 7	Transcriptomic data collected before and after quality control (QC). S ₈ -1-3 are the biological replicates of <i>Sulfurimonas denitrificans</i> grown with cyclooctasulfur and T-1 and T-2 are the two biological replicates grown with thiosulfate.....	32
Table 8	Summary of numbers of 16S rRNA, genes and identified proteins for the three most abundant genera in Crab Spa (<i>Sulfurimonas</i> , <i>Sulfurovum</i> and <i>Arcobacter</i>).....	33
Table 9	Number of sulfur oxidation genes (SOX) per dominant genus and sample LVP2 and LVP4.....	35
Table 10	Identification rates of proteins based on available genomic information divided by the number of identified proteins (Genes:Proteins). This value represents the ratio of genes that identified one protein. This value can be used as a measure of how the used database represented the active community of a system.....	36
Table 11	Overview of <i>S. denitrificans</i> protein identification counts for the two growth conditions cyclooctasulfur (S8) and thiosulfate (S2O3). Exclusive identifications are proteins that were detected in at least one replicate of one condition, but were absent in all replicates of the other condition.	47

Zusammenfassung

Crab Spa ist eine stabile hydrothermale Quelle und ist Teil des 9 ° N Ost-Pazifischen Rückens (EPR). Bemerkenswerterweise sind die physikochemischen Bedingungen in Crab Spa seit seiner Entdeckung im Jahr 2007 weitgehend konstant geblieben und bieten eine einzigartig stabile Umgebung, in der sich eine gut angepasste und stabile mikrobielle Gemeinschaft entwickelt hat. Diese mikrobielle Gemeinschaft wird von der Klasse der *Campylobacteria* dominiert, die bis zu 90% der Gemeinschaft ausmacht. Über die Stoffwechselwege, die es den *Campylobacteria* ermöglichen, die Bakteriengemeinschaft im Crab Spa zu dominieren, ist jedoch wenig bekannt. Um diese grundlegende Frage zu beantworten, wurde ein zweigleisiger Ansatz gewählt, der darin bestand, erstens die dominanten Stoffwechselwege in situ zu bestimmen und zweitens dieselben Stoffwechselwege und ihre Kontrollen unter definierten Bedingungen in vitro im Modell-Campylobacterium *Sulfurimonas denitrificans* genauer zu untersuchen.

Die metagenomische Analyse von zwei Umweltproben lieferte den Entwurf zur Bestimmung des metaproteomischen Profils der mikrobiellen Gemeinschaft von Crab Spa. Damit konnten die dominanten Organismen und deren wichtigste Stoffwechselwege identifiziert werden, welche die mikrobielle Gemeinschaft von Crab Spa antreiben. Etwa 90% der Gene für die Transkription und Proteinsynthese der Metagenomsequenzen gehörten nur drei Gattungen von *Campylobacteria* an: *Sulfurimonas*, *Sulfurovum* und *Arcobacter*. Die metaproteomischen Analysen bestätigten, dass die aktive mikrobielle Gemeinschaft von Campylobakterien dominiert wurde, die eine Kohlenstofffixierung über den reduktiven TCA-Zyklus durchführten, der hauptsächlich durch die Oxidation von Schwefelwasserstoff und Schwefel mit Nitrat und Sauerstoff angetrieben wurde. Die Analyse ergab, dass die Wege zwischen verschiedenen Mitgliedern der Bakterien aufgeteilt sein könnten. Die Proteine, die an Elektronenakzeptor-assoziierten Stoffwechselwegen, insbesondere der Denitrifikation, beteiligt sind, machten bis zu 20% des gesamten Metaproteoms aus, was als Anpassung an die Knappheit an Elektronenakzeptoren in Crab Spa gesehen werden könnte. Umgekehrt machten Proteine, die in Elektronendonator-assoziierten Stoffwechselwegen involviert sind, weniger als 0,1% des Metaproteoms aus, was mit der hohen Konzentration des Elektronendonors zu tun haben könnte. Um dieser Hypothese nachzugehen, wurden Chemostat-Experimente mit *S. denitrificans* entweder unter Elektronenakzeptor- oder -donor-Limitierung durchgeführt. Diese Experimente bestätigten, dass die Elektronenakzeptor Limitierung zu einer erhöhten Expression von Elektronenakzeptor-Proteinen führt. Eine höhere Expression von

Elektronendonor-Proteinen wurde jedoch unter Elektronendonor Limitierung nicht beobachtet. Neben Schwefelwasserstoff kann elementarer Schwefel im Crab Spa als wichtiger Elektronendonor dienen. Bisher waren jedoch keine Informationen darüber verfügbar, wie *Campylobacteria* elementaren Schwefel nutzen könnten. Zu diesem Zweck wurde *S. denitrificans* entweder mit Thiosulfat oder Cyclooctasulfur (S₈) als alleinigen Elektronendonoren gezogen und das Transkriptom mit dem Proteom verglichen. Die Ergebnisse zeigten eine unterschiedliche Expression des SOX-Schwefeloxidationsweges (*soxCDYZ* und *soxABXYZ*) als Reaktion auf die beiden unterschiedlichen Schwefelverbindungen. Basierend auf diesen Erkenntnissen wurde ein Modell für die Oxidation von Cyclooctasulfur vorgeschlagen, dass auch für andere schwefeloxidierende *Campylobacteria* gilt und bei der Interpretation von metatranskriptomischen und proteomischen Umweltdaten hilft (Götz, Pjevac, *et al.*, 2018; Lahme *et al.*, 2020). Insgesamt tragen die in dieser Arbeit vorgestellten Ergebnisse zu einem besseren Verständnis der an Hydrothermalquellen ablaufenden mikrobiellen Prozesse bei.

Summary

Crab Spa, is a stable diffuse-flow hydrothermal vent site located at the 9°N hydrothermal vent field on the East Pacific Rise (EPR). Remarkably, the physicochemical conditions at Crab Spa have remained largely constant since its discovery in 2007 providing a uniquely stable environment in which a well-adapted and stable microbial community has evolved. This microbial community is dominated by the class *Campylobacteria*, accounting for up to 90% of the community. Little is known, however, about the metabolic pathways that allow the *Campylobacteria* to dominate the bacterial community at Crab Spa. To address this fundamental question, a two-pronged approach was taken consisting of first determining the dominant metabolic pathways in situ, and second to study those same metabolic pathways and their controls in more detail under defined conditions in vitro in the model campylobacterium *Sulfurimonas denitrificans*.

Metagenomic analysis of two environmental samples provided the blueprint to determine the metaproteomic profile of the Crab Spa microbial community. This allowed to identify the dominant organisms and their major metabolic pathways sustaining the microbial community at Crab Spa. About 90% of the genes for transcription and protein synthesis of the metagenome sequences belonged to just three genera of *Campylobacteria*: *Sulfurimonas*, *Sulfurovum* and *Arcobacter*. The metaproteomic analyses confirmed that the active microbial community was dominated by *Campylobacteria*, carrying out carbon fixation via the reductive TCA cycle predominantly fueled by the oxidation of sulfide and sulfur with nitrate and oxygen. The analysis further revealed that pathways might be partitioned between different members of the bacterial community. Proteins involved in electron acceptor–related pathways, in particular denitrification, accounted for up to 20% of the whole metaproteome, which could be seen as an adaptation to the scarcity of electron acceptors at Crab Spa. Conversely, proteins related to electron donor–associated metabolic pathways accounted for less than 0.1% of the metaproteome, possibly in response to the high concentration of the electron donor. To follow up on this hypothesis, chemostat experiments with *S. denitrificans* were performed under either electron-acceptor or -donor limitation. These experiments confirmed that electron-acceptor limitation lead to the elevated expression of electron-acceptor proteins. However, a higher expression of electron-donor proteins was not observed under electron-donor limitation. Besides hydrogen sulfide, elemental sulfur has the potential to serve as an important electron donor at Crab Spa. However, up to now no information was available on how *Campylobacteria* might be able to utilize elemental sulfur. For this, *S. denitrificans* grew with

either thiosulfate or cyclooctasulfur (S₈) as sole electron donors and its transcriptome and proteome was compared. The results revealed a differential expression of the SOX sulfur oxidation pathway (*soxCDYZ* and *soxABXYZ*) in response to the two different sulfur compounds. Based on these findings, a model for the oxidation of cyclooctasulfur was proposed that also applies to other sulfur-oxidizing *Campylobacteria* and helps in the interpretation of environmental metatranscriptomic and –proteomic data (Götz, Pjevac, *et al.*, 2018; Lahme *et al.*, 2020). The presented results help to better understand the microbial processes at hydrothermal vents.

1 Introduction

When the idea of plate tectonic arose, it was predicted that the plate movements could create weak spots in the oceans crust, forming an environment that supports hydrothermal activity (Tivey, 2007). In 1977 near the Galapagos islands, the first deep-sea hydrothermal vents were found (Lonsdale, 1977; Corliss *et al.*, 1979). Surprisingly, these systems supported a large community of organisms, with particular high abundances of the giant tube worm *Riftia pachyptila*, but why and how the system supported such a community was just speculative at the time and only discovered later (Cavanaugh *et al.*, 1981; Felbeck, 1981; Markert *et al.*, 2007; Gardebrecht *et al.*, 2012). Despite some exceptions most active hydrothermal vent fields are located in the deep ocean making them difficult to study. After their discovery, the focus shifted to high temperature hydrothermal vents because the energy input into the seawater seemed more important (Tivey, 2007; Sievert and Vetriani, 2012) than low temperature diffuse flow hydrothermal vents which were always the focus of biologists(Urich *et al.*, 2014). The hydrothermal fluid circulation is known to be an important sink and source for various chemical elements with implications for the ocean's chemistry. Magnesium especially gives insight to the seawater to hydrothermal fluid ratio, as with higher temperatures it is removed from seawater when smectite/ chlorite precipitates (Von Damm *et al.*, 1985; Tivey, 2007). So far the best studied hydrothermal vent study sites for US and European research institutions are the Juan de Fuca Ridge, East Pacific Rise, Lau Basin and Mid-Atlantic Ridge (Tivey, 2007).

This thesis focuses on a specific deep sea hydrothermal diffuse flow vent called Crab Spa, which is situated at the 9° N deep-sea hydrothermal vent field on the East Pacific Rise (EPR) (McNichol *et al.*, 2018). This vent was discovered in 2007, one year after a volcanic eruption (Tan *et al.*, 2016), and it has been frequently sampled, demonstrating that physicochemical conditions have stayed remarkably stable not only over days, but over months and years (Reeves *et al.*, 2014; McNichol *et al.*, 2016, 2018). At Crab Spa, deep-sea cold seawater mixes below the seafloor with hot hydrothermal fluids, creating favorable redox conditions conducive for the growth of chemoautotrophic microorganisms (Sievert and Vetriani, 2012). The composition of exiting fluids is dependent on several factors such as seawater chemistry, rock chemistry and the structure of the rock (Tivey, 2007). Other study sites often experience variable temperature and mixing conditions making it difficult to study microbial communities as they constantly must adapt to those variable conditions (Pjevac *et al.*, 2018 and references therein). Changing physicochemical conditions could favor one organism

over the other depending on energy source availability and temperature changes (McNichol *et al.*, 2016, 2018).

It is well established that microorganisms are at the base of the food chain at hydrothermal vents (Sievert and Vetriani, 2012). Special sophisticated technologies are required to study these extreme and difficult to access environments which limits the sample amount, sampling time and sample size. Limited numbers of samples from hydrothermal vents make a statistical analysis difficult, and it requires modern laboratory and computational tools to process the few samples available. To get a general picture of the functionality of the microbial system at such diffuse flow vents, so called “-omics” approaches are used. Metagenomics was one of the first approaches to reveal the microbial community and their biochemical potential in deep-sea vent systems. It has been shown that for example in marine sediments up to 90% of the DNA recovered is from non-living organisms (Torti *et al.*, 2015), which possess questions on how reliable Metagenomics is in revealing active microbial communities. To study the functionality of the system two other methods have been previously used at hydrothermal vents in combination with metagenomes. Metatranscriptomics measures the RNA content in the system consisting of ribosomal RNA and mRNA (messenger RNA). It is known that mRNA outside of the organism can have a half-life time of only a couple seconds to minutes (Selinger *et al.*, 2003), which makes it difficult to study when sampling times can be several hours. Because the half-life time of proteins is in the range of hours (Maier *et al.*, 2011), when studying the expressed enzymes of the microbial community metaproteomics is used to complement transcriptomic data sets. However, with current technology, 100fmol of protein is needed for detection (Silva *et al.*, 2006), which is a significant amount if the microbial community is highly diverse. Thus, metaproteomics provides an overview on the most abundantly expressed metabolic pathways. Only a few meta-omics studies, especially metaproteomic studies, on vent habitats exist but give first insights into these special marine habitats (Urich *et al.*, 2014; Stokke *et al.*, 2015; Fortunato *et al.*, 2018; Pjevac *et al.*, 2018).

1.1 Energy metabolism at hydrothermal vents

The process of ‘chemoautotrophy’ was discovered by Winogradsky more than half a century before the discovery of hydrothermal vents (Dworkin, 2012). Chemolithoautotrophy is described as a process that uses a chemical redox potential to generate energy in the absence of light (chemolitho-) to fix carbon dioxide (-autotrophy) (Figure 1). This process, driven by bacteria, provides the base of the food chain at hydrothermal vents with the generation of

complex carbohydrates, lipids and proteins (Tuttle and Jannasch, 1979; Tuttle *et al.*, 1983). This system thrives on inorganic chemical energy sources provided through the mixing of seawater rich in electron acceptors and reduced hydrothermal vent fluids rich in electron donors. Electron acceptors such as oxygen or nitrate are used by bacteria in combination with electron donors such as sulfur or hydrogen sulfide to produce energy in the form of ATP, which is then being used to fix carbon dioxide (CO₂) into organic matter.

Chemoautotrophy occurs in many other environments such as sediments or redox zones in the water column of various sea basins (Madrid *et al.*, 2001; Vetriani *et al.*, 2003; Grote *et al.*, 2007). What sets hydrothermal vent systems apart from other redox systems is the active mixing event that supports a high rate of productivity in the subsurface (McNichol *et al.*, 2018). In these hydrothermal vent systems, Campylobacteria have been identified through DNA sequencing as the most abundant and active bacteria. The main identified genera of Campylobacteria are *Sulfurimonas*, *Sulfurovum* and *Arcobacter* but minor genera such as *Caminibacter*, *Nautilia*, *Nitratiruptor*, *Nitratifractor*, *Sulfuricurvum*, *Sulfurospirillum*, and *Thioreductor* (Sievert and Vetriani, 2012). Related campylobacterial genera are also found in other redox environments such as redox zones in the Baltic sea, Black Sea or Cariaco basin (Madrid *et al.*, 2001; Vetriani *et al.*, 2003; Grote *et al.*, 2007). Based on genomic and biochemical information these bacteria use the reverse tricarboxylic acid cycle for carbon fixation (Hügler *et al.*, 2005; Hügler and Sievert, 2011) and a combination of oxygen or nitrate reduction with sulfide, sulfur, thiosulfate or hydrogen oxidation (Figure 1).

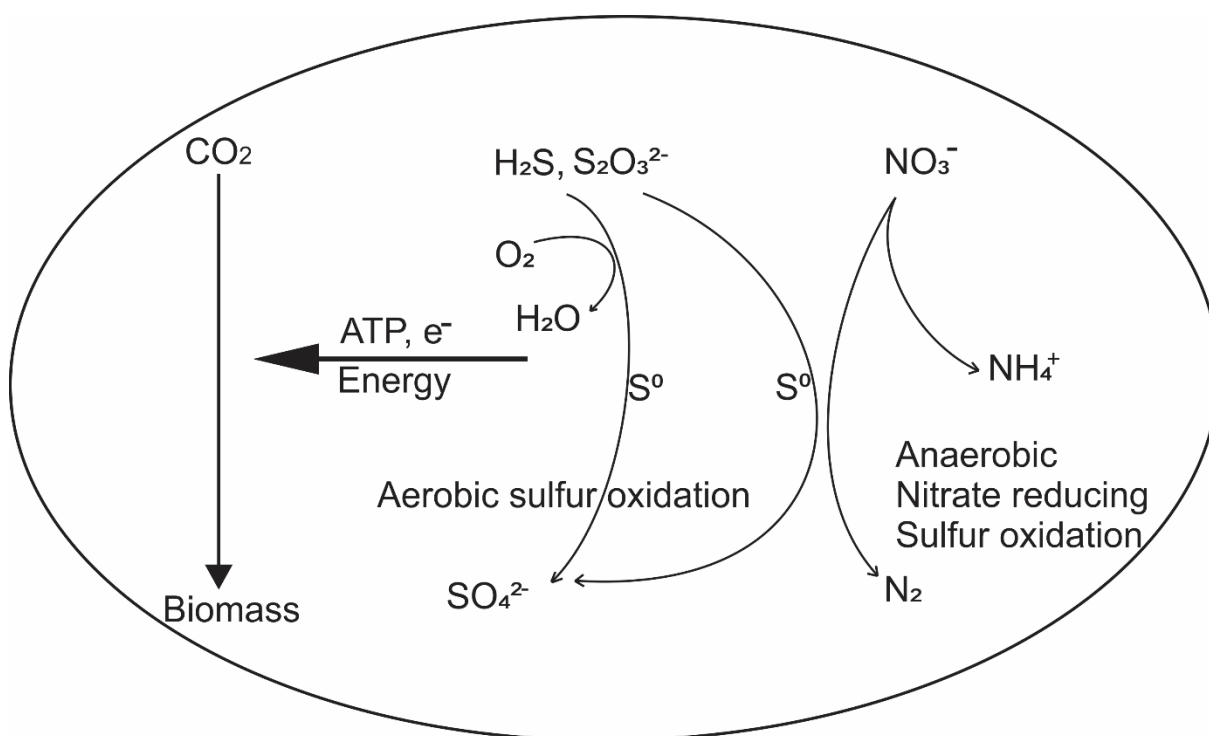


Figure 1 Chemolithoautotrophic model of biochemical redox-reactions. Reduced sulfur compounds or hydrogen are oxidized and oxidized nitrate or oxygen is reduced. These redox reactions result in energy in form of ATP which is used to fix carbon dioxide into biomass (carbon compounds).

The reverse tricarboxylic acid cycle consists of eight enzymes that cycle oxaloacetate to citrate which is then converted back to oxaloacetate and acetyl-CoA by the ATP Citrate lyase (Hügler and Sievert, 2011). In this cycle carbon dioxide and water are used in reactions to synthesize carbon compounds. Carbon dioxide is fixed in two steps of the eight reactions. First during the conversion of succinyl-CoA (four carbon atoms) to alpha-ketoglutarate (five carbon atoms) and second from alpha-ketoglutarate to Isocitrate (six carbon atoms). The energy needed for carbon fixation is mainly provided by sulfur oxidation (Sox system or sulfide quinone oxidoreductase-SQR) or hydrogen oxidation (hydrogenases), which is coupled to nitrate reduction (denitrification or dissimilatory nitrate reduction- DNRA) or oxygen reduction (Cytochrome c oxidase cbb₃ or Cytochrome aa₃ quinol oxidase). This was confirmed in hydrothermal sediments (Urich *et al.*, 2014), redox zones in the water column (Grote *et al.*, 2012), hydrothermal vents and chimney wall surfaces (Takai *et al.*, 2005; Sievert and Vetriani, 2012; Stokke *et al.*, 2015; Pjevac *et al.*, 2018).

Parts of the following three paragraphs have been published in (Götz, Pjevac, et al., 2018).

Sulfur can occur in high concentrations in hydrothermal vent environments. Sulfur is of central importance in biogeochemical cycles and exists in many oxidation states (Sievert *et al.*, 2007). As an essential component of biomass, sulfur is assimilated into organic compounds and is also involved either as electron acceptor or donor in energy yielding processes in chemolithoautotrophic, photolithoautotrophic, and heterotrophic microorganisms (Kletzin *et al.*, 2004; Friedrich *et al.*, 2005; Robertson and Kuenen, 2006; Sievert *et al.*, 2007; Dahl *et al.*, 2008; Finster, 2008; Sievert and Vetriani, 2012). Elemental sulfur accumulates in visible amounts in various environments, including marine sediments, microbial mats, hydrothermal vents, glacial shields, oxygen minimum zones and volcanic soils (Ruby *et al.*, 1981; Woodruff and Shanks, 1988; Raiswell, 1992a; Taylor and Wirsén, 1997; Alonso-Azcárate *et al.*, 2001; Engel *et al.*, 2004; Zopfi *et al.*, 2004; Lavik *et al.*, 2009; Cosmidis and Templeton, 2016; Lau *et al.*, 2017). Elemental sulfur occurs mostly in the form of zero-valence sulfur (S^0) with cyclooctasulfur (S_8) as the most common and stable form (Steudel and Eckert, 2003).

During microbial sulfide (S^{2-}) oxidation, S^0 (in the form of S_8 , polymeric sulfur (S_μ) or sulfur chains) is often produced and deposited as an intermediate oxidation product (Friedrich *et al.*, 2001; Prange *et al.*, 2002; Dahl and Prange, 2006; Sievert *et al.*, 2007; Sievert, Hügler, *et al.*, 2008). In various S^0 -rich natural and engineered environments, members of the genus *Sulfurimonas* and other sulfur-oxidizing *Campylobacteria*, such as *Sulfurovum* sp. and *Sulfuricurvum* sp., are highly abundant (Macalady *et al.*, 2008; Legatzki *et al.*, 2011; Hubert *et al.*, 2012; Meyer *et al.*, 2013; Pjevac *et al.*, 2014; Gulmann *et al.*, 2015; Zhang *et al.*, 2015; Li *et al.*, 2016; McNichol *et al.*, 2016). In marine sediments and at hydrothermal vents, it has been proposed that especially *Sulfurimonas* and *Sulfurovum* species occupy the niche for S^0/S_8 oxidation (Pjevac *et al.*, 2014; Meier *et al.*, 2017). Considering the extremely low solubility and reactivity of S_8 (Franz *et al.*, 2007; Kamyshny, 2009; Pjevac *et al.*, 2014), neutrophilic S_8 -oxidizing microorganisms most likely need a specific activation or solubilization mechanism to make S_8 available for their energy metabolism, as has been shown for acidophilic sulfur-oxidizing bacteria (Rohwerder and Sand, 2003; Mangold *et al.*, 2011; Chen *et al.*, 2012). To date, *Sulfurimonas denitrificans*, the type strain of the genus *Sulfurimonas*, is the only known neutrophilic microorganism with the demonstrated capability of S_8 oxidation (Pjevac *et al.*, 2014; Götz, Pjevac, *et al.*, 2018).

During aerobic sulfur oxidation, oxygen is reduced to water in a reaction performed by a Cytochrome c oxidase cbb_3 or Cytochrome aa_3 quinol oxidase (Xie *et al.*, 2011; Dahle *et al.*, 2013; Ulrich *et al.*, 2014; Pjevac *et al.*, 2018). Both these oxidases have been shown to be

adapted to different oxygen concentrations. Cbb₃ is adapted to lower oxygen concentration in comparison to aa₃. During anaerobic sulfur oxidation nitrate is reduced to either nitrogen gas in the four-step denitrification pathway or reduced by the dissimilatory nitrate reductase to ammonium. The first step in both nitrate reducing pathways is performed by the periplasmic nitrate reductase (Nap) which catalyzes the reaction from nitrate (NO₃⁻) to nitrite (NO₂⁻). As an alternative to sulfur compounds as electron donors it was shown with *S. denitrificans* that hydrogen oxidation in combination with denitrification is more efficient for growth (Han and Perner, 2014). Hydrogen oxidation seems to be more important at higher temperatures (>25°C) than at lower temperatures (<25°C) within and between diffuse flow hydrothermal vents (Fortunato *et al.*, 2018; McNichol *et al.*, 2018).

1.2 Questions and rationale of the thesis

1.2.1 Metaproteomics on Crab Spa diffuse-flow hydrothermal vent microbial community to determine the dominant metabolic pathways in situ

Over the last decade, Crab Spa has been studied extensively in comparison to other hydrothermal vent sites. It is known what kind of bacterial groups exist and what their metabolic potential looks like. Incubation studies with natural communities have provided information on productivity and under what conditions which bacteria can succeed (McNichol *et al.*, 2016, 2018). What we do not know is what pathways are actively expressed and utilized by the microorganisms in situ. For this reason, metaproteomics was chosen as the method to answer the question of what metabolic pathways are actively expressed in the microbial community contained in the diffuse-flow effluent from Crab Spa, which serves as an access point to the subseafloor biosphere of this diffuse-flow hydrothermal vent system (McNichol *et al.*, 2018). These samples provide insights to the microbial community structure/ how different community members co-exist and their most dominantly expressed biochemical pathways. The question to answer about the diffuse flow hydrothermal vent system at Crab Spa was, what are the most expressed pathways that drive the microbial community and indirectly support a diverse animal community at and around Crab Spa?

1.2.2 Cultivation experiments of *Sulfurimonas denitrificans* under limiting conditions in chemostats and elemental sulfur in batch culture to measure metabolic pathway changes in vitro

Single bacterial strain isolates are often used as model organisms to better understand their physiology and adaptations to changing environmental conditions in vitro. In 1975, *S. denitrificans* was isolated as *Thiomicrospira denitrificans* from Dutch Wadden Sea mud flats using a defined medium with thiosulfate ($S_2O_3^{2-}$) as electron donor and nitrate as electron acceptor to simulate chemosynthetic growth (Timmer-ten Hoor, 1975). In 2006, *Tms. denitrificans* was reclassified as *S. denitrificans* as part of the *Epsilonproteobacteria* (Takai *et al.*, 2006) which are now known as *Campylobacteria* (Waite *et al.*, 2017). As a representative of chemolithoautotrophic *Campylobacteria*, the genome of the *S. denitrificans* was sequenced (Sievert, Scott, *et al.*, 2008), which revealed a versatile metabolic potential of this bacterium, similar to other r-strategists that are adapted to fluctuating substrate and redox conditions (Rogge *et al.*, 2017).

In this thesis, *S. denitrificans* was used in chemostat and batch culture experiments as a model organism for chemolithoautotrophic *Campylobacteria* to identify proteins that are actively expressed under varying growth conditions to help interpret the metaproteomic dataset. In chemostat cultures, *S. denitrificans* was grown with four electron donor/acceptor combinations: (i) with hydrogen and nitrate (ii) with thiosulfate and oxygen, (iii) nitrate limited and thiosulfate and (iv) thiosulfate limited and nitrate. This approach would provide clues on how these organisms could adapt to changing environments and how to interpret enzyme abundances in the environment. Batch culture experiments with elemental sulfur were performed to identify potential pathways for elemental octa sulfur (S_8) utilization in *S. denitrificans*. Here, chemostat experiments were not feasible due to the insoluble nature of elemental sulfur which would have been difficult to apply to the chemostat in constant amounts without blocking the chemostat tubing and to achieve steady-state conditions.

2 Material and Methods

2.1 Metaproteomics to identify the active chemoautotrophic community members inhabiting the seafloor at a deep-sea hydrothermal vent

In this first part of the thesis, the dominant biochemical pathways of the active microbial communities inhabiting the seafloor at a deep-sea hydrothermal vent were determined using a metaproteomic approach, complemented by 16S rRNA- and metagenomics-based analyses.

2.1.1 Sampling

The studied vent site is a diffuse-flow vent called Crab Spa located at the 9°N vent field on the East Pacific Rise (9°50.3981 N, 104°17.4942 W). The biomass required for the analyses was collected in situ on filters using a large volume pump (LVP, McLane, Falmouth, MA, USA) during cruise AT26-10 on R/V Atlantis. The LVP was dropped as a free-falling instrument from R/V Atlantis during cruise AT26-10 in January 2014. Once on the seafloor, it was moved by ROV Jason to the vent site and the intake nozzle was placed into the vent orifice. Pumping started at a pre-programmed time of 3 hours triggered by ROV Jason while monitoring the amount of fluid passing through a combination of a combusted GF-75 glass fiber filter (effective pore size 0.3 µm, Advantec, USA) on top of a polyethersulfone membrane filter (PES, 0.2 µm pore size, Sterlitech, USA) with a maximum pump rate of 2.8 L min⁻¹. The amount of hydrothermal fluid pumped through the filters was 422L and 345L for LVP2 (January 9, 2014) and LVP4 (January 9, 2014), respectively. Within 30 min of completion of the pumping, the LVP was released by ROV Jason and came back to the surface within 40 min, where it was picked up and brought on deck. Once on deck, the filters were taken out of the thermally insulated filter housing, cut into four different-sized pieces for subsequent metagenomic, metatranscriptomic, metaproteomic, and lipidomic analyses, and stored frozen at -80°C. Overall, the time interval between the end of the pumping and the preservation of the filter on board the ship was ≤ 2 hours.

2.1.2 DNA extraction (performed by Dr. Lara Gulmann, Research Associate in the laboratory of Dr. Sievert)

DNA was extracted from 1/4 (LVP2) or 1/8 (LVP4) of the large volume pump filters (GF-75, effective pore size 0.3 µm, on top of PES, 0.2 µm pore size) using a phenol:chloroform:IAA and chloroform extraction method. Amicon Ultra-15 30k filters were

used to wash and concentrate the extracted DNA. The filters were thawed on ice and separated using sterile tweezers into sterile 50mL conical tubes, exposing the filter surface. Extraction buffer {2mL of lysis buffer [730mM Sucrose, 40mM EDTA (pH 8.0), 50mM Tris (pH 8.3)], sterile DNA grade water, all DNA and RNA free, molecular grade reagents, lysis buffer was autoclaved before use} was added to each sample. The samples were exposed to 3 freeze/thaw cycles with 30 seconds in liquid nitrogen, and then thawing in a 40°C water bath. Another 4mL of lysis buffer was added to each sample along with 120µl lysozyme solution (5% Lysozyme [Fisher BP 535-1] in Lysis Buffer, 0.2µm filter sterilized) and the samples were incubated in a hybridization oven with constant rotation for 45 minutes. After the incubation, 300µL Proteinase K solution (1% Proteinase K (Fisher BP 1700-50) in Lysis Buffer) and 300µL 20% SDS (in DNA grade water, 0.2µm filter sterilized) were added to each sample. The filters were then incubated at 55°C for 2 hours in the rotating hybridization oven. After incubation, the lysate was transferred out of the tubes with the filters into a sterile Teflon tube for the filter extraction. To wash the filters an additional 3mL of lysis buffer was added to each tube which were incubated at 55°C for 25 minutes. This wash was then pooled with the first tube of lysate. In a chemical fume hood, using personal protective equipment, 9mL of Phenol:Chloroform:IAA (25:24:1; pH 8.0) were added to each tube of lysate. This was then mixed by inversion for 20 seconds and centrifuged using a clinical tabletop centrifuge at 2,500xg for 5 minutes to separate the aqueous and organic phases. The aqueous phase, on top, was carefully transferred to a new sterile Teflon tube. The organic phase was then washed with an extra 2mL of lysis buffer, mixed, and centrifuged at 2,500xg for 5 minutes. This aqueous phase was pooled with the first aqueous phase. The phenol extraction was then repeated twice. After the phenol extraction, a chloroform wash was performed: 9mL of chloroform:IAA (24:1) were added to the aqueous phases from the phenol extraction. This was mixed by inversion for 20 seconds and then spun 5 minutes at 2,500 x g, and followed with a second chloroform wash. The aqueous phase was filtered through Amicon Ultra-15 30k filters, which were spun at 1,000xg until only 250µL remained on the filter, and the flow-through was removed. Three washes of 2 mL sterile TE buffer followed, where 2 mL TE were added, the filter was spun at 1,000xg until 250µL were left, and then more TE was added. After these washes, the filters were spun until less than 250µL were left in the filter, and then this liquid was carefully removed using a pipette to avoid damaging the filter membrane and put in a sterile microcentrifuge tube. The membrane was then washed with 100µL sterile TE buffer, which was then pooled with the other concentrated DNA product in the microcentrifuge tube, which was stored at -80°C until

further analysis. The amount of DNA extracted from the filters was 468µg and 315µg for LVP2 and 4, respectively.

2.1.3 16S rRNA Sequencing and Analysis (performed by Clarissa Karthäuser, in the laboratory of Dr. Sievert)

The V1+V2+V3 region of the 16S rRNA gene was targeted with primers 27F and 519R (Caporaso *et al.*, 2010) in a single-step 30 cycle PCR using the HotStarTaq Plus Master Mix Kit (Qiagen, USA) under the following conditions: 94°C for 3 minutes, followed by 28 cycles of 94°C for 30 seconds, 53°C for 40 seconds and 72°C for 1 minute, after which a final elongation step at 72°C for 5 minutes was performed. Sequencing was performed at MR DNA (www.mrdnalab.com, Shallowater, TX, USA) utilizing Roche 454 FLX titanium instruments and reagents and following manufacturer's guidelines. The sequences were further processed in the software QIIME, which stands for "Quantitative insights into Microbial Ecology" (Caporaso *et al.*, 2010) by Clarissa Karthäuser. OTUs were picked with the script *pick_de_novo_otus.py* (Rideout *et al.*, 2014). Steps 4 (*assign_taxonomy.py*) and 7 (*make_otu_table.py*) were repeated using the Silva database and the RDP method (Wang *et al.*, 2007) instead of QIIMEs default. This led to a higher and more precise detection of some bacterial species. It also highly increased the amount of archaea sequences that could be assigned to a taxon.

2.1.4 Metagenomic Sequencing and Analysis

Metagenomic sequencing was carried out at the Bigelow Laboratory for Ocean Sciences (Maine, USA). Libraries were created with Nextera XT (Illumina) reagents following manufacturer's instructions, except for purification steps, which were done with column cleanup kits (QIAGEN), and library size selection, which was done with BluePippin (Sage Science, Beverly, MA), with a target size of 500±50 bp. Libraries were sequenced with NextSeq 500 (Illumina) in 2x150bp mode using v.1 reagents. The obtained sequence reads were quality-trimmed with Trimmomatic v0.32 using the following settings: -phred33 LEADING:0 TRAILING:5 SLIDINGWINDOW:4:15 MINLEN:36. Paired metagenomic reads were joined using flash version 1.2.11 and the following parameters: -x 0.05 -m 20 -M 150. For the analysis of the metagenome, genes were manually sorted into biochemical pathway categories and counted per genus in Excel. Metagenomes LVP2 and LVP4 are available on the MG-RAST server under the accession numbers mgm4679649.3 and mgm4679741.3, respectively.

2.1.5 Protein extraction from filter pieces

A quarter of each filter was used for the metaproteomic analysis. First, the soluble proteins were extracted from the filters following the protocol of Teeling *et al.*, 2012. The quarter filter piece was cut into small pieces and transferred into 1.8 mL Eppendorf tubes containing lysis buffer (50 mM Tris, 2% SDS, 10% Glycerol, 0.1 M DTT, pH 6.8) and glass beads (180 μ m diameter). Subsequently, the cells contained on the filter were disrupted with a bead beater (MP FastPrep®-24 Classic) 3-times for 30 sec at 6.5 m/s and 4 °C with a 5 min pause on ice in between runs. Beads and filter pieces were pelleted by centrifugation at 15,500 x g for 4 min at 4 °C. The supernatant (protein raw extract) was collected in ultracentrifugation tubes and further centrifuged at 100,000 x g for 1 h at 4 °C. The supernatant includes the soluble proteome and the remaining pellet was further used for an enrichment of membrane-bound proteins. The supernatant (soluble proteome) was combined 1:1 with cold acetone (-20 °C) to precipitate proteins overnight at -20°C. Afterwards, the proteins were pelleted for 10 min at 15,500 x g at 4 °C. and washed in cold 96 % ethanol (-20 °C). Finally, the pellet was dried in a vacuum centrifuge (Concentrator plus, Eppendorf) at 1,400 rpm, ambient temperature and 20 mbar vacuum.

Membrane bound proteins were enriched from remaining cell components in ultracentrifuge tubes as described in (Eymann *et al.*, 2004) without using Pefabloc: Pellets were homogenized with a 1 mL glass mortar/ tissue grinder in 2x 250 μ L high-salt buffer (20mM Tris-HCl, pH 7.5, 10mM EDTA, 1M NaCl) and further incubated with 2 mL high-salt buffer for 30 min at 4 °C on a rotary shaker and again ultra-centrifuged at 100,000 x g for 1 h at 4 °C. The remaining pellet was homogenized in 1 mL 100 mM Na₂CO₃-HCl, pH 11, 10 mM EDTA, 100 mM NaCl and incubated again for 30 min at 4 °C on a rotary shaker. The membrane fraction was ultra-centrifuged at 100,000 x g for 1 h at 4 °C. The obtained pellet was resuspended in 50mM triethylammonium bicarbonate, pH 7.8, homogenized in the 1 mL glass mortar and incubated on the rotary shaker for 30 min at 4 °C. For the last time the membrane fraction was ultra-centrifuged at 100,000 x g for 1 h at 4 °C. The remaining pellet was dried for 5 min in a vacuum centrifuge (Concentrator plus, Eppendorf) at 1,400 rpm, ambient temperature and 20 mbar vacuum.

For protein separation by polyacrylamide SDS PAGE, pellets containing the soluble and membrane-bound proteins were resuspended in sample buffer (0.1 M Tris-HCl pH 6.8, 10 % SDS, 20 % glycerol, 5 % mercaptoethanol, bromophenol blue), denatured at 90 °C for 10 min and loaded as 3 technical replicates onto precast mini gels (BioRad TGX, 4-20%). The samples

were run at 150 V for approximately 50 min. Gels were stained overnight with CBB- Coomassie Brilliant Blue (G250, Sigma Aldrich). On a glass plate, cleaned with methanol and double distilled water (ddH₂O), protein lanes were excised from the gels and divided into 10 equal-sized pieces for chemostat and batch culture samples of *S. denitrificans* and metaproteome LVP2. For LVP4 15 equal-sized gel pieces (subsamples) were excised. Each subsample was cut in small pieces and transferred into 2 mL Eppendorf cups. CBB was removed by incubating the gel pieces multiple times (until unstained) in a wash solution containing 200 mmol L⁻¹ NH₄HCO₃ and 30% acetonitril at 37°C for 30 min and metaproteome subsamples were further purified using ZipTip pipette tips (Millipore) according to the manufacturer's instructions. Destained gel pieces were dried for 15 min in an Eppendorf Concentrator plus at 1,400 rpm, ambient temperature and 20 mbar vacuum. For protein digestion, 2 µg mL⁻¹ trypsin solution (Promega, Madison, WI, USA) was added to dried gel pieces until covered (~50 µL) and incubated at room temperature for 30 min. Additional trypsin was added to cover rehydrated gel pieces and incubated at 37°C for 14-16 h. Thereafter, 50 µL ddH₂O was added to the incubated gel pieces, which were further sonicated for 15 min in an ultrasound bath (37 kHz, 600W \ FB15054 Fisherbrand) to elute the peptides. After sonication, the sample was centrifuged at 5,000 x g for 10 s. The peptide-containing supernatants were transferred into new tubes, and centrifuged at 250 x g under vacuum in an Eppendorf Concentrator to reduce the sample volume to 10 µL. The 10 µL peptide mixes were stored at -80 °C until measurement.

2.1.6 Proteomics and data analysis

ESI-MS/MS measurements, data filtering and data analysis were performed as recently described in (Ponnudurai *et al.*, 2017). Peptide mixes were separated by Nano HPLC (Easy-nLCII HPLC system, Thermo Fisher Scientific). 10 subsamples of LVP2 and 15 subsamples of LVP4 were loaded onto a 20cm nano-LC column with 10 µl buffer A (0.1% acetic acid) at a constant flow rate of 500 nL/min without trapping. Subsequently, peptides were eluted using a nonlinear 100 minutes gradient from 1 to 99% buffer B (0.1 % acetic acid in acetonitrile) with a constant flow rate of 300 nL/min and injected online into an LTQ Orbitrap Velos classic mass spectrometer (Thermo Fisher Scientific). Afterwards the column was washed with 99% buffer B for 5 minutes and equilibrated with 99% buffer A for 19 minutes. After a survey scan at a resolution of R = 30,000 within a scan range(m/z) of 300-2000 in the Orbitrap with activated lockmass correction, the five most abundant precursor ions were selected for fragmentation. Singly charged ions as well as ions without detected charge states were not selected for MS/MS analysis. CID fragmentation was performed for 30 ms with normalized collision energy of 35

and the fragment ions were recorded in the linear ion trap. All MS/MS spectra were searched against a target-decoy database containing genomes of cultivated organisms as well as concurrently obtained single cell genomes and metagenomes using the SORCERERTM system (SageN, Milpitas, CA, USA) with an integrated SEQUEST algorithm (Thermo Fisher Scientific, San Jose, CA, USA; version 27, revision 11). Peptide and protein identifications were filtered with 1% peptide false discovery rate (FDR) and 1% protein FDR in Scaffold (<http://www.proteomesoftware.com/>). Total spectral counts were extracted in Scaffold and normalized into normalized spectral abundance factors (NSAF) with the protocol described in (Zybailov *et al.*, 2006). For OrgNSAF (OrganismNSAF) the NSAF from all proteins of one genus were used and normalized to 100%. The NSAF and Org NSAF data can be found in Supplement Table 1. The mass spectrometry proteomics data for LVP2 and LVP4 are available through the ProteomeXchange Consortium (<http://proteomecentral.proteomexchange.org>) via the PRIDE partner repository (Vizcaíno *et al.*, 2016) with the dataset identifier PXD022871 and 10.6019/PXD022871.

Bubble diagrams were calculated in R (R-code in appendix) and the taxonomic distribution was analyzed with Excel using calculated %NSAF factors normalized to 100% and illustrated as pie charts.

2.2 Cultivation and proteomic analysis of *Sulfurimonas denitrificans* to assess adaptations to different growth conditions

To identify adaptations of *S. denitrificans* to different growth conditions and substrates relevant for its natural habitat, *S. denitrificans* was grown in a chemostat and as batch cultures using the anaerobic artificial seawater medium based on Timmer-ten Hoor (1975), further described in 2.2.1. The bicarbonate concentration in the medium was increased to 5 g L⁻¹ to buffer the pH. The batch culture approach was used to investigate the growth of *S. denitrificans* using either thiosulfate or octa-sulfur, whereas chemostats were used to investigate the response of *S. denitrificans* to electron donor or electron acceptor limitations, as well the response to the presence of oxygen and hydrogen.

2.2.1 Medium preparation and cultivation of *Sulfurimonas denitrificans*

Anaerobic artificial seawater medium (Table 1) was prepared in a Widdel flask (Plugge, 2005) and autoclaved at 121 °C for 30 to 45 min. Subsequently, the medium was cooled under a stream of N₂:CO₂ (80:20) and solutions 2.2.1.2 through 2.2.1.6 were added. In the end, the pH was adjusted to 7. For routine cultivation, the medium was dispensed into Hungate tubes that were purged with N₂:CO₂ (80:20) and sealed with butyl rubber stoppers. To have actively growing cultures available for the experiments, stock cultures of *S. denitrificans* were prepared in Hungate tubes and transferred weekly.

2.2.1.1 Artificial seawater medium (Solution A)

All components were dissolved in Milli-Q water and the solution was autoclaved at 121 °C for 30 to 45 min.

Table 1 Artificial seawater medium used as basis for the completion of the well-defined *S. denitrificans* medium.

Chemical substance	g L ⁻¹	Final concentration [mM]
NaCl	10	171
KNO ₃	2	20
NH ₄ Cl	1	18.7
MgSO ₄ x 7 H ₂ O	3.5	14.2
CaCl ₂ x 2H ₂ O	0.42	2.9
KCl	0.7	9.4
Trace element solution SL-6	1.0 <u>mL</u>	

Dest H₂O

Add to 1000 ml

2.2.1.2 Sodium hydrogen carbonate stock solution (Solution C)

Sodium hydrogen carbonate was dissolved in Milli-Q water, autoclaved one time at 121 °C for 20 min and later added to the sterile artificial seawater medium through a filter with a pore size of 0.22 micrometer (µm).

Table 2 Sodium hydrogen carbonate is used in the medium to buffer the pH of the medium.

Chemical substance	g L ⁻¹	Final concentration in chemostat medium [mM]
NaHCO ₃	90	119
Dest H ₂ O	Add to 1000 mL	

2.2.1.3 Iron(III) chloride stock solution (Solution D)

Iron(III) chloride was dissolved in sulfuric acid and added via a 0.22 µm pore size filter to the sterile artificial seawater medium after it had been cooled to room temperature.

Table 3 Iron(III) chloride in the medium serves as iron source needed for some enzymes.

Chemical substance	mg	mL ⁻¹	Final concentration in medium [µM]
FeCl ₃ x 7 H ₂ O	2		4.86
H ₂ SO ₄ (0.1 N)	1 mL		

2.2.1.4 Potassium phosphate stock solution (Solution E)

Potassium phosphate was dissolved in Milli Q water and added via a 0.22 µm pore size filter to the sterile artificial seawater medium after it had been cooled to room temperature.

Table 4 Potassium phosphate in the medium serves as phosphate source.

Chemical substance	g	L ⁻¹	Final concentration in medium [mM]
KH ₂ PO ₄	5		3.67
Dest H ₂ O	Add to 100 mL		

2.2.1.5 Selenite-tungstate solution (Widdel and Bak, 1992)

A stock solution was prepared with 100 mL boiled and N₂ gas flushed Milli Q water.

Table 5 Selenite-tungstate solution as supplements (Widdel and Bak, 1992)

Chemical substance	mg L ⁻¹	Final concentration in medium [mM]
NaOH	500	0.05
Na ₂ SeO ₃ x H ₂ O	3	0.000064
Na ₂ WO ₄ x 2H ₂ O	4	0.000048
Dest H ₂ O	Add 1000 mL	

2.2.1.6 Thiosulfate stock solution (Solution B)

Sodium thiosulfate was dissolved in Milli Q water and added via 0.22 µm pore size filter to the sterile artificial seawater medium after it had been cooled to room temperature and its pH adjusted to 7.

Table 6 Sodium thiosulfate in the medium serves as electron donor for *S. denitrificans*.

Chemical substance	g	L ⁻¹	Final concentration in medium [mM]
Na ₂ S ₂ O ₃ x 5 H ₂ O	10	40	
Dest H ₂ O	Add to 40 mL		

2.2.2 Batch culture experiments to study growth of *Sulfurimonas denitrificans* with either thiosulfate or octo-sulfur as electron donor.

This paragraph was published in (Götz, Pjevac, et al., 2018).

For the batch culture experiments, *S. denitrificans* was grown at 22°C in 2 L pyrex bottles containing 1 L of the anaerobic seawater medium (Timmer-ten Hoor, 1975) sealed with butyl rubber stoppers and purged with N₂:CO₂ (80:20, 1.1 atm). Two replicate cultures with thiosulfate at a final concentration of 40mM (T-1, T-2) and three replicate cultures in which case thiosulfate was substituted with 5 g L⁻¹ of pure octa-sulfur (S₈) (S₈-1, S₈-2, S₈-3) were set up. The S₈ was generated by Dr. Petra Pjevac at the University of Vienna (Austria) by dissolving zero-valence sulfur (S⁰) powder in CS₂ and subsequent precipitation by evaporation of CS₂ (Steudel and Eckert, 2003; A. Kamyshny, unpublished). Insoluble S₈ precipitates were ground, resuspended in water, and immediately added to the culture flasks.

2.2.3 Chemostat experiments to study the proteomic response of *Sulfurimonas denitrificans* to substrate limitation as well as the presence of oxygen and hydrogen.

Open parts of the chemostat were covered with aluminum foil before autoclaving. All chemostat vessels, connectors, lines and parts were autoclaved prior to the experiment at 120°C for 20min. For each of the three chemostats, 2 L of anaerobic artificial seawater medium was prepared separately in a 2 L Pyrex bottle. To avoid any contaminations, the system was assembled as cleanly as possible using a Bunsen burner and 70% ethanol on autoclaved connectors (Figure 2). The pH of the medium was adjusted to approximately 7 after adding all solutions except sodium thiosulfate. The chemostat was run under anaerobic conditions using the N₂:CO₂ (80:20) gas mixture that was continuously applied to the chemostat system (Figure 2). The dilution rate of the chemostat was set to be between 0.87 and 0.89 d⁻¹.

From the chemostat, subsamples were taken during steady state conditions (constant growth rate in addition to constant physicochemical conditions) for proteomic analysis. Steady state conditions were determined by cell counting (2.2.4) to determine a constant growth rate and ion chromatography to determine constant substrate concentrations (2.2.5). The chemostat experiments were run under four conditions: 1) nitrate limitation (5 mmol L⁻¹ NO₃: 6 mmol L⁻¹ S₂O₃), 2), thiosulfate limitation (12 mmol L⁻¹ NO₃: 8 mmol L⁻¹ S₂O₃), 3) hydrogen with nitrate, and 4) oxygen with thiosulfate. The experiments with hydrogen and oxygen were performed by Dr. Jesse McNichol, at the time a PhD student in the laboratory of Dr. Sievert. Chemostat experiments with hydrogen were performed under a fume hood and during experiments with oxygen, the oxygen concentration was monitored using an optode (Pts3, Presens, Germany).

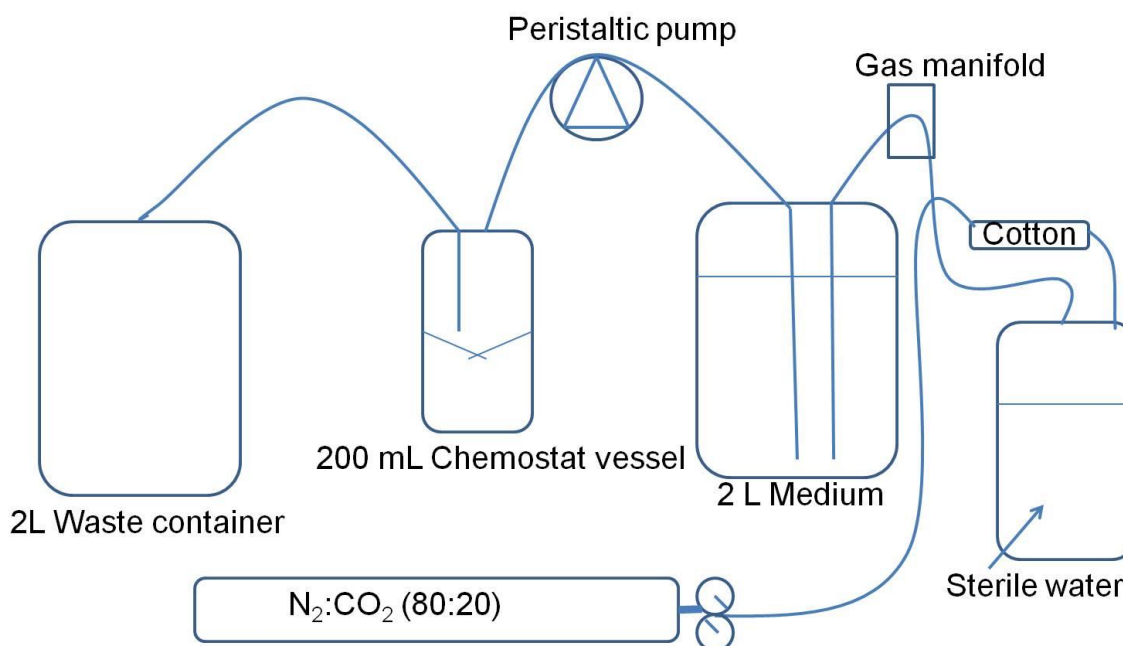


Figure 2 Schematic design of the used chemostat system. Incoming gas was filtered through cotton and sterile water before it was further directed into the 2 L medium tanks. Medium was pumped into the chemostat through a peristaltic pump. The gas was continuously redirected from the headspace of the medium tank into the chemostat and further to the waste container.

2.2.4 Cell counts using 4,6 Diamidin-2-phenylindol (DAPI)

Cell numbers were monitored daily using an established DAPI (4,6 Diamidin-2-phenylindol; excitation at 359nm and emission at 461nm in the blue spectra) staining method to visualize the cells under a fluorescence microscope at 1,000x magnification (Zeiss Axioscope). For that, two DAPI stained filters were prepared per sample / chemostat and for each filter 10 squares (100 x 100 μm) counted. For the fixation of the cells, 40 μL formaldehyde and for the staining 50 μL of a 200 pg mL^{-1} DAPI solution were added to 20-500 μL of the culture. Sterile filtered 1xPBS (phosphate buffered saline) buffer was used to bring the final volume to 2 mL.

The suspension was stained for 5 min and filtered through black 0.2 μm pore size Millipore filters using a vacuum pump. The filter was washed one time with sterile 1x PBS buffer, before the filter was mounted on a microscope slide on top of a drop of immersion oil. Another drop of oil was added on the filter and then a glass cover was put on top.

2.2.5 Analysis of ΣNH_3 , Nitrate, Nitrite, Sulfate, and Thiosulfate by Ion Chromatography

To ensure steady state and limitation conditions in the medium, the concentrations of nitrate, nitrite, ΣNH_3 , sulfate, and thiosulfate were measured by ion chromatography (IC) using a Dionex DX-500 IC System. Samples were diluted with MilliQ water before determining the concentration of anions (NO_3^- , NO_2^- , $\text{S}_2\text{O}_3^{2-}$ and SO_4^{2-}) and cations (ΣNH_3). Anions were chromatographically separated using a Dionex IonPac AS15 column and carbonate removal cartridge (Dionex CRD200) run isocratically with eluent consisting of 50% MilliQ water and 50% 75mM NaOH flowing at 1.2 mL/min. Carbonate removal is essential in getting accurate measurement for NO_2^- because both elute at around the same time. Cations were chromatographically separated using Dionex IonPac CS12A column run isocratically with eluent made up of 77% DI water and 23% 100mM H_2SO_4 flowing at 1.0 mL/min. Both anion and cation analyses were run in suppressed conductivity mode for increased sensitivity (suppressor current of 300 mA and 125 mA for anions and cations, respectively). Analytical uncertainty (2σ) was less than $\pm 3\%$.

2.2.6 Proteomic analysis of *Sulfurimonas denitrificans*

This paragraph was published in (Götz, Pjevac, et al., 2018).

For proteomics, 100 mL culture was harvested by centrifugation at 7,000 x g for 7 min at 20 °C in 50 mL centrifugation tubes. For transcriptomics, 100 mL culture was filtered onto 0.2 μm Teflon filters and immediately immersed in RNA later and stored at -20°C.

2.2.6.1 Protein isolation

This paragraph was published in (Götz, Pjevac, et al., 2018).

For the isolation of proteins, cell pellets were resuspended in 1 mL 1x Tris-EDTA (TE) buffer (pH 8; Sigma-Aldrich, St. Louis, MO, USA), containing cOmplete™ Protease inhibitor (Roche, Basel, Switzerland). To lyse cells, the suspensions were sonicated three times for 30 sec at 5 x 10% amplitude using the Sonoplus HD2070 sonication probe (Bandelin, Berlin, Germany). The obtained crude extracts were centrifuged for 10 min at 15,500 x g at 4°C. The raw protein extracts (supernatants) were concentrated by means of Amicon tubes (Ultra-15 3 kDa cutoff Merck Millipore, Kenilworth, NJ, USA), which were centrifuged for 30-60 min at 5,000 x g and 4°C as described in the manufacturer's instructions. Protein concentrations were determined using the Roti-Nanoquant protein assay (Carl Roth, Karlsruhe, Germany) as instructed by the manufacturer. Subsequently, 4 x loading buffer (200 mmol L⁻¹ Tris-HCl pH

6.8, 50 mmol L⁻¹ EDTA pH 8.0, 40 % glycerol, 8 % SDS, 0.08 % bromophenol blue, 1 mmol L⁻¹ dithiothreitol) was added to aliquots of ~25 µg protein, and samples were denatured for 10 min at 90°C. The denatured extracts and a Roti-Mark standard (Roti-Mark STANDARD, Carl Roth, Karlsruhe, Germany) were transferred onto a polyacrylamide SDS mini gel (10% Mini-PROTEAN, TGX Stain-free, BioRad, Hercules, CA, USA) and run approximately 20 min at 50 V and another 35 min at 150 V. The gel was fixed for 30 min in an ethanol: acetic acid: water (40:10:50) solution. The gel was stained overnight in a Coomassie Brilliant Blue (CBB) staining solution and further de-stained in distilled water.

2.2.6.2 Protein digestion

Parts of the protocol were published in (Götz, Pjevac, et al., 2018).

The proteins were extracted following the protocol described in section 2.1.5.

2.2.6.3 Mass spectrometry and proteome analysis (Götz, Pjevac, et al., 2018)

Parts of the protocol were published in (Götz, Pjevac, et al., 2018).

Peptide mixes were separated via chromatography on a reversed phase C18 column in a nano-ACQUITY-UPLC (Waters Corporation, Milford, MA, USA) as described by Otto *et al.* (2010). Mass spectrometry (MS) and MS/MS data were recorded with an online-coupled LTQ-Orbitrap mass spectrometer (Thermo Fisher Scientific Inc., Waltham, MA, USA). MS data were searched against a forward-decoy *S. denitrificans* protein database (Refseq Genome project: NC_007575.1, NCBI [National Center for Biotechnology Information]), which also included common laboratory contaminants, using Sequest (Thermo Fisher Scientific, San Jose, CA, USA; v 27.11). The protein false discovery rate (FDR) was 0.0% for all samples, with the exception of one technical replicate of T-1, in which case the FDR was 0.2%. Identifications were filtered in Scaffold (<http://www.proteomesoftware.com>) using the “Sequest” filter settings described by Heinz *et al.*, (2012). The total spectral count values of all proteins were exported for calculation of the normalized spectral abundance factors (NSAF, Zybailov *et al.*, 2006), which are given in Supplement Table 2 for the S₈ and thiosulfate replicates and for thiosulfate limitation, nitrate limitation, hydrogen and oxygen replicates in Supplement Table 3. The average of the NSAF and the standard deviation were calculated for the three biological replicates for S₈ (S₈ 1-3). For thiosulfate replicates, only two biological replicates were available (T-1 and T-2). However, two technical replicates were run for sample T-1 to assess the variability between runs. The NSAFs of the two technical replicates were averaged before being

averaged with the second biological replicate T-2 for statistical analyses. PSI-BLAST and DELTA-BLAST (Boratyn *et al.*, 2012) were used for domain analysis of hypothetical proteins. Further, the tools BOCTOPUS (boctopus.bioinfo.se) and PRED-TMMB (<http://bioinformatics.biol.uoa.gr///PRED-TMBB>) were used to search for beta-barrel topology. To detect signal peptides, SignalP 4.0 (<http://www.cbs.dtu.dk/services/SignalP/>) was used. The mass spectrometry proteomics data for S₈ (1-3) and the two thiosulfate replicates (T1-2) are available through the ProteomeXchange Consortium (<http://proteomecentral.proteomexchange.org>) via the PRIDE partner repository (Vizcaíno *et al.*, 2016) with the dataset identifier PXD009127.

2.2.6.4 RNA extraction, transcriptome sequencing and analysis (performed by Dr. Petra Pjevac, University of Vienna, Austria)

This paragraph was published in (Götz, Pjevac, et al., 2018).

The membrane filters with the cells were cut in pieces, put in a microcentrifuge tube containing extraction buffer provided with the mirVana miRNA isolation kit (Ambion, Carlsbad, CA, USA), and subjected to bead-beating. Subsequently, total RNA was extracted using the mirVana miRNA isolation kit, with subsequent turbo DNase (Ambion) treatment and purification with the Qiagen RNAeasy kit (Qiagen, Hilden, Germany) according to the manufacturers' instructions. Ribosomal RNA was not depleted. Total RNA extracts were sent to the Max Planck Genome Centre (Cologne, Germany) for preparation of RNAseq-libraries and subsequent sequencing of paired-end (2 x 150 bp) reads in the HiSeq2000 (Illumina). Sequencing statistics are provided in Table 7. Sequence reads were quality trimmed at a Phred score of 28 using the bbdduk function of BBMap v35.82 (<https://sourceforge.net/projects/bbmap/>), and mapped to a reference file of all open reading frames (ORFs) deposited in NCBI for the *S. denitrificans* genome (NCBI project NC_007575.1) using the bbmap function of BBMap v35.82. Sequences were mapped as paired reads with a minimal identity of 99%. For comparison between cultures, read counts were transformed to transcripts per million (TPM) values as described in Li *et al.* (2010). The transcriptome sequence data has been deposited in the European Nucleotide Archive (ENA) under the project accession number PRJEB25508.

Table 7 Transcriptomic data collected before and after quality control (QC). S₈-1-3 are the biological replicates of Sulfurimonas denitrificans grown with cyclooctasulfur and T-1 and T-2 are the two biological replicates grown with thiosulfate. Published in (Götz, Pjevac, et al., 2018).

Library	Reads total	Bases total	Reads after QC	Bases after QC	Mapped reads	% mapped
S ₈ -1	1.09E+07	1.64E+09	1.03E+07	1.09E+09	9.51E+06	93%
S ₈ -2	7.85E+06	1.18E+09	7.09E+06	7.10E+08	6.57E+06	93%
S ₈ -3	9.61E+06	1.44E+09	8.58E+06	7.72E+08	7.98E+06	93%
T-1	9.18E+06	1.38E+09	8.31E+06	8.38E+08	7.69E+06	92%
T-2	1.06E+07	1.58E+09	9.56E+06	9.67E+08	8.68E+06	91%

2.2.6.5 Statistical analysis

Parts of the protocol were published in (Götz, Pjevac, et al., 2018).

To test for statistically significant differences between the two (S₈ and T1-2) different growth conditions, the NSAFs and TPMs of all biological replicates of each growth conditions were used as the input parameters to calculate P-values based on the Welch's t-Test. Due to the small number of biological replicates available for the thiosulfate treatment (n=2), the Welch's rather than the Student's t-Test was selected, as a more stringent manner to statistically evaluate differences in gene transcription and protein expression between the two conditions. The student's t-Test was also used for a comparison of chemostat samples that were nitrate-limited (NL) and thiosulfate-limited (TL). Transcripts and proteins with a P-value smaller than 0.05 were considered to be statistically significantly different between the two conditions.

3 Results

3.1 MetaOmics analysis on Crab Spa diffuse-flow hydrothermal vent fluids

3.1.1 Taxonomic composition

The taxonomic composition of the seafloor microbial community of the deep-sea diffuse-flow vent Crab Spa was analyzed based on the single conserved taxonomic marker gene coding for 16S rRNA, as well as on a functional level based on the taxonomic affiliation of the metabolic genes and their proteins contained in the metagenome and the metaproteome, respectively (Figure 3 and Figure 4). All three approaches identified the three campylobacterial genera *Sulfurimonas*, *Sulfurovum* and *Arcobacter* as the dominant community members.

At the 16S rRNA level, each dominant genus was represented by hundreds of different OTUs (operational taxonomic units) (Table 8). The highest number of OTUs was found for *Sulfurovum* (LVP2=1,863, LVP4=1,6671), followed by *Sulfurimonas* (LVP2= 367, LVP4=318), and *Arcobacter* (LVP2= 552, LVP4=380). However, for each genus only three to eight OTUs were represented by more than 30 reads, indicating that the communities were dominated by a few species of each genus.

Table 8 Summary of numbers of 16S rRNA, genes and identified proteins for the three most abundant genera in Crab Spa (*Sulfurimonas*, *Sulfurovum* and *Arcobacter*)

Organism	16S rRNA LVP2	16S rRNA LVP4	Genes LVP2 (295,524 genes total)	Genes LVP4 (170,835 genes total)	Identified Proteins LVP2	Identified Proteins LVP4
<i>Sulfurimonas</i>	367	318	42,013	19,287	527	381
<i>Sulfurovum</i>	1,863	1,671	41,153	33,128	386	723
<i>Arcobacter</i>	552	380	28,394	14,616	258	233
	NCBI Genes	SAGs Genes	Identified Proteins NCBI		Identified Proteins SAGs (single cell genomes)	
<i>Sulfurimonas</i>	7,039	6,123	52		114	
<i>Sulfurovum</i>	4,610	11,828	35		217	
<i>Arcobacter</i>	5,226	2,501	18		43	

3.1.2 Metagenome: Metabolic potential

The metagenomes were analyzed to assess the metabolic potential of the studied microbial communities. These metagenomes were then compared to the actually expressed proteins identified through metaproteomic analyses. A total of 295,524 and 170,835 genes were identified in the metagenomes of LVP2 and LVP4, respectively, with ~38% of the genes (111,560 genes in LVP2; 67,031 genes in LVP4) belonging to the three dominant genera *Sulfurovum*, *Sulfurimonas* and *Arcobacter* (Table 8). Besides genes coding for ribosomal proteins and for the ATP synthase, which are markers of general activity, key genes that are involved in chemolithoautotrophic metabolism were among the most abundant genes (Figure 3). Of the chemolithoautotrophic key genes, 90% were assigned to *Campylobacteria*. Within the most abundant genes, reductive TCA cycle genes of the carbon fixation pathway were the most dominant, with most genes classified to *Campylobacteria*. One of the key genes of the rTCA cycle, the ATP citrate lyase, was present in high abundance. However, no ATP citrate lyase genes were identified for the genus *Arcobacter*. Key genes for other carbon fixation pathways were detected only in low abundance, mostly ribulose 1,5 bisphosphate carboxylase (RuBisCO) for carbon fixation encoded by Archaea. For respiratory processes, genes coding for the *cbb₃* cytochrome oxidoreductase involved in aerobic respiration and the periplasmic nitrate reductase (*napAB*), catalyzing the first step of either denitrification or DNRA (dissimilatory reduction of nitrate to ammonium), were the most abundant, with both being present in approximately equal abundance. In addition, the genes coding for the subsequent steps of the denitrification pathway, i.e., nitrite reductase (*nirS*), nitric oxide reductase (*norBC*) and nitrous oxide reductase (*nosZ*), and DNRA pathway, i.e., *napC*, were all present in roughly the same abundance, albeit in lower abundance than *napAB*. All genes indicative of aerobic respiration and denitrification were predominantly assigned to *Campylobacteria*. Furthermore, a polysulfide/thiosulfate reductase mostly assigned to *Sulfurimonas* could be identified, as well as adenylylsulfate reductases (*apr*) genes. Sulfide quinone reductase genes (*sqr*), genes coding for the sulfur oxidation multienzyme complex (Sox system), and the *apr* gene indicative of the reverse DSR pathway could be identified as marker genes coding for proteins involved in the oxidation of electron donors, with *sqr* being present in higher abundance than the *sox* and *apr* genes. Among the *sox* genes, it is noteworthy that the genes of the *soxABXYZ* cluster were less represented than genes of the *soxCDYZ* cluster (Table 9). Genes of *sqr* and *sox* were predominantly assigned to the campylobacterial genera *Sulfurimonas*, *Sulfurovum*, and *Arcobacter*, while *apr* genes of the reverse DSR pathway were mainly assigned to

Deltaproteobacteria. In addition, the metagenomes revealed the metabolic potential for hydrogen oxidation (*hypF*), mainly encoded by *Sulfurovum* and *Sulfurimonas*.

Table 9 Number of sulfur oxidation genes (SOX) per dominant genus and sample LVP2 and LVP4.

	Sulfurimonas LVP2	Sulfurimonas LVP4	Sulfurovum LVP2	Sulfurovum LVP4	Arcobacter LVP2	Arcobacter LVP4
<i>soxA</i>	2	-	3	4	4	-
<i>soxB</i>	1	-	9	7	12	7
<i>soxC</i>	41	29	22	15	10	5
<i>soxX</i>	-	-	2	2	5	-
<i>soxY</i>	16	3	9	8	3	1
<i>soxZ</i>	7	4	6	5	1	-

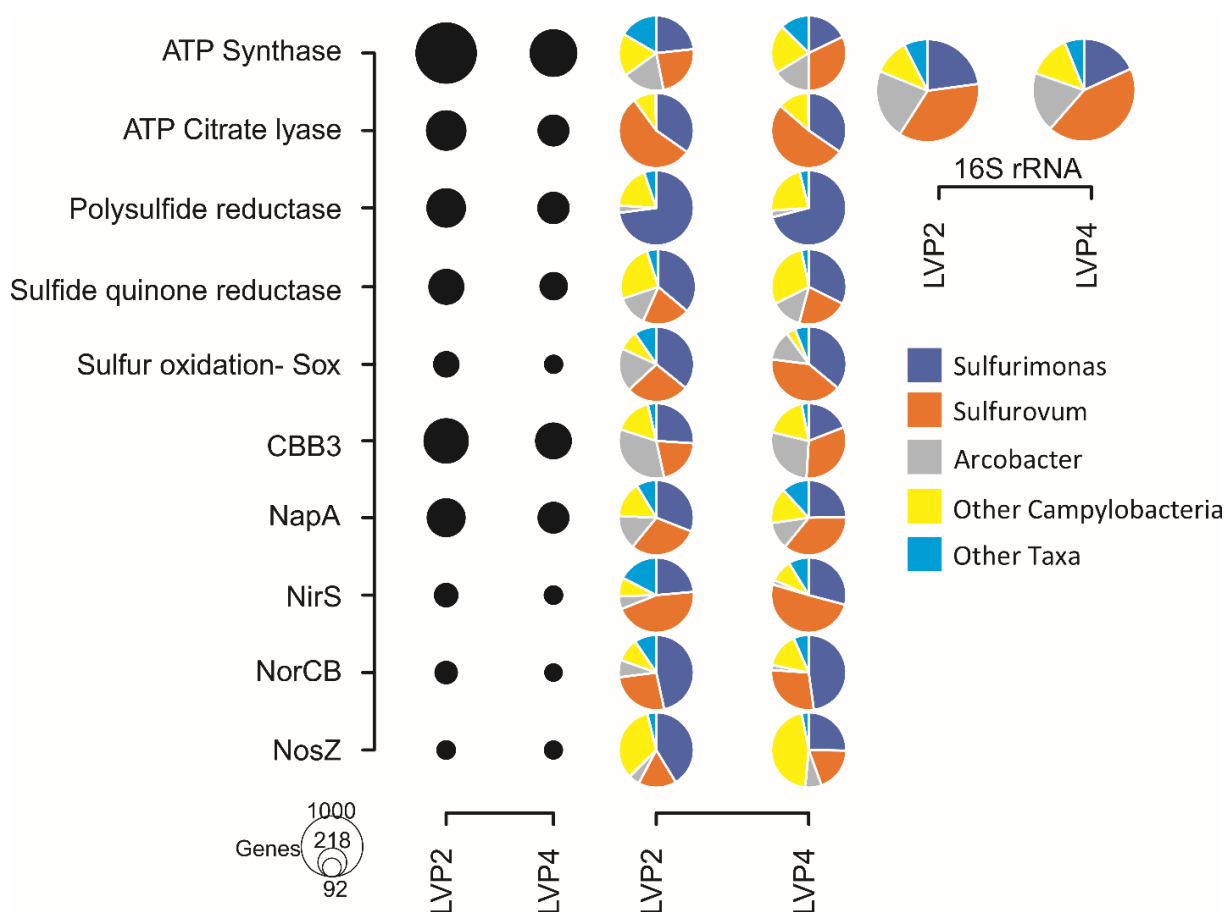


Figure 3 Functional genes of the metagenomes and 16S rRNA diversity of the Crab Spa microbial community of samples LVP2 and LVP4 are shown. Over 90% of the microbial community of Crab Spa is dominated by *Campylobacteria*, which is also mirrored in functional genes of the metagenomes. The Sox system consists of the genes *soxABCXYZ*. CBB3 stands for the *ccb₃* cytochrome oxidoreductase, NapA for nitrate reductase, NirS nitrite reductase, NorCB nitric oxide reductase and NosZ for the nitrous oxide reductase.

3.1.3 Metaproteome: Active community members and their utilized pathways

Metaproteomics was used to identify active pathways utilized by dominant bacterial community members. Combined, 4,466 proteins could be identified from the two metaproteomes (LVP2 and LVP4). Functions were assigned to 3,943 proteins, leaving 524 hypothetical proteins with unknown functions (Figure 4). LVP2 and LVP4 shared 70% of the identified proteins. 68% (1669/2445) and 65% (1777/2725) of all proteins were detected in more than one technical replicate of LVP2 and LVP4, respectively. As in the metagenome, the three genera that dominated the metaproteome were *Sulfuriomonas*, *Sulfurovum*, and *Arcobacter*, accounting for 56% of the identified proteins (2,508/4,466). The remaining 44% of the identified proteins (1,958/4,466) classified mainly to other campylobacterial genera, such as *Caminibacter*, *Nautilia*, *Nitratiruptor*, *Nitratifractor*, *Sulfuricurvum*, *Sulfurospirillum*, and *Thioreductor* (18% = 795/4,466) as well as to a lesser extent to various other taxa, including *Alpha*-, *Beta*-, *Gamma*- and *Deltaproteobacteria*, *Bacteroidetes*, *Archaea* and also viruses.

The effectiveness of the three components of the combined target-decoy database (single cell genomes, metagenomes, and reference genomes of cultured organisms) to identify proteins was determined for the three most dominant genera (*Sulfurimonas*, *Sulfurovum*, *Arcobacter*) by calculating the ratio of number of genes assigned to each genus in comparison to the number of identified proteins (Table 10). Here, a low ratio means it took fewer genes to identify one protein, and it can be seen that the single cell genomes provided the best identification rates for all three genera. Both metagenomes and the single cell genomes provided a better identification rate in comparison to the NCBI reference genomes of cultured organisms (Table 10).

Table 10 Identification rates of proteins based on available genomic information divided by the number of identified proteins (Genes:Proteins). This value represents the ratio of genes that identified one protein. This value can be used as a measure of how the used database represented the active community of a system.

Organism group	Metagenome Genes:Protein	Single Cell Genomes Genes:Protein	NCBI genomes Genes:Protein
Sulfurimonas	68	54	135
Sulfurovum	67	55	132
Arcobacter	88	58	290

Both metaproteomes shared similar relative abundance profiles of the identified proteins in different categories and their taxonomic assignments (Figure 4). Ribosomal proteins and ATP synthase, which are general markers for cellular activity, are the most abundant protein groups in the metaproteome. All ribosomal proteins were classified to *Campylobacter* (Figure 4), while only a small fraction of ATP synthase proteins were classified to taxa other than *Campylobacter* (Figure 4).

Proteins of the reductive tricarboxylic acid cycle (rTCA cycle) were among the most abundant proteins, with the identified ATP citrate lyase being the second most abundant protein next to ATP synthase (Figure 5). No proteins indicative of carbon fixation pathways other than the rTCA cycle were detected. In comparison to ribosomal proteins, rTCA cycle enzymes showed a different taxonomic distribution, as only a small fraction could be classified to *Arcobacter*. The ATP citrate lyase was primarily dominated by *Sulfurimonas* and *Sulfurovum*, followed by various other *Campylobacter* (Figure 5). No ATP citrate lyase proteins were classified as *Arcobacter*, in line with the metagenomic analysis.

The metaproteome identified denitrification and microaerobic respiration via the *cbb*₃ cytochrome oxidoreductase as the two main respiratory processes. All denitrification enzymes are present in the metaproteomes, with the nitrate reductase (NapA) and the nitrite reductase (NirS) being present in higher relative abundance compared to the nitric oxide reductase (NorBC) and nitrous oxide reductase (NosZ). However, it has to be kept in mind that NorBC is most likely underrepresented in the metaproteome, as membrane bound enzymes are not extracted with the same efficiency as soluble proteins by the used extraction procedure. Among Nap and NirS proteins, the genus *Sulfurovum* was highly represented, but it was less represented among NorBC and NosZ proteins. On the other hand, the genus *Sulfurimonas* was less represented among Nap proteins and most highly represented among NirS and NosZ, while NorBC was dominated by other *Campylobacter*. While *Arcobacter* was identified in low abundance among the NapA and NirS proteins, it was not represented among NorBC. However, *Arcobacter* was found in higher relative abundance among the *cbb*₃-type cytochrome oxidoreductase proteins (CBB₃).

In contrast to the metagenome, only a small number of proteins indicative of sulfur metabolism were identified. Both the sulfide quinone reductase (Sqr) and enzymes of the sulfur oxidation complex (SOX) were present in low relative abundance (<0.1% NSAF). Among the Sox proteins, only SoxCZY of the SoxCDY₂Z₂ operon were identified. While Sqr was identified in similar abundance between *Sulfurovum*, *Sulfurimonas*, and other *Campylobacter*, Sox

proteins were mainly classified as *Sulfurovum*. In addition, adenylylsulfate reductase predominantly of gammaproteobacterial origin was identified in low relative abundance. Multiple thiosulfate/polysulfide reductases were present at a higher relative abundance and in line with the metagenome mainly assigned to *Sulfurimonas*. No other enzymes known to be involved in the sulfur metabolism of chemolithoautotrophs could be identified.

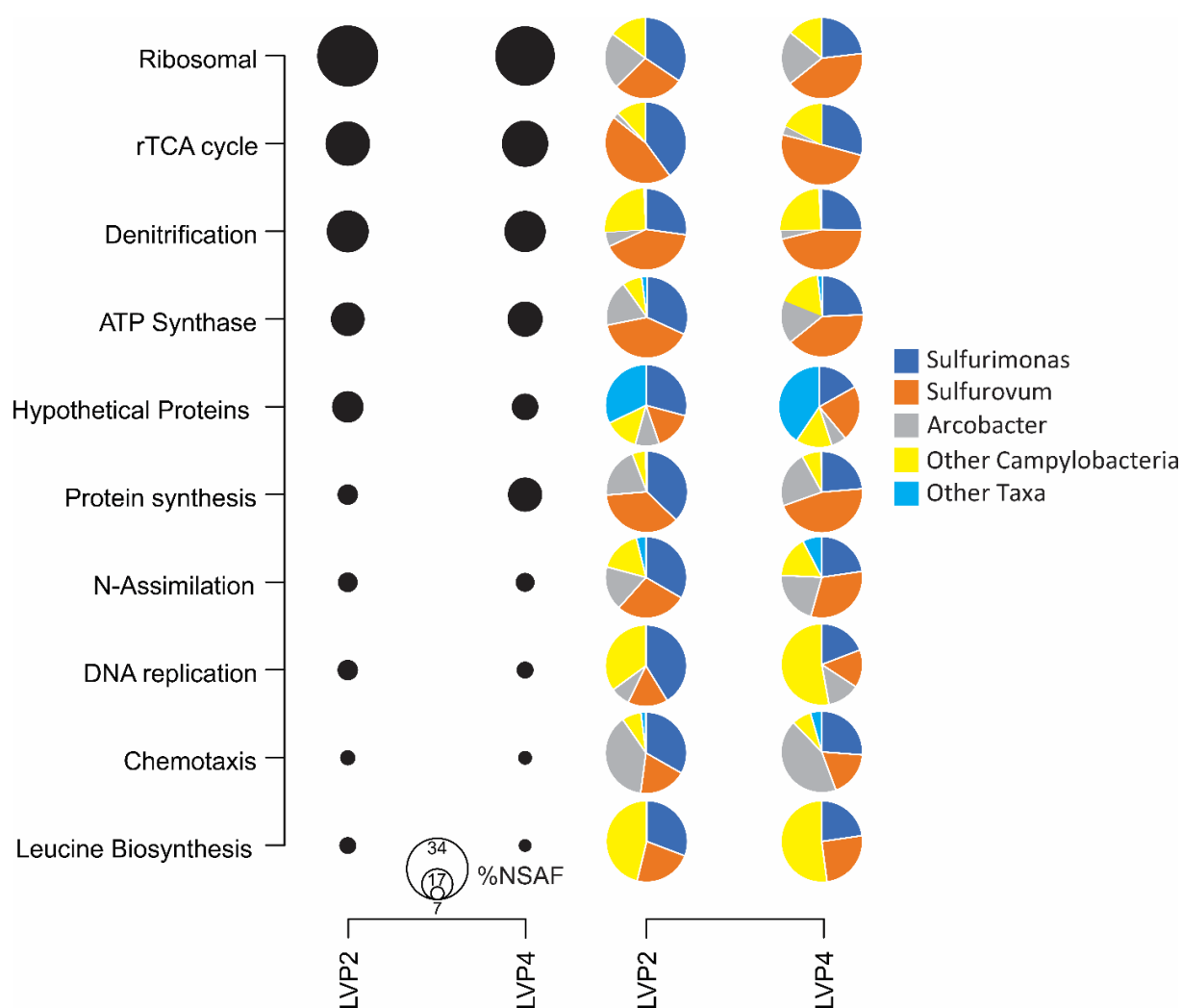


Figure 4 Bubble chart including the abundance and taxonomic differentiation of the most abundant pathways at Crab Spa. The black bubbles indicate the abundance with different radii, that represent the percentage of the normalized spectral abundance factor (%NSAF) for LVP2 and LVP4. Pie charts show the distribution of different taxa within these protein groups. The hypothetical proteins show the highest variability in taxa (turquoise) compared to all other abundant protein groups that are mainly dominated by *Sulfurimonas* (blue), *Sulfurovum* (orange), *Arcobacter* (grey) and other Camylobacteria (yellow- including e.g. Thioreductor, Nitratiraptor, Nitratiraptor).

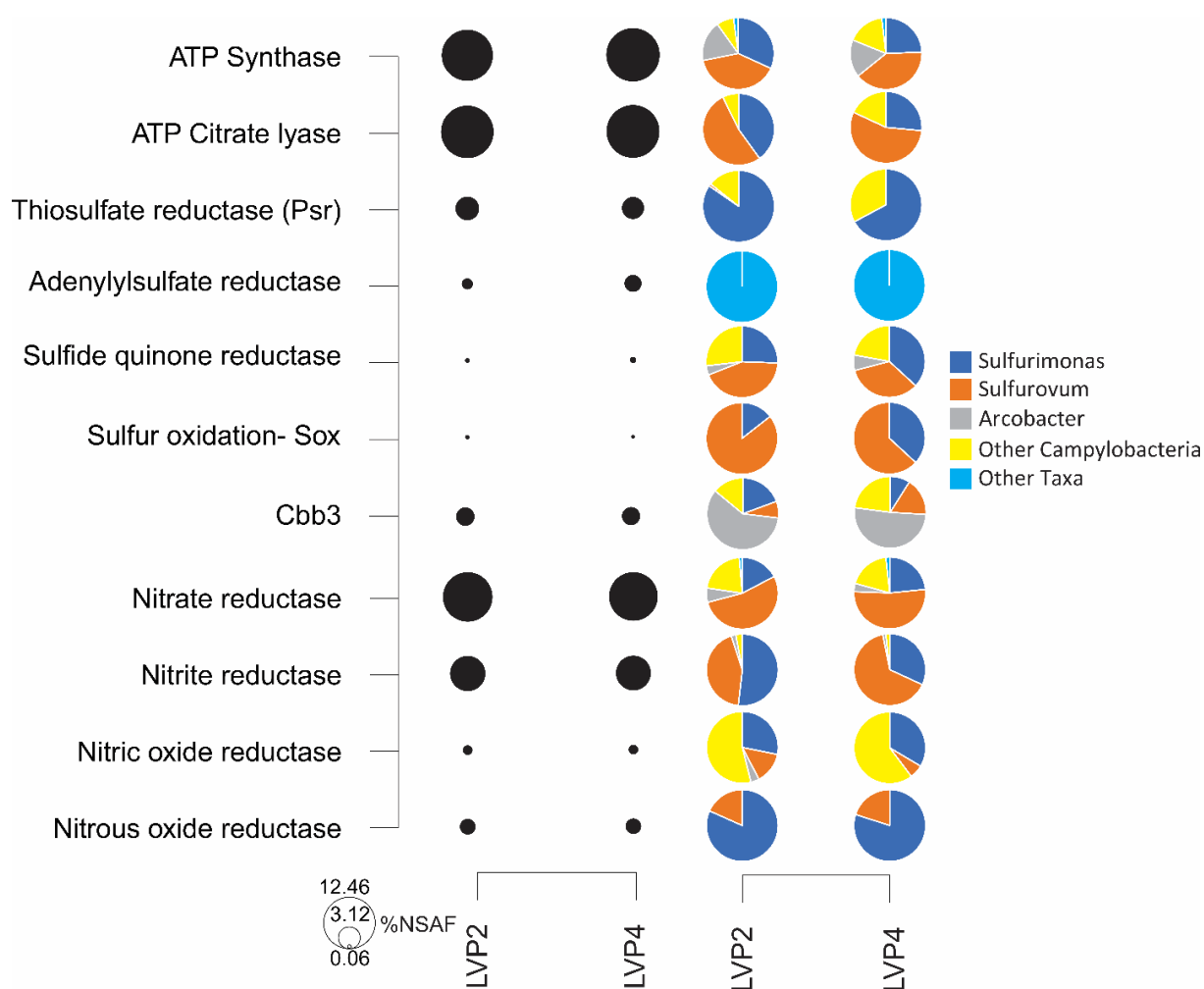


Figure 5 This bubble chart shows the abundance of enzymes involved in the energy metabolism of the Crab Spa most abundant community members. The most abundant enzymes presented are the ATP-synthase, ATP citrate lyase, Nitrate reductase and Nitrite reductase, all mostly dominated by *Sulfurimonas* and *Sulfurovum* species.

3.1.4 Comparison of the metaproteomic profiles between the three dominant genera of Crab Spa

In order to portray the most abundant protein categories for each dominant genus, the organism-specific normalized spectral abundance factor (OrgNSAF) was calculated (Figure 6). This calculation provides a direct comparison of the three dominant genera and their identified protein groups, allowing the identification of traits that might differentiate them from each other. Based on this analysis, there seems to be no obvious difference between the genera *Sulfurimonas* and *Sulfurovum*, besides the presence of the thiosulfate/polysulfide reductase in *Sulfurimonas*. The rTCA cycle and denitrification pathway were most dominant, with an average OrgNSAF of 18% and 13% in *Sulfurimonas* and 19% and 17% in *Sulfurovum*, respectively.

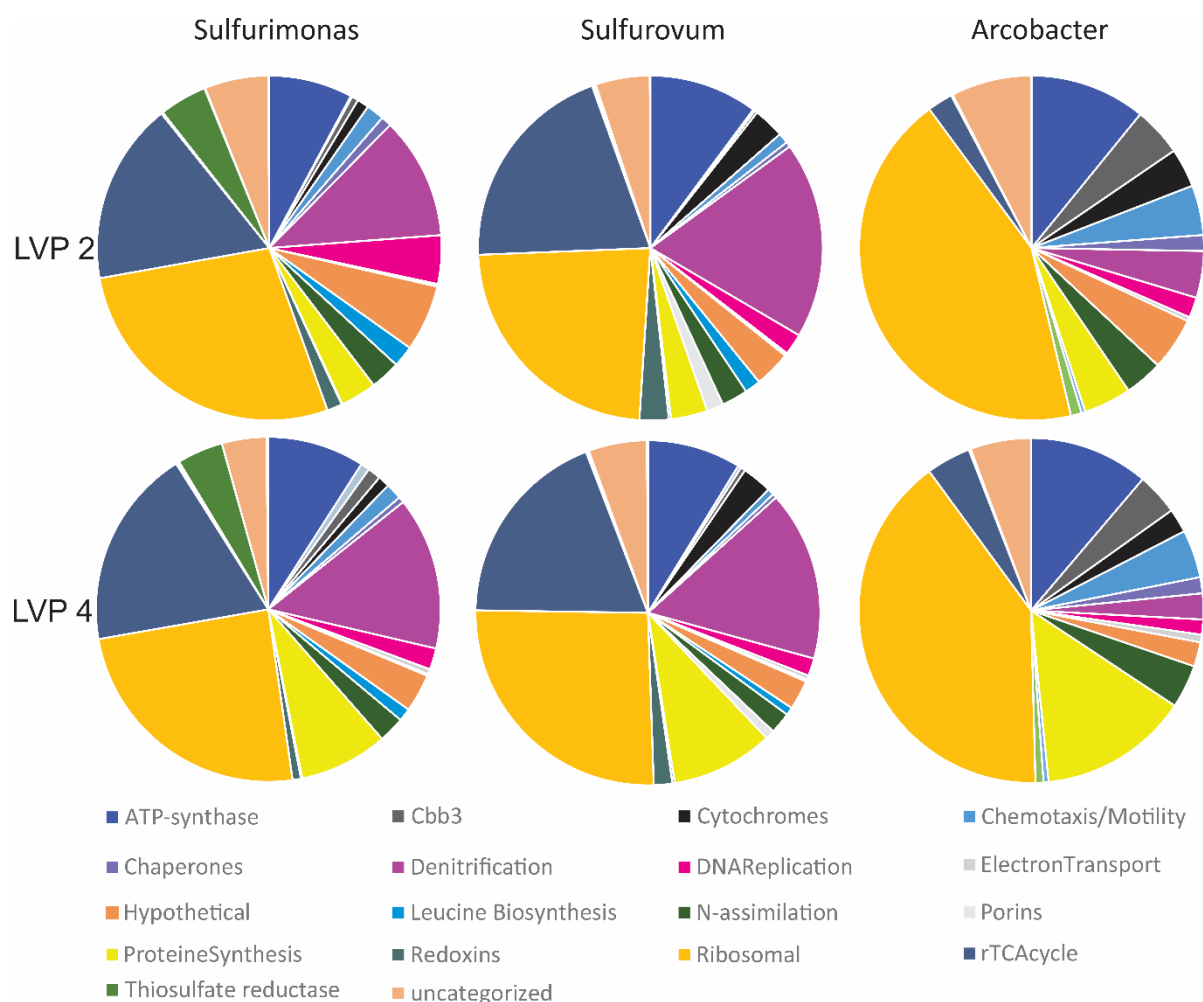


Figure 6 Pie-Charts that show protein categories normalized to 100% to the three most abundant genera (*Sulfurimonas*, *Sulfurovum* and *Arcobacter*) with organism specific normalized spectral abundance factors (OrgNSAF). The protein category distribution in *Sulfurimonas* and *Sulfurovum* is similar but differs in comparison to *Arcobacter*. Thiosulfate reductase proteins are only found in *Sulfurimonas* species and not in *Sulfurovum* or *Arcobacter*. The rTCA cycle and denitrification pathway are over 10% more abundant in *Sulfurimonas* and

Sulfurovum than in *Arcobacter*. The Cbb3 cytochrome c oxidoreductase is 3% more abundant as well as ribosomal proteins which are 20% more abundant in *Arcobacter*.

In comparison, the OrgNSAF profile was quite different for *Arcobacter*. The relative abundance of ribosomal proteins was about 17% higher compared to the other two genera. In addition, the OrgNSAFs for *Arcobacter* for the denitrification pathway and for the rTCA cycle were only 3%, and the OrgNSAF of the cbb₃ cytochrome oxidoreductase was 3% and 3.5% higher in comparison to *Sulfurimonas* and *Sulfurovum*, respectively.

Generally, motility proteins, which were present in the metaproteomes at a total of 2% NSAF (Figure 4), were more highly represented within the *Arcobacter* genus compared to *Sulfurimonas* and *Sulfurovum*. Specifically, the three dominant genera differ in their representation of proteins of the chemotaxis apparatus and flagellar proteins, with flagellar proteins being more highly represented in *Arcobacter* and proteins of the chemotaxis apparatus being more highly represented in *Sulfurimonas* and *Sulfurovum* (Figure 7).

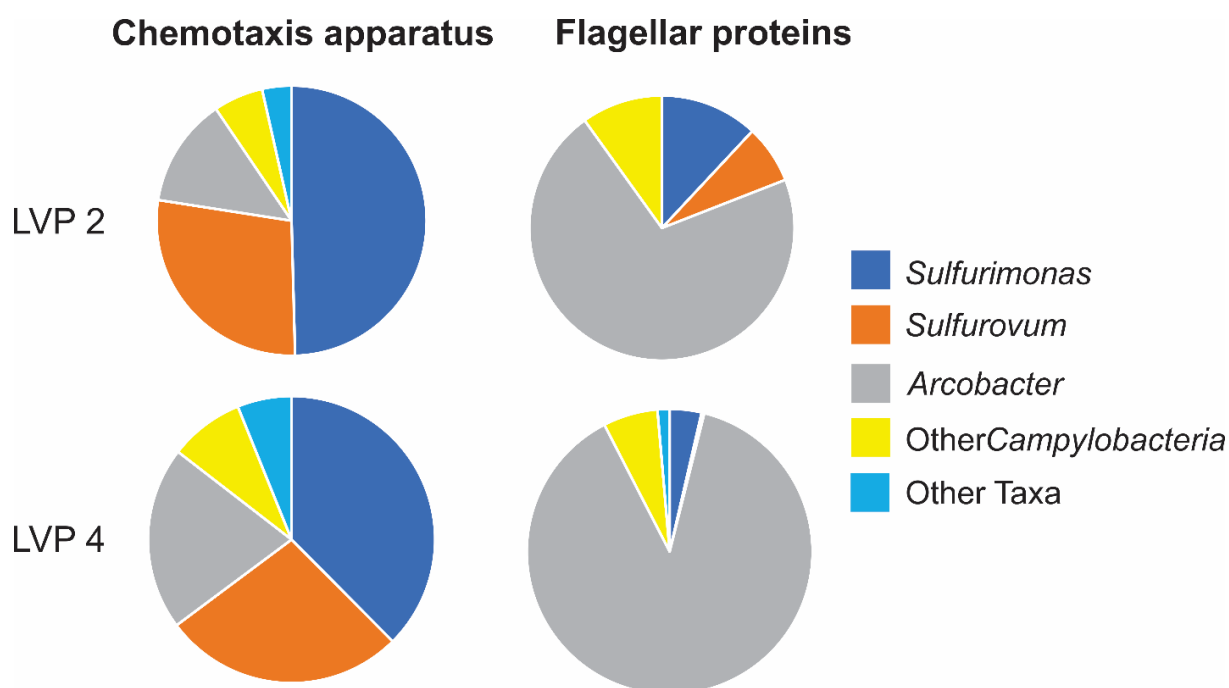


Figure 7 Taxonomic distribution in identified Chemotaxis apparatus and Flagellar proteins (total chemotaxis proteins 2.35 % normalized spectral abundance factor in LVP2 and 1.95%NSAF in LVP4). *Arcobacter* species dominate flagellar proteins whereas *Sulfurimonas* and *Sulfurovum* dominate chemotaxis apparatus proteins.

3.2 Chemostat experiments with *Sulfurimonas denitrificans* as a model organism for chemoautotrophy.

After first observations from the metaproteome samples of Crab Spa, it was decided to perform chemostat experiments with a model organism for chemolithoautotrophic *Campylobacteria*, *S. denitrificans*, under nitrate (NL) or thiosulfate limitation (TL), monitoring cell growth and ion concentrations (Figure 8). Previously, this bacterium was also grown in chemostats with hydrogen and nitrate (HN) and thiosulfate with oxygen (TO) by Dr. Jesse McNichol.

3.2.1 Growth and ion concentration in the chemostat of limitation experiments

In thiosulfate limitation experiments (A, B and C) initial thiosulfate concentration started with 5-8 mmol L⁻¹, sulfate concentration 14 mmol L⁻¹ and nitrate concentration 12 mmol L⁻¹. In all three chemostats A, B and C the thiosulfate concentration dropped to zero and increased slightly to around 100-200 μmol L⁻¹ in A and C and 800 μmol L⁻¹ in B (Figure 8). The ratio of sulfate to thiosulfate and nitrate stayed relatively stable in both thiosulfate limitation and nitrate limitation experiments. In nitrate limitation experiments (D, E and F), the initial thiosulfate concentration was 6 mmol L⁻¹, sulfate concentration 13-14 mmol L⁻¹, and nitrate concentration 5 mmol L⁻¹. In all three chemostats D, E and F, the nitrate concentration dropped to zero and stayed stable until the end of the experiment (Figure 8). Samples for proteomic analysis were taken at the last sampling point of the plots in Figure 8.

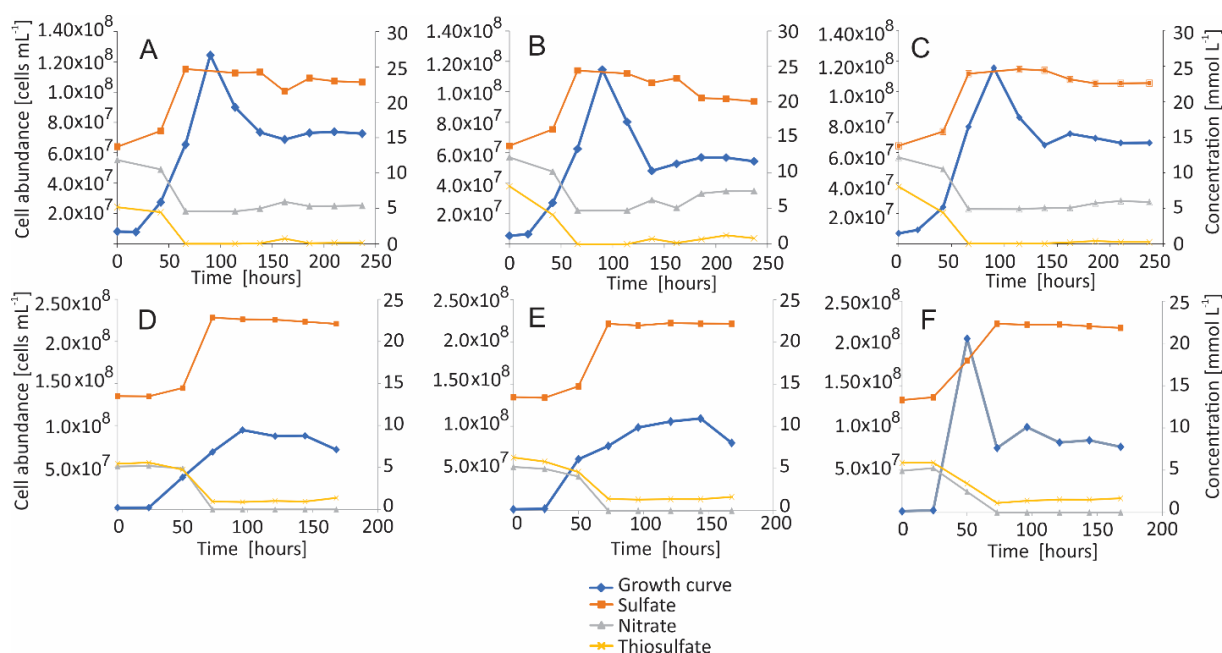


Figure 8 Growth curves are indicated in blue and ion concentrations measured by ion-chromatography are indicated in red (Sulfate), grey (Nitrate) and yellow (Thiosulfate). A, B and C are indicative for three individual chemostats which were run simultaneously under thiosulfate limitation (TL) and D, E and F under nitrate limitation (NL). Steady state conditions were determined by the stable ion concentrations within the medium. Samples for proteomic analysis were taken on the last sampling point.

3.2.2 Proteomics on *Sulfurimonas denitrificans* chemostat cultures

The proteomic profile of *S. denitrificans* was analyzed at four different growth conditions in three chemostats. The focus was on relevant enzymes of the energy metabolism to identify regulatory effects under the different growth conditions (nitrate limitation, thiosulfate limitation, thiosulfate and oxygen, hydrogen and nitrate). The ATP citrate lyase of the central carbon fixation pathway, the rTCA cycle, shows no significant difference between the four conditions. Activity markers such as ribosomal proteins and ATP synthase proteins seem to have a higher abundance when *S. denitrificans* is grown with thiosulfate/oxygen or hydrogen/nitrate. In Figure 9, the relative abundance of denitrification enzymes (Figure 9A), sulfur oxidation enzymes (Figure 9B), hydrogenases (Figure 9C) and *cbb₃* cytochrome oxidoreductase (Figure 9D) under the different growth conditions are summarized.

The abundance of denitrification enzymes was different depending on the growth condition of *S. denitrificans* (Figure 9A). Especially NirS and NosZ show strong differences in abundance. When nitrate is limited (NL) there is a trend of increased abundance of denitrification enzymes and when nitrate is not available (TO) the abundance of NirS and NosZ

doubles. The abundance of denitrification enzymes under thiosulfate-limiting conditions (TL) is higher in comparison to the abundance when grown with hydrogen (HN).

In Figure 9B, the expression of the *S. denitrificans* sulfur oxidation clusters are shown for thiosulfate limitation (TL) and nitrate limitation (NL). When thiosulfate is limited, the expression of SoxCD of cluster2 (SoxCDY₂Z₂) is higher in comparison to nitrate limiting conditions. In addition, cluster1 (SoxABXY₁Z₁) seems to be down-regulated under thiosulfate-limiting conditions in comparison to nitrate-limiting conditions. Further, in cultures grown with hydrogen and nitrate, SoxA,X,Y₁ are not detected and SoxB and SoxZ₂ show a low abundance in absence of thiosulfate (Supplement Table 3).The sulfide quinone reductase (SQR) has an equally high abundance regardless of the growth condition.

Under hydrogen/nitrate (HN) conditions, hydrogenase WP_011373064.1 and HypB are upregulated (Figure 9C). In the absence of hydrogen, there is still a baseline abundance of hydrogenase enzymes. Similar results are found for cbb₃ cytochrome oxidoreductase (Figure 9D). In the absence of oxygen (TL, NL and HN), there is a low base-line abundance of FixNOQP proteins, but when oxygen becomes available FixO and FixP get upregulated (Figure 9D).

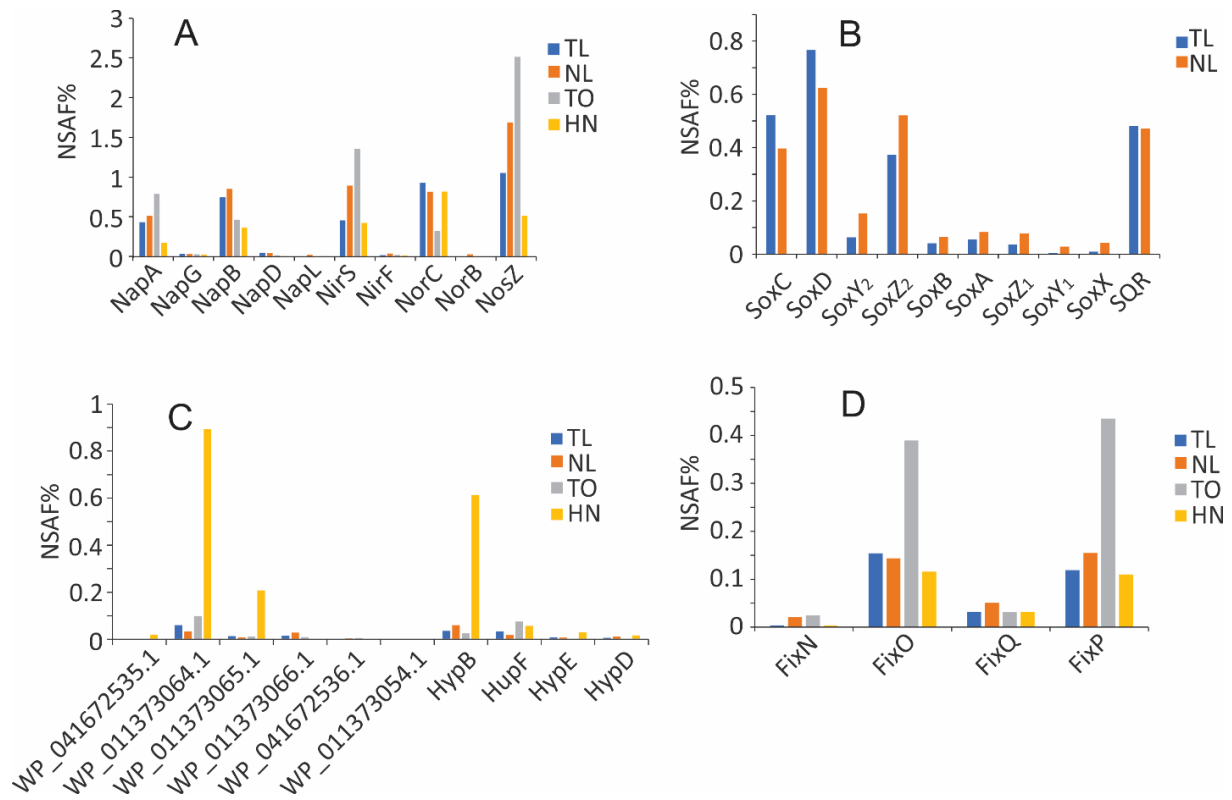


Figure 9 Proteomic results for the expression of denitrification enzymes (A), sulfur oxidation enzymes (B), hydrogenases (C) and the *cbb₃* cytochrome oxidoreductase (D) in *Sulfurimonas denitrificans* under thiosulfate limitation (TL), nitrate limitation (NL), thiosulfate and oxygen (TO) and hydrogen and nitrate (HN). Protein expression is given as normalized spectral abundance factor (NSAF%).

3.3 S₈ metabolism in *Sulfurimonas denitrificans*

These results have been published in (Götz, Pjevac, et al., 2018).

3.3.1 Growth characteristics

The growth rate of thiosulfate-grown cultures was 1.8-times higher compared with cultures grown on cyclooctasulfur (2.7 day^{-1} vs. 1.5 day^{-1}), corresponding to a doubling time of ~6 h and ~11 h for thiosulfate- and S₈-grown cultures, respectively (Figure 10). Thiosulfate-grown cultures also had a significantly shorter lag phase, which might be related to the easier accessibility of thiosulfate than of S₈. One of the three S₈-grown cultures had a significantly extended lag phase, but once growth started, the growth rate was similar to the other two cultures.

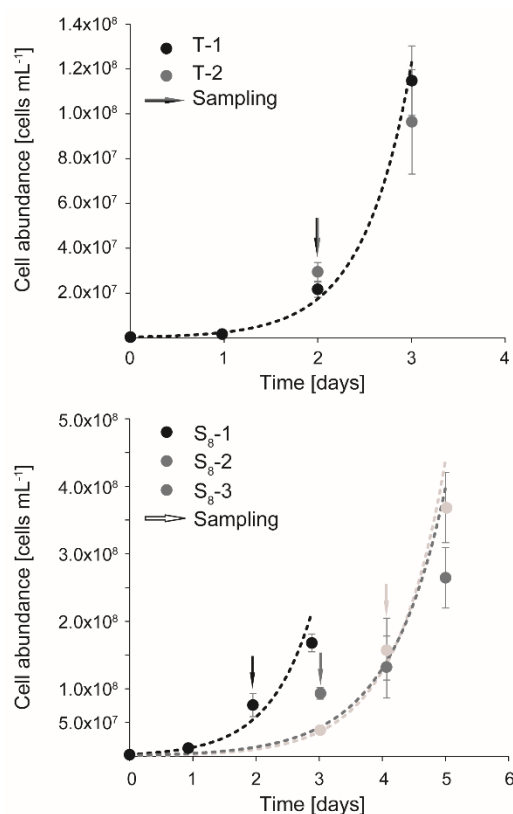


Figure 10 Growth curves (dotted lines) of *S. denitrificans* cultures grown on thiosulfate (upper panel) or cyclooctasulfur (lower panel), as determined via cell counts after DAPI staining. Arrows indicate the time of sampling of the biological replicates. Published in (Götz, Pjevac, et al., 2018).

3.3.2 The transcriptome and proteome of thiosulfate- versus S₈-grown cells are largely similar

Transcriptomic and proteomic data were obtained from either thiosulfate- or S₈-grown cultures sampled in early exponential phase. Overall, reads mapping to 97.7 % of the genes in the genome (2,114 and 2,104 out of 2,164) were detected in the transcriptome of cultures grown with thiosulfate or S₈, respectively. In the proteome, 38.8% and 37% of proteins encoded in the genome (822 and 784 out of 2,119 protein coding genes) were identified in thiosulfate- and S₈-grown cultures, respectively (Table 11). 122 and 84 proteins were detected exclusively in thiosulfate- and S₈-grown cultures, respectively, while 176 and 200 proteins were identified in only one of the analyzed replicates of thiosulfate- and in S₈-grown cultures, respectively (Table 11).

Table 11 Overview of S. denitrificans protein identification counts for the two growth conditions cyclooctasulfur (S₈) and thiosulfate (S₂O₃). Exclusive identifications are proteins that were detected in at least one replicate of one condition, but were absent in all replicates of the other condition. Published in (Götz, Pjevac, et al., 2018).

	S ₈ grown cultures	S ₂ O ₃ ²⁻ grown cultures
Identified proteins total	784	822
Only in one replicate	200	176
Exclusive proteins	84	122
>1% NSAF	19	10

In general, a classification into clusters of orthologous genes (COG) showed similar profiles of transcribed protein coding genes and identified comparable sets of proteins between thiosulfate- and S₈-grown cultures (Figure 11). Genes of the translational apparatus (including tRNA ligases and ribosomal subunits) accounted for up to one third of the classifiable transcripts and proteins under both conditions, followed by transcribed genes and proteins of the energy metabolism (Figure 11). The most apparent difference among functional genes is the increased transcription level of genes that encode proteins of the flagellar apparatus in S₈-grown cultures (Figure 11).

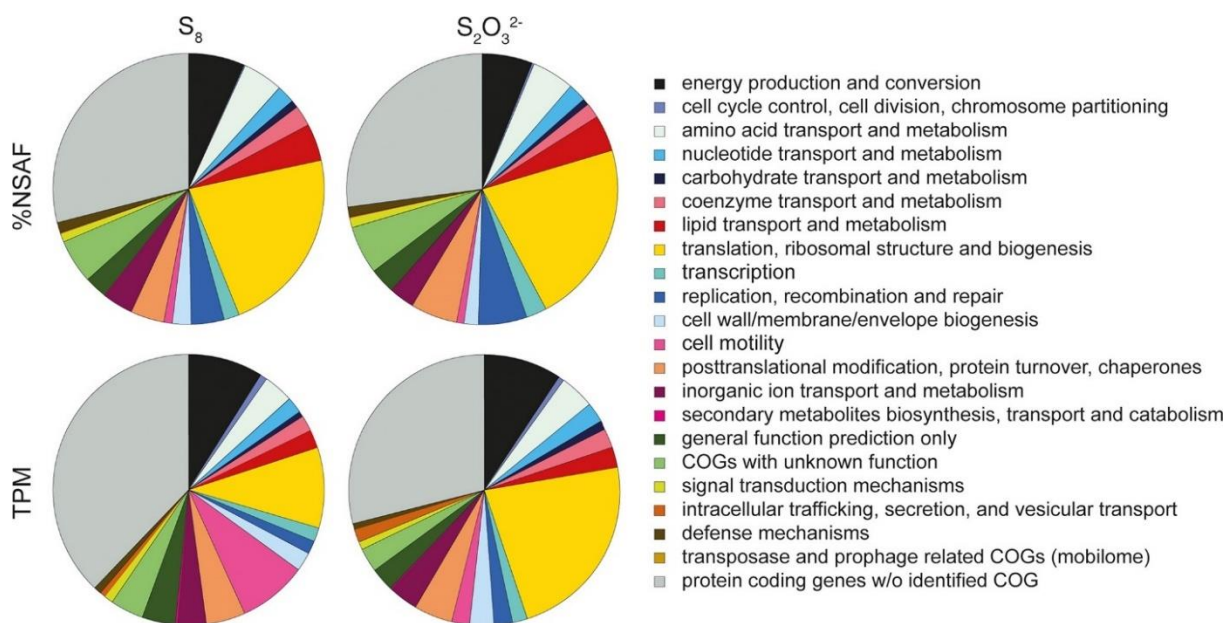


Figure 11 Distribution of COG categories in the *S. denitrificans* proteome (%NSAF = Normalized Spectral Abundance Factor) and transcriptome (TPM = Transcripts Per Million) on cyclooctasulfur (S_8) or thiosulfate ($S_2O_3^{2-}$). Published in (Götz, Pjevac, *et al.*, 2018).

Since transcriptome sequencing was performed without rRNA depletion to minimize sample processing biases, the majority of the transcriptomic reads (88.2-94.0%) mapped onto rRNA-encoding genes from one of the four rRNA operons encoded by *S. denitrificans*. No differences were observed for ribosomal RNA in thiosulfate- and S_8 -grown cultures. In addition, proteins of the small and large ribosomal subunits showed little variance in their abundance, which is expected since all subunits and the ribosomal RNA form functioning ribosomes. However, a significant differences in the transcription of genes encoding ribosomal small and large subunit proteins were found, which were transcribed at a significantly higher level in thiosulfate-grown cultures. The expression of an alternative indicator for growth - the translation elongation factor TU (EF-TU; WP_011371980.1) - was also found (Pedersen *et al.*, 1978), which also had a higher expression level in the transcriptome and higher levels of abundance in the proteome in thiosulfate-grown cultures (Supplement Table 2).

Although the differences in transcriptomic and proteomic profiles between cells grown with the two different electron donors were subtle (Figure 12), a small number of proteins showed statistically significant differences in relative abundance. One of these proteins (WP_011373531.1) was present at significantly higher levels (2.9 x increase) in S_8 -grown cultures, compared to thiosulfate-grown cultures. This hypothetical protein was also

differentially regulated in the transcriptome, but in the opposite manner - it was transcribed at higher levels under the thiosulfate condition compared to the S_8 condition. Based on analyses using BOCTOPUS, PRED-TMMB and SignalP 4.0, WP_011373531.1 contains a beta-barrel structure and a predicted signal peptide. It also contains a phenylalanine at the C-terminal position, as well as hydrophobic amino acids at positions -3, -5, -7, and -9 relative to the C-terminus, which have previously been reported to be important for the assembly into the outer membrane (Struyvé *et al.*, 1991; Tommassen, 2010). These indications suggest that it is an outer membrane protein. Protein domain analysis (DELTA-BLAST and PSI-BLAST, NCBI) of this hypothetical protein further showed that the first 177 amino acids of WP_011373531.1 have similarity to the conserved domain of the outer membrane protein family OprD and the major outer membrane protein of *Campylobacter* (Campylo_MOMP), suggesting an involvement in transport and/or adhesion (Yoshihara *et al.*, 1998; Zhang *et al.*, 2000). However, based on the low overall similarity, a functional classification cannot be inferred at present. A protein BLAST-based comparison of alignment length and amino acid sequence identity revealed the presence of homologs of this putative outer membrane protein (>70% alignment fraction, >30% amino acid identity) in various campylobacterial species (e.g., *Sulfurimonas*, *Sulfurovum*, *Sulfuricurvum*, *Nitratiruptor*) that are also implicated in elemental sulfur utilization (Campbell *et al.*, 2006; Sievert, Hügler, *et al.*, 2008a; Sievert and Vetriani, 2012).

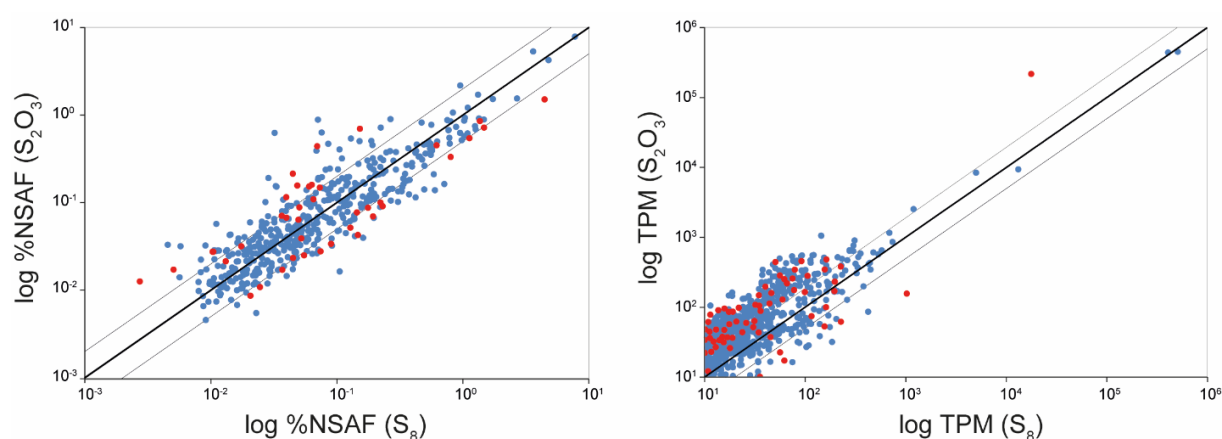


Figure 12 Distribution of the proteomic (left) and transcriptomic (right) expression of *S. denitrificans* cultures grown on cyclooctasulfur (x-axis) versus thiosulfate (y-axis). Proteins and ORFs with statistically significant differences in expression are depicted in red. Published in (Götz, Pjevac, *et al.*, 2018).

3.3.3 Flagella-related proteins and transcripts are differentially abundant

Significant differences in gene transcription levels were observed for a large number of genes involved in flagella biosynthesis and motility (Figure 13). Flagella-related genes were generally upregulated in cultures grown with S_8 as electron donor. In contrast, the differences in the expression of proteins of the flagellar apparatus were not as pronounced between the growth conditions, but the flagellar hook protein FlgE and flagellin were found in considerably higher relative abundance in the proteome of S_8 -grown cultures (Supplement Table 2).

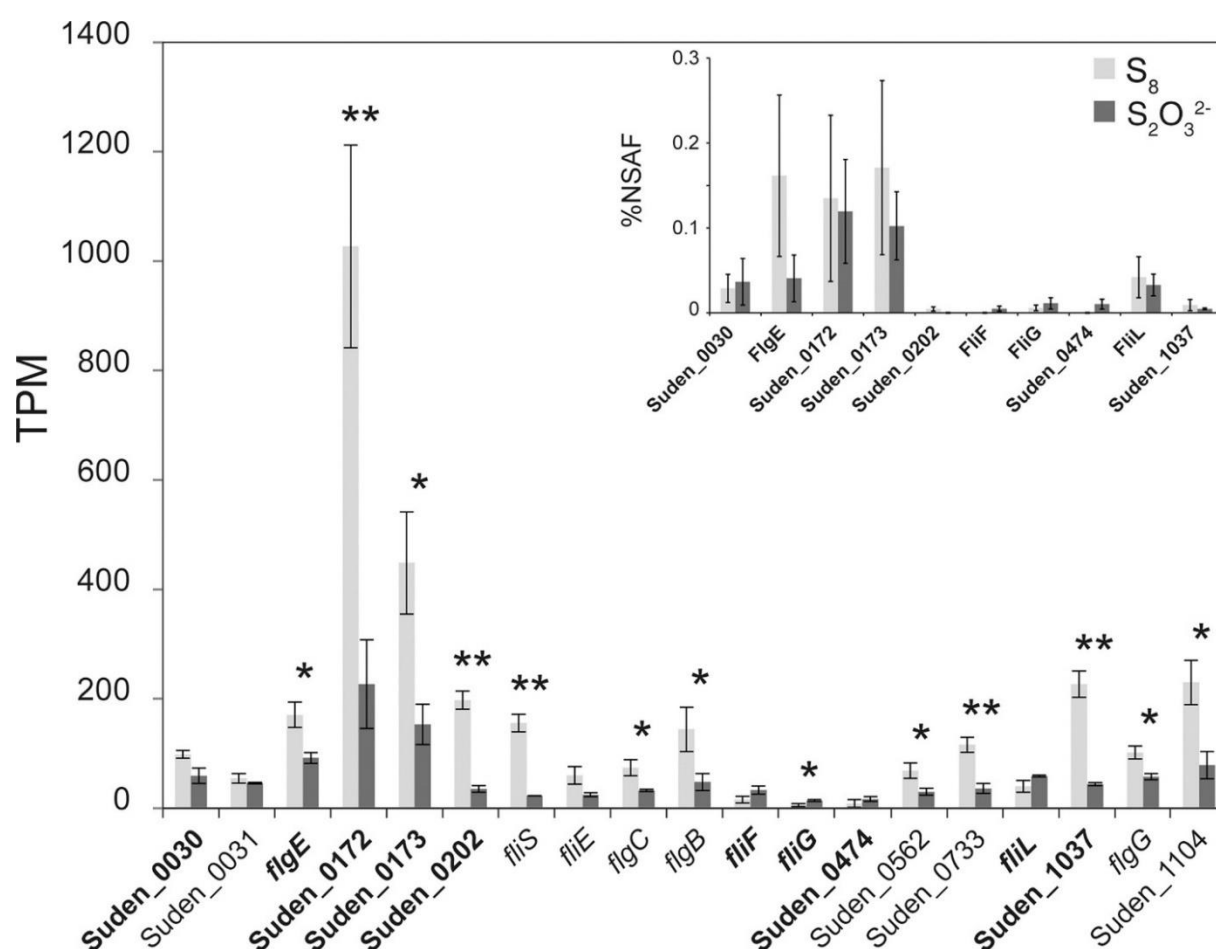


Figure 13 The relative abundance of transcripts (TPM = Transcripts Per Million) and proteins (%NSAF = Normalized Spectral Abundance Factor) related to flagellar biosynthesis and motility. Light bars show the average values of *S. denitrificans* grown on cyclooctasulfur (S_8) and dark bars show the average of cultures grown on thiosulfate. Statistically-significant differences are denoted with one ($p < 0.05$) or two ($p < 0.01$) asterisks. Genes indicated in bold were also identified in the proteomic dataset. Suden_0030: Flagellar hook capping protein = WP_011371666.1; Suden_0031: Flagellar hook protein = WP_011371667.1; FlgE: Flagellar hook = WP_011371668.1, Suden_0032: Suden_0172: Flagellin-like = WP_011371808.1; Suden_0173: Flagellin-like = WP_011371809.1; Suden_0202: Flagellar hook-associated protein 2-like = WP_011371838.1; FliS: Flagellar protein = WP_041672386.1, Suden_0203; FliE: Flagellar hook-basal body complex protein

= WP_011371998.1, Suden_0363; FlgC: Flagellar basal-body rod protein = WP_011371999.1, Suden_0364; FlgB: Flagellar basal-body rod protein = WP_011372000.1, Suden_0365; FliF: Flagellar M-ring protein = WP_011372107.1, Suden_0472; FliG: Flagellar motor switch protein = WP_011372108.1, Suden_0473; Suden_0474: putative flagellar assembly protein = WP_011372109.1; Suden_0562: Flagellar P-ring protein = WP_011372195.1; Suden_0733: Flagellar L-ring protein = WP_011372366.1; FliL: Flagellar basal body-associated protein = WP_011372470.1, Suden_0840; Suden_1037: putative flagellin = WP_011372667.1; FlgG: Flagellar basal-body rod = WP_011372733.1, Suden_1103; Suden_1104: Flagellar basal body rod protein = WP_011372734.1. Published in (Götz, Pjevac, *et al.*, 2018).

3.3.4 Genes and proteins of central biochemical pathways

Growing with nitrate as the electron acceptor with thiosulfate or cyclooctasulfur as the sole electron donor, *S. denitrificans* gains energy through denitrification coupled to sulfur oxidation. The generated energy mainly fuels carbon fixation through the reductive tricarboxylic acid (rTCA) cycle. Accordingly, all transcripts and proteins of the rTCA cycle were identified. In the genome, two copies of succinate dehydrogenase/fumarate reductase were identified previously, one being membrane-bound and one being cytoplasmic (Sievert *et al.*, 2008). It was previously proposed that the membrane-bound form might play a direct role in the rTCA cycle by transferring electrons derived from the oxidation of hydrogen or sulfur via the quinone pool (Sievert, Scott, *et al.*, 2008). In line with this hypothesis, the putatively membrane-bound succinate dehydrogenase/fumarate reductase (SDH; EC 1.3.5.1; WP_011372658.1-WP_011372660.1) was found in the transcriptomes and proteomes under both growth conditions, while the cytoplasmic succinate dehydrogenase/fumarate reductase (WP_011371673.1-WP_011371674.1) only displayed a low transcription level and was not identified in the proteome (Supplement Table 2).

For the reduction of nitrate, it could be confirmed that all transcripts and all proteins involved in the canonical dissimilatory denitrification pathway were present (Figure 14), including the nitric oxide reductase cNOR, which had previously been questioned to be functional due to the absence of *norD* and *norQ* in the genome (Sievert, Scott, *et al.*, 2008). In contrast, neither the transcripts nor the proteins of the proposed alternative non-electrogenic quinone-oxidizing nitric oxide reductase (gNOR, WP_011371739.1-WP_011371741.1; Sievert, Scott, *et al.*, 2008) could be detected (Supplement Table 2). The comparatively low abundance of the nitrous oxide reductase (NorB, NorC) in the proteome compared to the other enzymes of the denitrification pathway is most likely due to the fact that NorB is an integral membrane protein and NorC is anchored in the membrane. Membrane associated proteins are

not extracted with the same efficiency as soluble proteins by the used extraction procedure, resulting in their lower representation in the proteome. The same bias applies for the membrane bound components of the nitrate reductase complex (NapFGH).

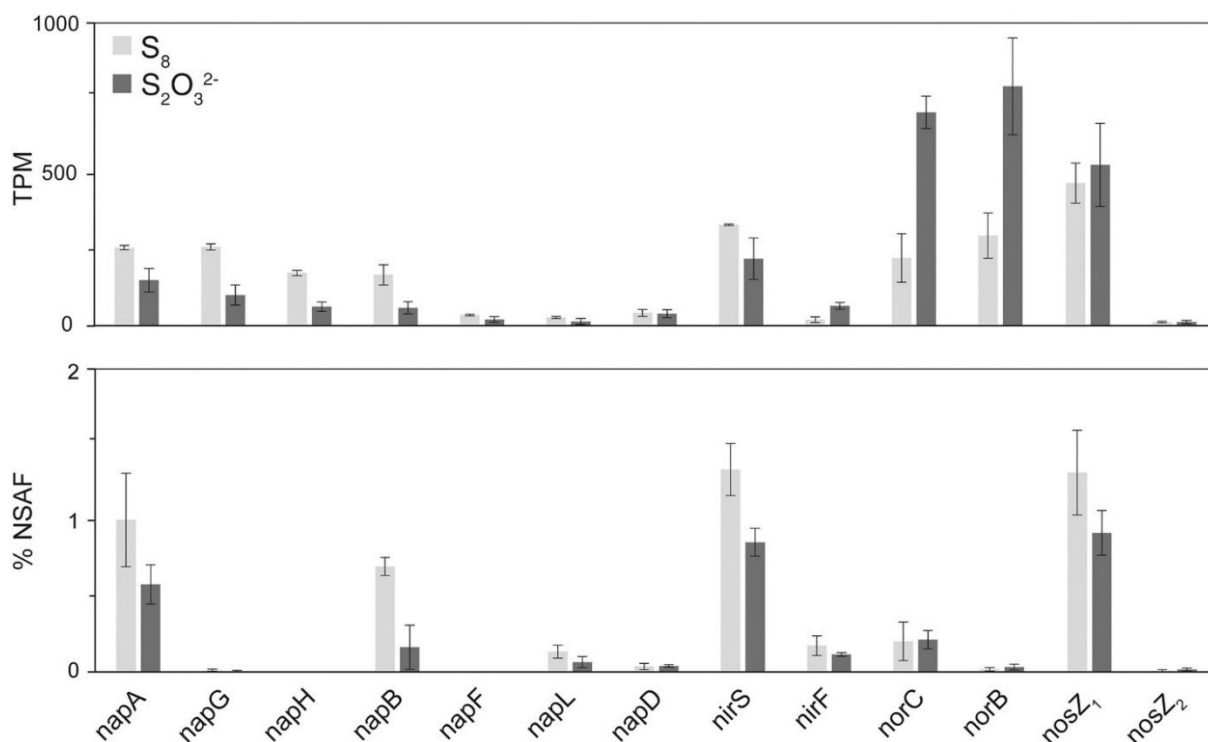


Figure 14 Expression of *S. denitrificans* transcripts (upper panel; TPM = Transcripts Per Million) and proteins (lower panel; %NSAF = Normalized Spectral Abundance Factor) involved in denitrification. Light bars show the average values of *S. denitrificans* grown on cyclooctasulfur (S₈) and dark bars show the average of cultures grown on thiosulfate. *napAGHBFLD* = Nitrate reductase (napA = WP_011373143.1, Sude_n_1514; napB = WP_011373146.1, Sude_n_1517; napG = WP_041672542.1, Sude_n_1515; napH = WP_041672543.1, Sude_n_1516; napF = WP_011373147.1, Sude_n_1518; napL = WP_011373148.1, Sude_n_1519; napD = WP_011373150.1, Sude_n_1521); *nirSF* = nitrite reductase (nirS = WP_011373599.1, Sude_n_1985; nirF = WP_011373602.1, Sude_n_1988); *norCB* = nitric oxide reductase (norC = WP_011373597.1, Sude_n_1983; norB = WP_011373598.1, Sude_n_1984); *nosZ1,2* = nitrous oxide reductase (nosZ1 = WP_011372928.1, Sude_n_1298; nosZ2 = WP_011373385.1, Sude_n_1770). Published in (Götz, Pjevac, *et al.*, 2018).

With respect to sulfur compound metabolism, transcripts and proteins of the periplasmic SOX (sulfur oxidation) multienzyme complex were detected, confirming the use of the SOX system for sulfur oxidation in *S. denitrificans*, as has previously been shown for the campylobacterium *Sulfurovum* sp. NCB37-1 (Yamamoto *et al.*, 2010). The transcripts of both sox operons, i.e., *soxABXY₁Z₁* and *soxCDY₂Z₂*, showed a trend of increased transcription levels in thiosulfate grown-cultures. However, the transcripts of *soxABXY₁Z₁* were more strongly

upregulated with thiosulfate, as the transcription ratios for *soxABXY₁Z₁* between S₈ and thiosulfate ranged from 0.3-0.6, while those of *soxCDY₂Z₂* ranged from 0.65-0.8 (Figure 15). In the proteomes of S₈-grown cultures, SOX proteins of the *soxABXY₁Z₁* operon were hardly detected, while they were present in significantly higher abundance with thiosulfate (Figure 15). In contrast, the sulfur dehydrogenase proteins, i.e., SoxCD, were significantly more abundant in the proteome of S₈-grown cultures, although still present with thiosulfate (Figure 15). Regardless of the supplied electron donor, the SoxY and SoxZ proteins of the *soxCDY₂Z₂* operon were not only the two most abundant proteins of the SOX multienzyme system, but of both proteomes under both growth conditions overall (Figure 15, Supplement Table 2), suggesting that they play an important role under both conditions. In addition, a protein encoded by gene WP_011373670.1 that is located next to *soxCDY₂Z₂* is present in the transcriptome and proteome under both growth conditions (Figure 15, Supplement Table 2). The 340 amino acids-long protein has a signal peptide indicating a periplasmic location, and based on BLAST search it further contains a metallo-hydrolase-like_MBL-fold with all the conserved residues of the active site and three putative metal-binding sites, suggesting it has a hydrolytic function. Transcript reads and protein abundance of the sulfide:quinone oxidoreductase (SQR), a sulfide-oxidizing enzyme, and the putative membrane-bound polysulfide reductase, a polysulfide-reducing complex, which might be involved in the reduction of polysulfide, were low, and no significant differences between growth conditions was observed (Figure 15).

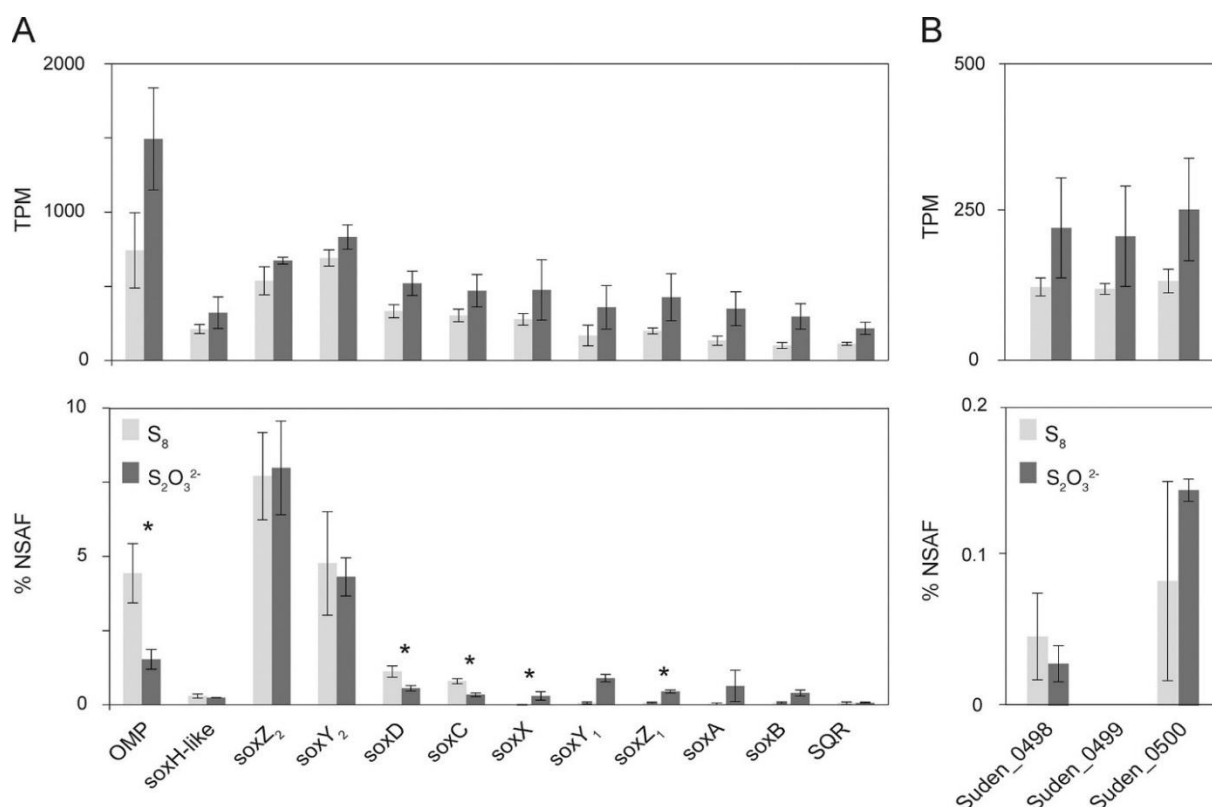


Figure 15 The relative abundance of expressed SOX (sulfur oxidation multienzyme complex) and SQR (sulfide quinone reductase) proteins (%NSAF = Normalized Spectral Abundance Factor) and transcripts (TPM = Transcripts Per Million). Light bars show the average values of *S. denitrificans* grown on cyclooctasulfur (S₈) and dark bars show the average of cultures grown on thiosulfate. Statistically significant differences (p<0.05) are denoted with an asterisk. OMP (outer membrane protein) = WP_011373531.1, Suden_1917; soxH-like = WP_011373670.1, Suden_2056; SOX (sulfur oxidation multienzyme complex): soxZ2Y2DC: soxZ2 = WP_011373671.1, Suden_2057; soxY2 = WP_011373672.1, Suden_2058; soxD = WP_011373673.1, Suden_2059; soxC = WP_011373674.1, Suden_2060 ; soxXY1Z1AB: soxX = WP_011371896.1, Suden_0260; soxY1 = WP_011371897.1, Suden_0261; soxZ1 = WP_011371898.1, Suden_0262; soxA = WP_011371899.1, Suden_0263; soxB = WP_011371900.1, Suden_0264) and SQR (sulfide quinone reductase = WP_011372252.1, Suden_0619). B) The relative abundance of transcripts (upper panel; TPM = Transcripts Per Million) and proteins (lower panel; %NSAF = Normalized Spectral Abundance Factor) of the proposed polysulfide reductase (Suden_0498-Suden_0450: WP_011372132.1- WP_011372134.1). Published in (Götz, Pjevac, *et al.*, 2018).

3.3.5 Transcribed and translated genes involved in alternative energy metabolism

The *S. denitrificans* genome reflects the potential to use alternative energy sources to generate energy for carbon fixation (Sievert, Scott, *et al.*, 2008). Transcription of genes that are involved in the metabolism of compounds which were not provided in the medium were also detected. The assessment of transcriptomic data revealed that genes of a *cbb3*-type cytochrome *c* oxidase (*fixNOQP* cluster involved in aerobic respiration) as well as genes encoding a

membrane-bound [Ni,Fe]-uptake hydrogenase (*hydABC* cluster involved in hydrogen oxidation) were transcribed in all cultures (Figure 16). In addition, FixO and HydB were identified at low relative abundance in the proteomes under both cultivation conditions (Supplement Table 2), whereas the proposed cytoplasmic hydrogenase putatively involved in direct electron transfer as part of the rTCA cycle (WP_011373066.1; WP041672536.1; Sievert, Scott *et al.*, 2008) was not expressed under either cultivation condition (Supplement Table 2). Genes encoding the membrane-bound formate dehydrogenase complex were transcribed at higher relative levels in the S₈-grown cultures (Figure 16), but no proteins of the complex were identified (Supplement Table 2).

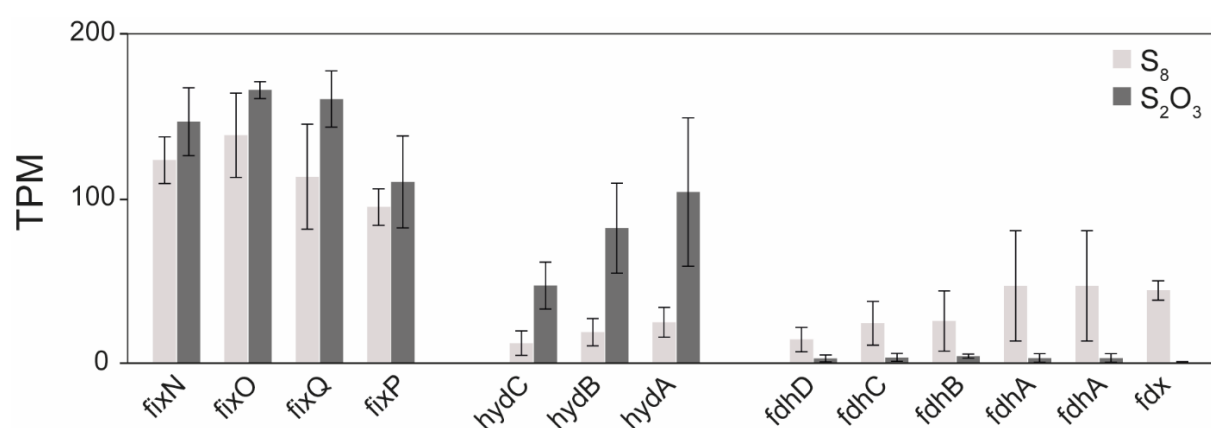


Figure 16 Gene expression (TPM = Transcripts Per Million) of the *cbb3*-type cytochrome c oxidase (*fixNOQP*, *fixN* = WP_011371717.1, Suden_0081; *fixO* = WP_011371718.1, Suden_0082; *fixQ* = WP_011371719.1, Suden_0083; *fixP* = WP_011371720.1, Suden_0084), the membrane bound [Ni,Fe]-uptake hydrogenase (*hydCBA*, *hydC* = WP_041672535.1, Suden_1434; *hydB* = WP_011373064.1, Suden_1435; *hydA* = WP_011373065.1, Suden_1436) and the membrane bound formate dehydrogenase (*fdhDCBAA*, *fdhD* = WP_011372449.1, Suden_0817; *fdhC* = WP_011372450.1, Suden_0818; *fdhB* = WP_011372451.1, Suden_0819; *fdhA* = WP_011372452.1, Suden_0820; *fdhA* = WP_041672204.1, Suden_0821; *fdx* = WP_011372455.1, Suden_0824). Light bars show the average values of *S. denitrificans* grown on cyclooctasulfur (S₈) and dark bars show the average of cultures grown on thiosulfate. Published in (Götz, Pjevac, *et al.*, 2018).

4 Discussion

Crab Spa is located at 9°N on the East Pacific Rise and has been used as a model system for studying chemoautotrophy at deep-sea vents, which are known to be fluctuating in their physicochemical composition (Lowell *et al.*, 1995; Von Damm, 1995; Shank *et al.*, 1998; Le Bris *et al.*, 2006; Scheirer *et al.*, 2006; Damm and Lilley, 2013). Crab Spa is a very stable diffuse flow vent systems and has been studied more intensely in the last decade (Sievert and Vetriani, 2012; McNichol *et al.*, 2016, 2018). In comparison to the surrounding seawater, exiting fluids have elevated levels of methane, sulfide and ammonium, but are depleted in oxygen and nitrate, which is a reflection of the growth of chemoautotrophs in the subseafloor environment (McNichol *et al.*, 2016, 2018). The temperature as well as the chemistry of electron donor and acceptor composition has been monitored since 2007 (McNichol *et al.*, 2016, 2018, Reeves *et al.*, 2014) and surprisingly has not changed much between 2007 and 2014 when the samples were taken for the analyses presented in this thesis. Since 2007, these stable physicochemical conditions led to a well-adapted and overall stable subseafloor microbial community that is responsible for the depletion of oxygen and nitrate (McNichol *et al.*, 2016). Using 16S rRNA sequencing techniques, *Campylobacteria* have been identified as the dominant bacterial community at various hydrothermal vent systems, including Crab Spa (López-García *et al.*, 2003; Hügler *et al.*, 2005; Nakagawa *et al.*, 2005; Sogin *et al.*, 2006; Huber *et al.*, 2007; Nakagawa and Takai, 2008; Sievert, Hügler, *et al.*, 2008; Sievert and Vetriani, 2012; McNichol *et al.*, 2016, 2018, Urich *et al.*, 2014). In hydrothermal sediments they have been identified to make up 70% of the bacterial community (Urich *et al.*, 2014). This abundance is also reflected in the presented data in which *Campylobacteria* dominate Crab Spa fluids based on 16S rRNA sequence information (by over 90%), key genes identified in the metagenome (Figure 3), and key enzymes identified in the metaproteome (Figure 4). Remarkably, all three approaches show almost perfect congruence, indicating that the microbial community is mainly composed of organisms active under the prevailing environmental conditions. The metaproteome revealed and confirmed that the three major genera *Sulfurimonas*, *Sulfurovum*, and *Arcobacter* are driving the Crab Spa diffuse-flow vent community (McNichol *et al.*, 2016, 2018). The dominant genera show a high micro-diversity, similarly to what has been found at other diffuse-flow deep-sea vents (Huber *et al.*, 2007).

Little is known about the key metabolic pathways that allow *Campylobacteria* to dominate the microbial community at Crab Spa. A two-pronged approach was taken to identify the dominant active microorganisms and their metabolic pathways. I focused on results

obtained from environmental metaproteomic datasets from large volume pump samples obtained from Crab Spa. Previous studies provided evidence for electron acceptor limitation of the microbial community at Crab Spa (McNichol et al., 2016, 2018). The high abundance of proteins involved in electron-acceptor-related processes observed in the metaproteome thus led to questions regarding the regulation of proteins involved in energy metabolism by *Campylobacteria* under either electron donor or acceptor limitation. To answer those questions, the campylobacterial model organism *Sulfurimonas denitrificans* was used in batch- and continuous culture experiments under various growth conditions. Samples from those growth experiments were processed to analyze the proteome and determine the major metabolic pathways active in *S. denitrificans* under the different conditions.

4.1 *Campylobacteria* at Crab Spa

The database for a proteomic analysis is critical. To avoid false positive results during the identification of proteins, it is essential to create an organism specific gene library as close as possible to the study site. In this thesis, I used a combination of two metagenomes created from the same filters that were used for the metaproteomic analyses. In addition, single cell genomes, provided by the research group of Ramunas Stepanauskas, and genomes of select cultures available at NCBI were used in combination with the metagenomes to create a robust database for the metaproteomic analysis. There has not been a direct metric of how good each part of a database performs regarding the identification of proteins within the metaproteome. Here, ratios were calculated of how many genes per identified protein were available in the database (Table 10). It might not be surprising, but site-specific single cell genomes and metagenomes identified more proteins in comparison to genomes of cultured organisms available from NCBI. Based on these results, single cell genomes from the in situ samples performed best and should thus always be the first pick, followed by metagenomes, to create site-specific databases for metaproteomic analysis of any environment.

Differences in the distribution of taxa were observed between metabolic genes in the metagenome and proteins in the metaproteome. For example, based on the metagenome, the energy marker gene ATP synthase had a 1/5 distribution of each of the three dominant genera, 1/5 of other *Campylobacteria*, and 1/5 of other remaining taxa. In contrast, in the metaproteome over 75% of the ATP synthase belonged to the three dominant genera, with the remaining 25% belonging to other *Campylobacteria*. These observations can be explained by methodological differences between genomics and proteomics analyses. It is obvious that metaproteomics is a suitable approach to determine major active metabolic pathways in a complex environmental

system, whereas metagenomics reveals only the metabolic potential of the microbiomes. However, metagenomes are essential as they serve as templates for the identification of the proteins in mass spectrometry analyses.

4.1.1 Metabolism of *Campylobacteria* in the environment

The three main genera *Sulfurimonas*, *Sulfurovum* and *Arcobacter* revealed strong similarities as well as differences in detected enzymes of their biochemical pathways (Figure 6). *Sulfurimonas* and *Sulfurovum* show an almost identical protein profile (Figure 6), with the only exception of the occurrence of the thiosulfate reductase in *Sulfurimonas*. Unfortunately, the biochemical function of the thiosulfate reductase is not known. However, Blast searches suggest a similarity to polysulfide reductases, which might indicate an electron acceptor system (Dietrich and Klimmek, 2002) alternative to denitrification in *Sulfurimonas* species. This is further supported by a recent study showing the capability of sulfur reduction in *Sulfurimonas* sp. NW10, suggesting the involvement of a periplasmic and cytoplasmic polysulfide reductases in *Sulfurimonas* species (Wang *et al.*, 2020). It is therefore strongly suggested to investigate the thiosulfate reductase functionality which might belong to the polysulfide reductases and could be a factor differentiating *Sulfurimonas* from *Sulfurovum*, and thus driving niche specialization.

The data identified the rTCA cycle, primarily utilized by *Sulfurimonas* and *Sulfurovum*, as the major carbon fixation pathway of the productive subseafloor biosphere of Crab Spa, reaching carbon fixation rates up to 321 μg carbon per liter per day (McNichol *et al.*, 2018). The dominance of the rTCA cycle is similar to what has been reported for hydrothermal sediments (Urich *et al.*, 2014), biofilms on hydrothermal chimney walls (Stokke *et al.*, 2015a; Pjevac *et al.*, 2018) and in line with the operation of the rTCA cycle in *Campylobacteria* in general (Hügler *et al.*, 2005; Takai *et al.*, 2005; Hügler and Sievert, 2011). Interestingly, 4% NSAF rTCA cycle enzymes were identified for *Sulfurovum* species compared to 2% NSAF for *Sulfurimonas* species. However, in culture experiments it was observed that rTCA cycle enzymes of *Sulfurimonas* species showed higher specific activities compared to *Sulfurovum lithotrophicum* (Hügler *et al.*, 2005; Takai *et al.*, 2005). This might be an indication that *Sulfurovum* species generally require more rTCA cycle enzymes to achieve comparable carbon fixation rates to *Sulfurimonas* species. For *Arcobacter*, the third dominant genus among the identified *Campylobacteria*, the pyruvate ferredoxin oxidoreductase was the only identified enzyme of the rTCA cycle. Since it also occurs in the oxidative TCA cycle, it is not possible to infer the carbon metabolism of *Arcobacter* species in the Crab Spa subseafloor biosphere. *Arcobacter* species most likely have a different role in the Crab Spa diffuse-flow hydrothermal

vent system. A higher relative abundance of ribosomal proteins (Figure 6) leads to the question of whether the genus *Arcobacter* is more metabolically active, although fewer proteins were detected overall in comparison to the other two dominant genera. The ability of *Arcobacter* species in Crab Spa to use oxygen as the electron acceptor with a cytochrome cbb₃ oxidoreductase could also be validated, which is consistent with microaerophilic growth in other *Arcobacter* (Wirsen *et al.*, 2002; Sievert *et al.*, 2007). One striking difference in comparison to the other two genera was found in proteins related to motility. Here, *Arcobacter* is dominating flagellar proteins, which indicates strong mobility and might give them the proposed ability to form colonies in the form of mats (Wirsen *et al.*, 2002) and therefore act as primary colonizers on surfaces in the subseafloor biosphere. In contrast, *Sulfurimonas* and *Sulfurovum* species dominate chemotaxis proteins which are necessary to sense chemical gradients (Berg, 1975), which, as proposed r-strategists (Rogge *et al.*, 2017), allows them to adapt quickly to a changing environment.

4.1.2 Difference in abundance of enzymes in relation to substrate concentration

In a previous metaproteogenomic study, discrepancies between the metabolic potential (metagenome) and the actual metabolism revealed by metaproteomics were found to be unexpectedly large (Pjevac *et al.*, 2018). Here, a similar observation was made as a relatively high number of genes involved with the electron donor metabolism (SQR, SOX) were identified in the metagenome, but only a low number of proteins (<0.1 %NSAF) were identified in the metaproteome. In contrast, for electron acceptor metabolism (specifically denitrification), the abundance of genes in the metagenome was equally high as the corresponding proteins in the metaproteome. One plausible explanation for this is that the metabolic potential is given by active and non-active bacteria of the community. In addition, one strand of DNA is theoretically sufficient for DNA sequencing techniques (Sims *et al.*, 2014), whereas the amount of protein needed for detection is 100 fmol, which converts to over 60 billion molecules (Silva *et al.*, 2006). On the one hand, potentially active pathways and enzymes could be missed due to the detection limits of proteomics, but on the other hand, the observed differences between genes and protein abundance can tell us something about the importance of the pathways required in the system.

When essential substrates like nitrate or oxygen become limited in the system, one way to make efficient use of the limited resource is an upregulation of the translation for those enzymes (Harder and Dijkhuizen, 1983). In short, increase the amount of enzyme to capture its

limited substrate. The correlation of enzyme abundance to limited substrate concentration was confirmed in experiments with the deltaproteobacterium *Desulfovibrio vulgaris* under sulfate limiting conditions in chemostats (Villanueva *et al.*, 2008). In support of this hypothesis, the chemostat experiments with *S. denitrificans* demonstrated that under electron acceptor limitation an upregulation for the expression of denitrification enzymes was triggered (Figure 9). When nitrate was completely absent in the system and oxygen was the sole electron acceptor, the denitrification pathway was most upregulated. This could indicate another adaptation in *Sulfurimonas* species, which have been described as *r*-strategist (Rogge *et al.*, 2017) and primary colonizers (López-García *et al.*, 2003), to have metabolic pathways readily available when substrates are absent or available in low concentrations. In contrast, the limitation of the electron donor (thiosulfate) did not trigger a pronounced upregulation of the associated enzymes, only trends are observed (Figure 9). Only when the substrates oxygen or hydrogen were available, did the associated proteins become upregulated, which could indicate a quick response system in contrast to a continuous expression of denitrification enzymes even in the absence of nitrate (Figure 9).

In the limited electron acceptor environment of Crab Spa, the denitrification pathway has one of the highest relative abundances in both metaproteomes and is dominated by the genera *Sulfurimonas* and *Sulfurovum*. The fact that the denitrification pathway is present in such high abundance might highlight that chemolithoautotrophy is mainly occurring in the absence of oxygen, which is similar to findings in hydrothermal sediments (Urich *et al.*, 2014). Although denitrification is highly abundant in hydrothermal sediments, it is in contrast to bacterial communities growing as biofilms on hydrothermal chimney walls which showed a significantly higher representation of oxygen-reducing terminal oxidases (Pjevac *et al.*, 2018), in line with the fact that those communities are more exposed to the surrounding seawater. Especially abundant in the metaproteome are the nitrate reductase (Nap) and the nitrite reductase (Nir). Both of these enzymes are dominated by the genus *Sulfurovum*, whereas nitric oxide reductase (Nor) and nitrous oxide reductase (Nos) are dominated by the genus *Sulfurimonas*. Surprisingly, NirS, NorB and NosZ have a similar frequency in the metagenome, but in the metaproteome NorB and NosZ have a lower abundance in comparison to NapA and NirS. The low abundance of NorB can be explained because membrane bound proteins are not easily enriched during protein isolation. Nonetheless, the difference in abundance of Nap and Nir to Nor and Nos raised the question of whether the denitrification pathway is partitioned between *Sulfurimonas* and *Sulfurovum* species. Can this partitioning be described as metabolic handoffs as previously described by Anantharaman *et al.* (2016)? With the data obtained in this

study, it is not possible to infer if the denitrification pathway is entirely available in an organism's genome or if it is truncated. However, the proteomic data suggests that the first two steps in the denitrification pathway might be primarily performed by *Sulfurovum* and whereas the last two steps might be mainly catalyzed by *Sulfurimonas*. Similar to Crab Spa, *Sulfurovum* also dominated the first two enzymes of the denitrification pathway in a biofilm colonizing the outside of a black smoker chimney wall, whereas *Bacteroidetes* species dominated the last two enzymes of the denitrification pathway, which lead Stokke *et al.* (2015) to conclude that the denitrification pathway is partitioned between *Sulfurovum* and *Bacteroidetes*. Here, *Bacteroidetes* species were only present in low abundance, but the results support the observation that *Sulfurovum* performs only a partial denitrification. Similar to the conclusions of Stokke *et al.* (2015), the current data suggest a partitioning of the denitrification pathway in which *Sulfurovum* predominantly performs the first two steps and *Sulfurimonas* the last two steps. Similarly, there could be a partitioning between organisms carrying out the oxidation of sulfide to sulfur and the subsequent oxidation of sulfur, but the paucity of detected proteins involved in the oxidation of electron donors precludes us from any conclusions in that regard.

Surprisingly, not many proteins of the sulfur oxidation pathway could be identified in the sulfur rich hydrothermal environment of Crab Spa, which is in contrast to the metabolic potential identified in the metagenomes, but similar to observations made in other hydrothermally influenced environments (Urich *et al.*, 2014; Pjevac *et al.*, 2018). In many environments, such as marine sediments, microbial mats, hydrothermal vents, glacial shields, oxygen minimum zones and volcanic soils, it is well known that sulfur is available in many oxidation states and occurs in high concentrations (Ruby *et al.*, 1981; Woodruff and Shanks, 1988b; Raiswell, 1992; Taylor and Wirsén, 1997; Alonso-Azcárate *et al.*, 2001; Engel *et al.*, 2004; Zopf *et al.*, 2004b; Lavik *et al.*, 2009; Cosmidis and Templeton, 2016; Lau *et al.*, 2017). Zero-valence sulfur (S^0) is often quite abundant, with cyclooctasulfur (S_8) as the most stable and common form (Steudel and Eckert, 2003; Götz, Pjevac, *et al.*, 2018). During microbial sulfide (S^{2-}) oxidation, S^0 in the form of S_8 , polymeric sulfur (S_μ) or sulfur chains is often produced and deposited as an intermediate oxidation product (Friedrich *et al.*, 2001; Prange *et al.*, 2002; Dahl and Prange, 2006; Sievert *et al.*, 2007; Sievert, Hügler, *et al.*, 2008; Götz, Pjevac, *et al.*, 2018). Members of the genus *Sulfurimonas* and other sulfur-oxidizing *Campylobacteria*, such as *Sulfurovum* and *Sulfuricurvum*, are highly abundant in various S^0 -rich natural and engineered environments (Macalady *et al.*, 2008; Legatzki *et al.*, 2011; Hubert *et al.*, 2012; Meyer *et al.*, 2013; Pjevac *et al.*, 2014; Gulmann *et al.*, 2015; Zhang *et al.*, 2015; Li *et al.*, 2016; McNichol *et al.*, 2016; Götz, Pjevac, *et al.*, 2018). It has been proposed that

especially *Sulfurimonas* and *Sulfurovum* species occupy the niche for S^0/S_8 oxidation in sediments and at hydrothermal vents (Pjevac *et al.*, 2014; Meier *et al.*, 2017), but the pathways are not known. To date, *S. denitrificans* is the only neutrophilic microorganism capable of S_8 oxidation (Pjevac *et al.*, 2014), which prompted culture experiments with *S. denitrificans* utilizing S_8 as sole electron donor to elucidate the underlying mechanisms and to identify proteins that could be indicative of this process in the environment. The results of these experiments are further discussed in the next chapter and were previously published in (Götz, Pjevac, *et al.*, 2018).

4.2 Importance of sulfur oxidation for *Sulfurimonas denitrificans* and its implications for redox environments

Large parts of this section have been published in (Götz, Pjevac, et al., 2018).

Here, proteomic and transcriptomic analyses were used to investigate the metabolism of *Sulfurimonas denitrificans* with either S_8 or thiosulfate as the sole electron donor. The combined application of proteomic and transcriptomic profiling provides a comprehensive assessment of the microbial response to different physiological conditions. In some instances, it was observed that there was not a strict correlation between transcribed genes and detected proteins, which could be explained either by posttranscriptional regulation (Picard *et al.*, 2009; Van Assche *et al.*, 2015), the initiation of transcription before proteins reached levels high enough for their detection, or the longer lifetime of proteins compared to transcripts.

In the batch culture experiments with *S. denitrificans*, the detection of 42% of the predicted proteins encoded in the genome is comparable to what was found for the gram-positive bacterium *Bacillus subtilis*, but lower than for example the 70% reported for the thaumarchaeon “*Candidatus Nitrosopelagicus brevis*” (Hahne *et al.*, 2010; Santoro *et al.*, 2015). The number of transcribed genes and identified proteins was similar under both growth conditions. This similarity of the transcriptomic and proteomic profiles was mirrored in the broad COG categories (Figure 11), and differences between the growth conditions were restricted to individual mRNA and protein categories.

Ribosomal RNA levels as well as protein levels of ribosomal subunits did not vary significantly between the two growth conditions, despite higher growth rates with thiosulfate. Similar observations have been made previously and it was concluded that rRNA levels in combination with the growth rates are not always a good indicator for microbial activity (Blazewicz *et al.*, 2013). However, in cultures grown with thiosulfate, transcription of

ribosomal subunit genes was significantly higher in relation to rRNA gene transcription levels, which, together with elevated transcript and protein levels of the elongation factor TU, likely reflects the higher growth rates and higher overall activity in cultures grown with thiosulfate. One of the most abundant proteins of the *S. denitrificans* proteome was identified as a hypothetical protein (WP_011373531.1), which is likely to play an important role for *Sulfurimonas* species and other *Campylobacteria* as apparent homologs are present in genomes of various *Campylobacteria*. Homologues In S_8 -grown cultures, this protein showed an almost threefold increase in relative abundance. Possibly, this protein could be involved in the activation of S_8 , similar to the outer membrane protein identified in *A. caldus* (Ramírez *et al.*, 2004; Mangold *et al.*, 2011; Chen *et al.*, 2012), although no similarity was observed between these proteins. On the other hand, transcripts showed an opposite trend with the level of WP_011373531.1 gene expression being higher under the thiosulfate condition, making a specific role in S_8 metabolism less certain. However, the relative abundance of the transcripts is influenced by the absolute number of identified transcripts and translation could further be prevented by posttranscriptional regulation, making the proteomic data overall a better indicator for the involvement of the protein under different growth conditions. Thus, although it is presently not possible to assign a function to this protein, the results indicate that it may play a fundamental role in the cells' metabolism, including the possibility of its involvement in S_8 metabolism. To resolve the role of this protein in *S. denitrificans*, and potentially other *Campylobacteria*, more work is needed. Such experiments, however, were beyond the scope of this thesis, since they would rely on heterologous gene expression assays or a genetic system for *S. denitrificans*, which is currently not available.

4.2.1 The expression of genes and proteins involved in energy metabolism

Chemoautotrophic bacteria gain energy through redox reactions. In the present experiments, *S. denitrificans* coupled the reduction of nitrate with the oxidation of thiosulfate or cyclooctasulfur to gain energy for growth. All proteins of the canonical denitrification pathway were identified, but no protein of the proposed alternative non-electrogenic gNOR system (Sievert, Scott, *et al.*, 2008). To the best of my knowledge, this provides the first validation of a functional cNOR system that lacks the components encoded by *norD* and *norQ*, which are absent from the genome of *S. denitrificans* and other *Campylobacteria* (Sievert, Scott, *et al.*, 2008).

Besides the utilization of nitrate, *S. denitrificans* can utilize oxygen using a *cbb3*-type cytochrome *c* oxidase (Sievert, Scott, *et al.*, 2008). All genes were transcribed under both conditions (Figure 16), which could be either an indicator for the presence of small amounts of oxygen in the batch culture system, for example by leakage through the butyl stoppers, or for constitutive transcription. In addition, genes for the membrane bound [Ni,Fe]-uptake hydrogenase and genes for the formate dehydrogenase were transcribed (Figure 16), although no hydrogen or formate was provided in the cultivation medium. Notably, even though low level of transcripts for hydrogenase could be detected in the absence of hydrogen, the transcripts for the hydrogenase are highly upregulated in the presence of hydrogen (unpublished data) which further confirms the present observations of upregulated proteins within the proteome of *S. denitrificans* grown with hydrogen (Figure 9). The simultaneous transcription (at a low level) of genes for the utilization of alternative substrates could be an additional mechanism to react quickly when either oxygen or hydrogen become available in the environment.

4.2.2 Flagella likely facilitate attachment to S₈

Cyclooctasulfur is a solid substrate, which likely requires the attachment of cells to make it accessible (Mangold *et al.*, 2011; Pjevac *et al.*, 2014). Proteins of the flagellar apparatus have been shown to play a critical role in attachment and biofilm formation, including in *Campylobacter* (e.g. O'Toole and Kolter, 1998; Pratt and Kolter, 1998; Ottemann and Lowenthal, 2002; Joshua *et al.*, 2006; Haiko and Westerlund-Wikström, 2013). Previously, Mangold and colleagues identified a flagellar basal-body rod protein (FlgC) to be up-regulated in S⁰-grown vs. tetrathionate-grown cultures of *A. caldus*, facilitating attachment to the solid substrate (Mangold *et al.*, 2011). Interestingly, the only COG category that showed differences between the two growth conditions encompassed genes of the flagellar apparatus. Specifically, transcriptomic data showed a significantly higher expression of genes involved in flagella biosynthesis and flagella motility in S₈-grown cultures (Figure 13). Thus, it is proposed that the increased transcription of flagella-related genes as well as the higher relative abundance of FlgE (flagellar hook protein) and flagellin in S₈-grown cultures is indicative of attachment and biofilm formation on cyclooctasulfur particles. On the other hand, genes related to chemotaxis showed a trend of higher expression in thiosulfate-grown cultures, indicating that chemotaxis is more important in sensing gradients of the soluble substrate thiosulfate. In this context, it is important to note that while the original strain used in the experiments has been described as non-motile, *S. denitrificans* has regained motility during cultivation in the Sievert laboratory (unpublished data). This is attributed to the spontaneous excision of the transposon that was

shown to interrupt a flagellin biosynthesis operon, as its genome otherwise contains all genes required for a fully functional flagellar apparatus (Sievert, Scott, *et al.*, 2008).

4.2.3 The mechanism of thiosulfate- and S₈-oxidation

With the exception of the potential involvement of the hypothetical protein in the activation and transport of S₈ into the cell, it was not possible to identify a possible mechanism for the activation of cyclooctasulfur, as has for example been proposed for acidophilic sulfur-oxidizing bacteria (Rohwerder and Sand, 2003; Mangold *et al.*, 2011; Chen *et al.*, 2012). However, the data confirm the previously hypothesized differential regulation of the two SOX gene clusters present in *S. denitrificans* in response to the available sulfur substrate (Sievert, Scott, *et al.*, 2008; Meier *et al.*, 2017; Pjevac *et al.*, 2018), allowing us to propose a possible oxidation pathway. In thiosulfate-grown cultures, the first gene cluster encoding *soxABXY₁Z₁* was highly transcribed and the corresponding proteins were found in significantly higher abundance compared to growth with S₈, confirming their involvement in thiosulfate oxidation as previously proposed (Friedrich *et al.*, 2001, 2005). The differential abundance of the SoxABXY₁Z₁-proteins is in contrast to the phototrophic sulfur-oxidizing gammaproteobacterium *A. vinosum*, for which no differences were observed in response to different sulfur compounds (Weissgerber *et al.*, 2014). Under both growth conditions, *soxY₂Z₂* was highly transcribed and the corresponding proteins were highly abundant in *S. denitrificans*, suggesting that it plays an important role in the oxidation of both thiosulfate and S₈ (Figure 4). In contrast, SoxCD proteins were significantly more abundant in S₈-grown cultures. Although the *soxABXY₁Z₁*-operon was present in the transcriptome, it was nearly undetectable in the proteome, suggesting that it might be under post-transcriptional control and not translated into functional proteins when *S. denitrificans* is grown with S₈ (Picard *et al.*, 2009; Van Assche *et al.*, 2015) or translated at low levels preventing the detection of the proteins by the used methods. Thus, it is proposed that the oxidation of S₈ is mediated mainly by *soxCDY₂Z₂*, and the low abundance of transcripts and in particular of proteins of the *soxABXY₁Z₁* operon in S₈-grown cultures is interpreted as another reflection of baseline activity and for metabolic flexibility, allowing *S. denitrificans* to quickly respond to the availability of thiosulfate. This interpretation is in line with qPCR data that showed the presence of *soxB* transcripts in low abundance in hydrogen-grown *S. denitrificans* cultures lacking reduced sulfur compounds, and their increased abundance in the presence of thiosulfate, while *soxD* transcripts remained more or less unchanged, pointing to its constitutive expression (unpublished data).

4.2.4 An alternative model for sulfur oxidation in *Sulfurimonas denitrificans*

Based on the observations on the differential abundance of the SOX proteins during growth on thiosulfate versus S₈ and previous results (Friedrich *et al.*, 2001b, 2005; Sauvé *et al.*, 2007; Grabarczyk and Berks, 2017), a sulfur oxidation model for the oxidation of S₈ by *S. denitrificans* is proposed that does not involve the SoxABXY₁Z₁ protein complex (Figure 17). At present, it is not possible to resolve how the sulfonate group bound to SoxY₂Z₂ is being hydrolyzed to form sulfate. One option could be that SoxB, which might be present in low abundance, could perform that function. However, another possibility might be that the putative periplasmic metallo-hydrolase encoded by WP_011373670.1 could perform this function. This scenario appears intriguing as this gene is located next to soxCDY₂Z₂ and homologs of this gene are found in other sulfur-oxidizing *Campylobacteria* with conserved synteny. The protein's catalytic domain has similarities to SoxH of *Paracoccus pantotrophus*. However, while *soxH* expression is specifically induced by thiosulfate, it is not required for sulfur oxidation in *P. pantotrophus* and its function is currently unknown (Rother *et al.*, 2001), although it has been described as a putative thiol hydrolase (Friedrich *et al.*, 2001b). Lastly, it might be possible that SoxCDY₂Z₂ can catalyze the reaction by itself, although there is at present no evidence to support this hypothesis. Future experiments need to be carried out to differentiate between these options. Thiosulfate oxidation by *S. denitrificans* proceeds mainly as proposed in the current sulfur oxidation model (Friedrich *et al.*, 2001, 2005; Grabarczyk and Berks, 2017). First, thiosulfate is activated via SoxXA and bound to a cysteine residue of SoxY in the SoxY₁Z₁ complex, followed by the hydrolysis of the outer sulfonate group of the bound thiosulfate by SoxB (Friedrich *et al.*, 2001). However, it is hypothesized that subsequently the sulfone group is being transferred to SoxY₂Z₂, where it is oxidized and hydrolyzed to sulfate as described above, in line with the high abundance of SoxCD and in particular SoxY₂Z₂ under both growth conditions. Based on the operon structure and the observed expression pattern, it is postulated that SoxY₂Z₂ interacts specifically with SoxCD. This way, it is proposed that SoxCDY₂Z₂ is always present, whereas SoxABXY₁Z₁ is only needed in the presence of thiosulfate. Biochemical and genetic studies will be required to validate this proposed model for the oxidation of S₈ and thiosulfate in *S. denitrificans* and other *Campylobacteria* with the same genetic arrangement of the SOX system.

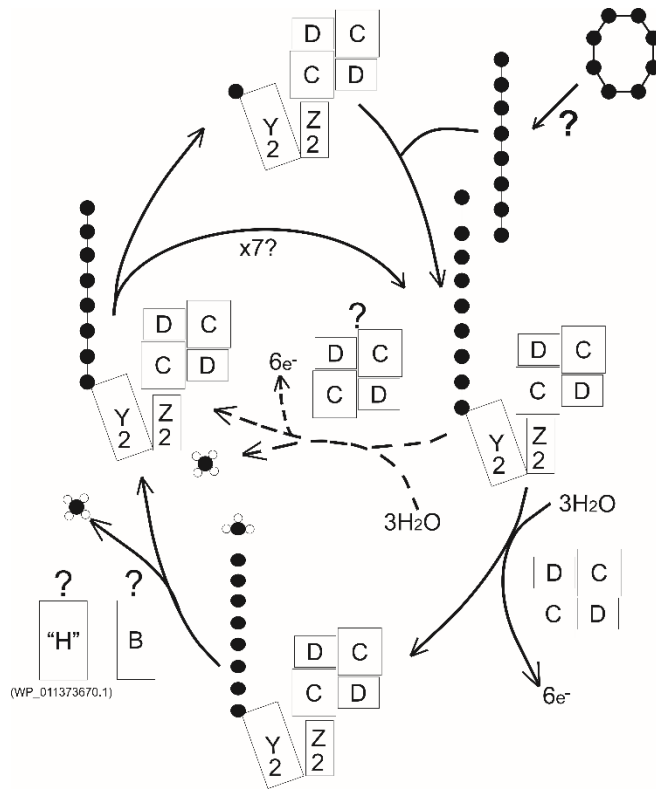


Figure 17 Model for the oxidation of elemental sulfur chains in *S. denitrificans*. The activation mechanism of cyclooctasulfur and the hydrolysis step resulting in the liberation of SO_4^{2-} from the outer sulfonate group (indicated with a '?') are currently unknown. The 'x7' indicates that the sulfur chain attached to SoxY2 might be oxidized completely (or in part) before accepting a new sulfur chain. Sulfur is indicated as black dot, whereas oxygen is indicated as small white circles on sulfur. Published in (Götz, Pjevac, *et al.*, 2018).

In addition to the described function in *S. denitrificans*, the *soxY₂Z₂* genes of the *soxCDY₂Z₂* operon show a much higher level of diversification between different *Sulfurimonas* and *Sulfurovum* species (up to 79% nucleotide sequence dissimilarity) than *soxY₁Z₁* of the *soxABXY₁Z₁* operon (Meier *et al.*, 2017). Moreover, the sequence similarity between the two SoxYZ copies in *S. denitrificans* and other *Campylobacteria* is very low. The amino acid sequence identity is 33% for the two SoxY proteins, and 28% (over a 61% alignment fraction) for the two SoxZ proteins of *S. denitrificans*. In fact, no significant identity, except for the export signal sequence, is detectable on the nucleotide level for either gene. This highly divergent intragenomic duplication, and the intergenomic diversification of the SoxY₂Z₂ proteins, is present in all currently available *Sulfurimonas* and *Sulfurovum* genomes (Meier *et al.*, 2017). Furthermore, a significantly higher expression level of SoxY₂Z₂ proteins when compared to SoxY₁Z₁ proteins has been found in the metaproteomes of *Campylobacteria*-dominated biofilms forming on black-smoker chimneys (Pjevac *et al.*, 2018). The

diversification of the SoxY₂Z₂ proteins could lead to different substrate preferences with respect to the chain length of the bound polysulfide or to differences in overall substrate-binding affinities, and may therefore be involved in niche partitioning between co-occurring *Sulfurimonas* and *Sulfurovum* species, whereas the SoxY₁Z₁ proteins are specific for thiosulfate, explaining their lower diversity and lower abundance in environmental samples, where thiosulfate is usually present in lower concentrations than elemental sulfur or polysulfide (Zopfi *et al.*, 2004). Potentially, the ratio of the SoxCD to SoxAB proteins (SoxCD/SoxAB: S₈:19; TS:0.9) and SoxY₂Z₂ to SoxY₁Z₁ proteins (SoxY₂Z₂/ SoxY₁Z₁: S₈:89; TS:9) , and to a lesser extent that of the transcripts (*soxCD/soxAB*: S₈:2.7; TS:1.5 and *soxY₂Z₂/soxY₁Z₁*: S₈:3.3; TS:1.9), could be used as an indicator for the type of sulfur compound being utilized by *Sulfurimonas* and possibly other sulfur-oxidizing *Campylobacteria* in the environment. In the metaproteomes analyzed here, only some proteins of the SoxCDY₂Z₂ cluster and no proteins of the SoxABXY₁Z₁ cluster were identified, suggesting that elemental sulfur is likely an important electron donor at Crab Spa.

5 Conclusion and Outlook

The post-genomic analysis of microbial communities is needed to reveal the most active and abundant biochemical pathways of a system. This aids in the understanding of the overall functionality of the ecosystem and with that gives clues to what extent our knowledge from cultured representatives matches. The data suggest that the Crab Spa microbial community mirrors the chemistry of the seafloor biosphere in the up and down regulation of proteins involved in the energy metabolism of the three most dominant genera *Sulfurimonas*, *Sulfurovum* and *Arcobacter*. To investigate a functional difference between *Sulfurimonas* and *Sulfurovum* a higher resolution of their proteomes and biochemical analysis of key-enzymes of unknown function in cultured representatives is needed as well as an improved and more detailed database fueled by quick sequencing of single cell genomes. A more single cell genome focused database would allow to distinguish between single species for each genus and thus might solve the riddle of micro-diversity as a part of the complexity of a system. Technological advancements are needed to provide higher resolutions of proteomes and to create more single cell genome focused databases.

Parts in the following conclusion have been published in (Götz, Pjevac, et al., 2018).

Multiple adaptation mechanism of *Sulfurimonas denitrificans* to various substrates in both batch and chemostat cultures were identified. Since post-genomic analysis does not only answer questions, but rather opens a whole list of unanswered questions, culture experiments in addition to genetics and biochemical analysis of single proteins are needed. Here, transcriptomics and proteomics were applied as two powerful approaches to identify biochemical pathways involved in the oxidation of two different sulfur compounds by *S. denitrificans*. The data show that in response to the available sulfur substrate, the SOX system in *S. denitrificans* is differentially regulated. Based on the available data, a model for the oxidation of cyclooctasulfur in *S. denitrificans* was proposed, which further has been confirmed and supported by the results of Lahme *et al.* (2020). Further a hypothetical protein was identified that may play a central role in the metabolism of reduced sulfur compounds. In the future, genetic and biochemical studies are needed on abundant hypothetical proteins to investigate their function. Especially in the present case, the potential involvement of the identified hypothetical protein in the activation of S₈ needs clarification. A validation of the proposed model for sulfur oxidation in *S. denitrificans*, which is likely active in other sulfur-oxidizing *Campylobacteria*, is needed to understand the usage of the available elemental sulfur

in Crab Spa and other hydrothermal environments. In addition to the advanced understanding of the r-strategist *Sulfurimonas*, the data presented in this thesis will aid in the interpretation of environmental metatranscriptomic and –proteomic data sets derived from redox environments dominated by *Campylobacteria*.

6 References

- Alonso-Azcárate, J., Bottrell, S.H., and Tritlla, J. (2001) Sulfur redox reactions and formation of native sulfur veins during low grade metamorphism of gypsum evaporites, Cameros Basin (NE Spain). *Chem Geol* **174**: 389–402.
- Berg, H.C. (1975) Chemotaxis in bacteria. *Annu Rev Biophys Bioeng* **4**: 119–136.
- Blazewicz, S.J., Barnard, R.L., Daly, R.A., and Firestone, M.K. (2013) Evaluating rRNA as an indicator of microbial activity in environmental communities: limitations and uses. *ISME J* **7**: 2061–2068.
- Boratyn, G.M., Schäffer, A.A., Agarwala, R., Altschul, S.F., Lipman, D.J., and Madden, T.L. (2012) Domain enhanced lookup time accelerated BLAST. *Biol Direct* **7**: 12.
- Campbell, B.J., Engel, A.S., Porter, M.L., and Takai, K. (2006) The versatile ϵ -proteobacteria: key players in sulphidic habitats. *Nat Rev Microbiol* **4**: 458–468.
- Caporaso, J.G., Kuczynski, J., Stombaugh, J., Bittinger, K., Bushman, F.D., Costello, E.K., *et al.* (2010) QIIME allows analysis of high-throughput community sequencing data. *Nat Methods* **7**: 335–336.
- Cavanaugh, C.M., Gardiner, S.L., Jones, M.L., Jannasch, H.W., and Waterbury, J.B. (1981) Prokaryotic Cells in the Hydrothermal Vent Tube Worm Riftia pachyptila Jones: Possible Chemoautotrophic Symbionts. *Science* **213**: 340–342.
- Chen, L., Ren, Y., Lin, Jianqun, Liu, X., Pang, X., and Lin, Jianqiang (2012) Acidithiobacillus caldus Sulfur Oxidation Model Based on Transcriptome Analysis between the Wild Type and Sulfur Oxygenase Reductase Defective Mutant. *PLOS ONE* **7**: e39470.
- Corliss, J.B., Dymond, J., Gordon, L.I., Edmond, J.M., Herzen, R.P. von, Ballard, R.D., *et al.* (1979) Submarine Thermal Springs on the Galápagos Rift. *Science* **203**: 1073–1083.
- Cosmidis, J. and Templeton, A.S. (2016) Self-assembly of biomorphic carbon/sulfur microstructures in sulfidic environments. *Nat Commun* **7**: ncomms12812.
- Dahl, C., Friedrich, C., and Kletzin, A. (2008) Sulfur Oxidation in Prokaryotes. In *eLS*. John Wiley & Sons, Ltd.
- Dahl, C. and Prange, A. (2006) Bacterial Sulfur Globules: Occurrence, Structure and Metabolism. In *Inclusions in Prokaryotes*. Shively, D.J.M. (ed). Springer Berlin Heidelberg, pp. 21–51.
- Dahle, H., Roalkvam, I., Thorseth, I.H., Pedersen, R.B., and Steen, I.H. (2013) The versatile in situ gene expression of an Epsilonproteobacteria-dominated biofilm from a hydrothermal chimney. *Environ Microbiol Rep* **5**: 282–290.
- Damm, K.L.V. and Lilley, M.D. (2013) Diffuse Flow Hydrothermal Fluids from 9° 50' N East Pacific Rise: Origin, Evolution and Biogeochemical Controls. In *The Subseafloor Biosphere at Mid-Ocean Ridges*. American Geophysical Union (AGU), pp. 245–268.
- Dietrich, W. and Klimmek, O. (2002) The function of methyl-menaquinone-6 and polysulfide reductase membrane anchor (PsrC) in polysulfide respiration of Wolinella succinogenes. *Eur J Biochem* **269**: 1086–1095.
- Dworkin, M. (2012) Sergei Winogradsky: a founder of modern microbiology and the first microbial ecologist. *FEMS Microbiol Rev* **36**: 364–379.
- Engel, A.S., Porter, M.L., Stern, L.A., Quinlan, S., and Bennett, P.C. (2004) Bacterial diversity and ecosystem function of filamentous microbial mats from aphotic (cave) sulfidic springs dominated by chemolithoautotrophic “Epsilonproteobacteria.” *FEMS Microbiol Ecol* **51**: 31–53.
- Eymann, C., Dreisbach, A., Albrecht, D., Bernhardt, J., Becher, D., Gentner, S., *et al.* (2004) A comprehensive proteome map of growing Bacillus subtilis cells. *PROTEOMICS* **4**: 2849–2876.

- Felbeck, H. (1981) Chemoautotrophic Potential of the Hydrothermal Vent Tube Worm, *Riftia pachyptila* Jones (Vestimentifera). *Science* **213**: 336–338.
- Finster, K. (2008) Microbiological disproportionation of inorganic sulfur compounds. *J Sulfur Chem* **29**: 281–292.
- Fortunato, C.S., Larson, B., Butterfield, D.A., and Huber, J.A. (2018) Spatially distinct, temporally stable microbial populations mediate biogeochemical cycling at and below the seafloor in hydrothermal vent fluids. *Environ Microbiol* **20**: 769–784.
- Franz, B., Lichtenberg, H., Hormes, J., Modrow, H., Dahl, C., and Prange, A. (2007) Utilization of solid ‘elemental’ sulfur by the phototrophic purple sulfur bacterium *Allochromatium vinosum*: a sulfur K-edge X-ray absorption spectroscopy study. *Microbiology* **153**: 1268–1274.
- Friedrich, C.G., Bardischewsky, F., Rother, D., Quentmeier, A., and Fischer, J. (2005) Prokaryotic sulfur oxidation. *Curr Opin Microbiol* **8**: 253–259.
- Friedrich, C.G., Rother, D., Bardischewsky, F., Quentmeier, A., and Fischer, J. (2001) Oxidation of Reduced Inorganic Sulfur Compounds by Bacteria: Emergence of a Common Mechanism? *Appl Environ Microbiol* **67**: 2873–2882.
- Gardebrecht, A., Markert, S., Sievert, S.M., Felbeck, H., Thürmer, A., Albrecht, D., *et al.* (2012) Physiological homogeneity among the endosymbionts of *Riftia pachyptila* and *Tevnia jerichonana* revealed by proteogenomics. *ISME J* **6**: 766–776.
- Götz, F., Longnecker, K., Soule, M.C.K., Becker, K.W., McNichol, J., Kujawinski, E.B., and Sievert, S.M. (2018) Targeted metabolomics reveals proline as a major osmolyte in the chemolithoautotroph *Sulfurimonas denitrificans*. *MicrobiologyOpen* **7**: e00586.
- Götz, F., Pjevac, P., Markert, S., McNichol, J., Becher, D., Schweder, T., *et al.* (2018) Transcriptomic and proteomic insight into the mechanism of cyclooctasulfur- versus thiosulfate-oxidation by the chemolithoautotroph *Sulfurimonas denitrificans*: S₈ metabolism in *Sulfurimonas denitrificans*. *Environ Microbiol* **1**: 244–258.
- Grabarczyk, D.B. and Berks, B.C. (2017) Intermediates in the Sox sulfur oxidation pathway are bound to a sulfane conjugate of the carrier protein SoxYZ. *PLOS ONE* **12**: e0173395.
- Grote, J., Labrenz, M., Pfeiffer, B., Jost, G., and Jürgens, K. (2007) Quantitative Distributions of Epsilonproteobacteria and a *Sulfurimonas* Subgroup in Pelagic Redoxclines of the Central Baltic Sea. *Appl Environ Microbiol* **73**: 7155–7161.
- Grote, J., Schott, T., Bruckner, C.G., Glöckner, F.O., Jost, G., Teeling, H., *et al.* (2012) Genome and physiology of a model Epsilonproteobacterium responsible for sulfide detoxification in marine oxygen depletion zones. *Proc Natl Acad Sci U S A* **109**: 506–510.
- Gulmann, L.K., Beaulieu, S.E., Shank, T.M., Ding, K., Seyfried, W.E.J., and Sievert, S.M. (2015) Bacterial diversity and successional patterns during biofilm formation on freshly exposed basalt surfaces at diffuse-flow deep-sea vents. *Front Microbiol* **6**: 901.
- Hahne, H., Mäder, U., Otto, A., Bonn, F., Steil, L., Bremer, E., *et al.* (2010) A Comprehensive Proteomics and Transcriptomics Analysis of *Bacillus subtilis* Salt Stress Adaptation. *J Bacteriol* **192**: 870–882.
- Haiko, J. and Westerlund-Wikström, B. (2013) The Role of the Bacterial Flagellum in Adhesion and Virulence. *Biology* **2**: 1242–1267.
- Han, Y. and Perner, M. (2014) The Role of Hydrogen for *Sulfurimonas denitrificans*’ Metabolism. *PLOS ONE* **9**: e106218.
- Heinz, E., Williams, T.A., Nakjang, S., Noël, C.J., Swan, D.C., Goldberg, A.V., *et al.* (2012) The genome of the obligate intracellular parasite *Trachipleistophora hominis*: new insights into microsporidian genome dynamics and reductive evolution. *PLoS Pathog* **8**: e1002979.

- Huber, J.A., Welch, D.B.M., Morrison, H.G., Huse, S.M., Neal, P.R., Butterfield, D.A., and Sogin, M.L. (2007) Microbial Population Structures in the Deep Marine Biosphere. *Science* **318**: 97–100.
- Hubert, C.R.J., Oldenburg, T.B.P., Fustic, M., Gray, N.D., Larter, S.R., Penn, K., *et al.* (2012) Massive dominance of Epsilonproteobacteria in formation waters from a Canadian oil sands reservoir containing severely biodegraded oil. *Environ Microbiol* **14**: 387–404.
- Hügler, M. and Sievert, S.M. (2011) Beyond the Calvin Cycle: Autotrophic Carbon Fixation in the Ocean. *Annu Rev Mar Sci* **3**: 261–289.
- Hügler, M., Wirsén, C.O., Fuchs, G., Taylor, C.D., and Sievert, S.M. (2005) Evidence for Autotrophic CO₂ Fixation via the Reductive Tricarboxylic Acid Cycle by Members of the ϵ Subdivision of Proteobacteria. *J Bacteriol* **187**: 3020–3027.
- Joshua, G.W.P., Guthrie-Irons, C., Karlyshev, A.V., and Wren, B.W. (2006) Biofilm formation in *Campylobacter jejuni*. *Microbiology* **152**: 387–396.
- Kamysny, A. (2009) Solubility of cyclooctasulfur in pure water and sea water at different temperatures. *Geochim Cosmochim Acta* **73**: 6022–6028.
- Kletzin, A., Urich, T., Müller, F., Bandejas, T.M., and Gomes, C.M. (2004) Dissimilatory oxidation and reduction of elemental sulfur in thermophilic archaea. *J Bioenerg Biomembr* **36**: 77–91.
- Lahme, S., Callbeck, C.M., Eland, L.E., Wipat, A., Enning, D., Head, I.M., and Hubert, C.R.J. (2020) Comparison of sulfide-oxidizing *Sulfurimonas* strains reveals a new mode of thiosulfate formation in subsurface environments. *Environ Microbiol* **22**: 1784–1800.
- Lau, G.E., Cosmidis, J., Grasby, S.E., Trivedi, C.B., Spear, J.R., and Templeton, A.S. (2017) Low-temperature formation and stabilization of rare allotropes of cyclooctasulfur (β -S₈ and γ -S₈) in the presence of organic carbon at a sulfur-rich glacial site in the Canadian High Arctic. *Geochim Cosmochim Acta* **200**: 218–231.
- Lavik, G., Stührmann, T., Brüchert, V., Plas, A.V. der, Mohrholz, V., Lam, P., *et al.* (2009) Detoxification of sulphidic African shelf waters by blooming chemolithotrophs. *Nature* **457**: 581.
- Le Bris, N., Govenar, B., Le Gall, C., and Fisher, C.R. (2006) Variability of physico-chemical conditions in 9°50'N EPR diffuse flow vent habitats. *Mar Chem* **98**: 167–182.
- Legatzki, A., Ortiz, M., Neilson, J.W., Dominguez, S., Andersen, G.L., Toomey, R.S., *et al.* (2011) Bacterial and Archaeal Community Structure of Two Adjacent Calcite Speleothems in Kartchner Caverns, Arizona, USA. *Geomicrobiol J* **28**: 99–117.
- Li, B., Ruotti, V., Stewart, R.M., Thomson, J.A., and Dewey, C.N. (2010) RNA-Seq gene expression estimation with read mapping uncertainty. *Bioinformatics* **26**: 493–500.
- Li, R., Morrison, L., Collins, G., Li, A., and Zhan, X. (2016) Simultaneous nitrate and phosphate removal from wastewater lacking organic matter through microbial oxidation of pyrrhotite coupled to nitrate reduction. *Water Res* **96**: 32–41.
- Lonsdale, P. (1977) Clustering of suspension-feeding macrobenthos near abyssal hydrothermal vents at oceanic spreading centers. *Deep Sea Res* **24**: 857–863.
- López-García, P., Duperron, S., Philippot, P., Foriel, J., Susini, J., and Moreira, D. (2003) Bacterial diversity in hydrothermal sediment and epsilonproteobacterial dominance in experimental microcolonizers at the Mid-Atlantic Ridge. *Environ Microbiol* **5**: 961–976.
- Lowell, R.P., Rona, P.A., and Herzen, R.P.V. (1995) Seafloor hydrothermal systems. *J Geophys Res Solid Earth* **100**: 327–352.
- Macalady, J.L., Dattagupta, S., Schaperdoth, I., Jones, D.S., Druschel, G.K., and Eastman, D. (2008) Niche differentiation among sulfur-oxidizing bacterial populations in cave waters. *ISME J* **2**: 590–601.

- Madrid, V.M., Taylor, G.T., Scranton, M.I., and Chistoserdov, A.Y. (2001) Phylogenetic Diversity of Bacterial and Archaeal Communities in the Anoxic Zone of the Cariaco Basin. *Appl Environ Microbiol* **67**: 1663–1674.
- Maier, T., Schmidt, A., Güell, M., Kühner, S., Gavin, A.-C., Aebersold, R., and Serrano, L. (2011) Quantification of mRNA and protein and integration with protein turnover in a bacterium. *Mol Syst Biol* **7**: 511.
- Mangold, S., Valdés, J., Holmes, D., and Dopson, M. (2011) Sulfur Metabolism in the Extreme Acidophile *Acidithiobacillus Caldus*. *Front Microbiol* **2**: doi:10.3389/fmicb.2011.00017.
- Markert, S., Arndt, C., Felbeck, H., Becher, D., Sievert, S.M., Hügler, M., *et al.* (2007) Physiological Proteomics of the Uncultured Endosymbiont of *Riftia pachyptila*. *Science* **315**: 247–250.
- McNichol, J., Stryhanyuk, H., Sylva, S.P., Thomas, F., Musat, N., Seewald, J.S., and Sievert, S.M. (2018) Primary productivity below the seafloor at deep-sea hot springs. *Proc Natl Acad Sci* **115**: 6756–6761.
- McNichol, J., Sylva, S.P., Thomas, F., Taylor, C.D., Sievert, S.M., and Seewald, J.S. (2016) Assessing Microbial Processes in Deep-Sea Hydrothermal Systems via Incubations at In Situ Temperature and Pressure. *Deep Sea Res Part Oceanogr Res Pap.* **115**: 221–232.
- Meier, D.V., Pjevac, P., Bach, W., Hourdez, S., Girguis, P.R., Vidoudez, C., *et al.* (2017) Niche partitioning of diverse sulfur-oxidizing bacteria at hydrothermal vents. *ISME J.* **7**: 1545–1558.
- Meyer, J.L., Akerman, N.H., Proskurowski, G., and Huber, J.A. (2013) Microbiological characterization of post-eruption “snowblower” vents at Axial Seamount, Juan de Fuca Ridge. *Front Microbiol* **4**: <https://doi.org/10.3389/fmicb.2013.00153>.
- Möller, L., Laas, P., Rogge, A., Goetz, F., Bahlo, R., Leipe, T., and Labrenz, M. (2019) Sulfurimonas subgroup GD17 cells accumulate polyphosphate under fluctuating redox conditions in the Baltic Sea: possible implications for their ecology. *ISME J* **13**: 482.
- Nakagawa, S. and Takai, K. (2008) Deep-sea vent chemoautotrophs: diversity, biochemistry and ecological significance. *FEMS Microbiol Ecol* **65**: 1–14.
- Nakagawa, S., Takai, K., Inagaki, F., Hirayama, H., Nunoura, T., Horikoshi, K., and Sako, Y. (2005) Distribution, phylogenetic diversity and physiological characteristics of epsilon-Proteobacteria in a deep-sea hydrothermal field. *Environ Microbiol* **7**: 1619–1632.
- O’Toole, G.A. and Kolter, R. (1998) Flagellar and twitching motility are necessary for *Pseudomonas aeruginosa* biofilm development. *Mol Microbiol* **30**: 295–304.
- Ottemann, K.M. and Lowenthal, A.C. (2002) *Helicobacter pylori* uses motility for initial colonization and to attain robust infection. *Infect Immun* **70**: 1984–1990.
- Otto, A., Bernhardt, J., Meyer, H., Schaffer, M., Herbst, F.-A., Siebourg, J., *et al.* (2010) Systems-wide temporal proteomic profiling in glucose-starved *Bacillus subtilis*. *Nat Commun* **1**: 137.
- Pedersen, S., Bloch, P.L., Reeh, S., and Neidhardt, F.C. (1978) Patterns of protein synthesis in *E. coli*: a catalog of the amount of 140 individual proteins at different growth rates. *Cell* **14**: 179–190.
- Picard, F., Dressaire, C., Girbal, L., and Coccia-Bousquet, M. (2009) Examination of post-transcriptional regulations in prokaryotes by integrative biology. *C R Biol* **332**: 958–973.
- Pjevac, P., Kamysny, A., Dykma, S., and Mußmann, M. (2014) Microbial consumption of zero-valence sulfur in marine benthic habitats. *Environ Microbiol* **16**: 3416–3430.
- Pjevac, P., Meier, D.V., Markert, S., Hentscher, C., Schweder, T., Becher, D., *et al.* (2018) Metaproteogenomic Profiling of Microbial Communities Colonizing Actively Venting Hydrothermal Chimneys. *Front Microbiol* **9**: <https://doi.org/10.3389/fmicb.2018.00680>.

- Plugge, C.M. (2005) Anoxic Media Design, Preparation, and Considerations. In *Methods in Enzymology*. Environmental Microbiology. Academic Press, pp. 3–16.
- Ponnudurai, R., Kleiner, M., Sayavedra, L., Petersen, J.M., Moche, M., Otto, A., *et al.* (2017) Metabolic and physiological interdependencies in the *Bathymodiolus azoricus* symbiosis. *ISME J* **11**: 463.
- Prange, A., Chauvistré, R., Modrow, H., Hormes, J., Trüper, H.G., and Dahl, C. (2002) Quantitative speciation of sulfur in bacterial sulfur globules: X-ray absorption spectroscopy reveals at least three different species of sulfur. *Microbiology* **148**: 267–276.
- Pratt, L.A. and Kolter, R. (1998) Genetic analysis of *Escherichia coli* biofilm formation: roles of flagella, motility, chemotaxis and type I pili. *Mol Microbiol* **30**: 285–293.
- Raiswell, R. (1992) Evolution of the global biogeochemical sulphur cycle, scope 39 edited by P. Brimblecombe and A. Y. Lein. John Wiley and Sons, Chichester, 1989. No. of pages: 241. Price: £56.95 (hardback). *Geol J* **27**: 192–193.
- Ramírez, P., Guiliani, N., Valenzuela, L., Beard, S., and Jerez, C.A. (2004) Differential Protein Expression during Growth of *Acidithiobacillus ferrooxidans* on Ferrous Iron, Sulfur Compounds, or Metal Sulfides. *Appl Environ Microbiol* **70**: 4491–4498.
- Reeves, E.P., McDermott, J.M., and Seewald, J.S. (2014) The origin of methanethiol in midocean ridge hydrothermal fluids. *Proc Natl Acad Sci* **111**: 5474–5479.
- Rideout, J.R., He, Y., Navas-Molina, J.A., Walters, W.A., Ursell, L.K., Gibbons, S.M., *et al.* (2014) Subsampled open-reference clustering creates consistent, comprehensive OTU definitions and scales to billions of sequences. *PeerJ* **2**: e545.
- Robertson, L.A. and Kuenen, J.G. (2006) The Colorless Sulfur Bacteria. In *The Prokaryotes*. Dr, M.D.P., Falkow, S., Rosenberg, E., Schleifer, K.-H., and Stackebrandt, E. (eds). Springer New York, pp. 985–1011.
- Rogge, A., Vogts, A., Voss, M., Jürgens, K., Jost, G., and Labrenz, M. (2017) Success of chemolithoautotrophic SUP05 and *Sulfurimonas* GD17 cells in pelagic Baltic Sea redox zones is facilitated by their lifestyles as K- and r-strategists. *Environ Microbiol* **19**: 2495–2506.
- Rohwerder, T. and Sand, W. (2003) The sulfane sulfur of persulfides is the actual substrate of the sulfur-oxidizing enzymes from *Acidithiobacillus* and *Acidiphilium* spp. *Microbiology* **149**: 1699–1710.
- Rother, D., Henrich, H.-J., Quentmeier, A., Bardischewsky, F., and Friedrich, C.G. (2001) Novel Genes of the sox Gene Cluster, Mutagenesis of the Flavoprotein SoxF, and Evidence for a General Sulfur-Oxidizing System in *Paracoccus pantotrophus* GB17. *J Bacteriol* **183**: 4499–4508.
- Ruby, E.G., Wirsén, C.O., and Jannasch, H.W. (1981) Chemolithotrophic Sulfur-Oxidizing Bacteria from the Galapagos Rift Hydrothermal Vents. *Appl Environ Microbiol* **42**: 317–324.
- Santoro, A.E., Dupont, C.L., Richter, R.A., Craig, M.T., Carini, P., McIlvin, M.R., *et al.* (2015) Genomic and proteomic characterization of “*Candidatus Nitrosopelagicus brevis*”: An ammonia-oxidizing archaeon from the open ocean. *Proc Natl Acad Sci* **112**: 1173–1178.
- Sauvé, V., Bruno, S., Berks, B.C., and Hemmings, A.M. (2007) The SoxYZ Complex Carries Sulfur Cycle Intermediates on a Peptide Swinging Arm. *J Biol Chem* **282**: 23194–23204.
- Scheirer, D.S., Shank, T.M., and Fornari, D.J. (2006) Temperature variations at diffuse and focused flow hydrothermal vent sites along the northern East Pacific Rise. *Geochem Geophys Geosystems* **7**: <https://doi.org/10.1029/2005GC001094>.
- Selinger, D.W., Saxena, R.M., Cheung, K.J., Church, G.M., and Rosenow, C. (2003) Global RNA Half-Life Analysis in *Escherichia coli* Reveals Positional Patterns of Transcript Degradation. *Genome Res* **13**: 216–223.

- Shank, T.M., Fornari, D.J., Von Damm, K.L., Lilley, M.D., Haymon, R.M., and Lutz, R.A. (1998) Temporal and spatial patterns of biological community development at nascent deep-sea hydrothermal vents (9°50'N, East Pacific Rise). *Deep Sea Res Part II Top Stud Oceanogr* **45**: 465–515.
- Sievert, S., Kiene, R., and Schulz-Vogt, H. (2007) The Sulfur Cycle. *Oceanography* **20**: 117–123.
- Sievert, S. and Vetriani, C. (2012) Chemoautotrophy at Deep-Sea Vents: Past, Present, and Future. *Oceanography* **25**: 218–233.
- Sievert, S.M., Hügler, M., Taylor, C.D., and Wirsén, C.O. (2008) Sulfur Oxidation at Deep-Sea Hydrothermal Vents. In *Microbial Sulfur Metabolism*. Dahl, D.C. and Friedrich, D.C.G. (eds). Springer Berlin Heidelberg, pp. 238–258.
- Sievert, S.M., Scott, K.M., Klotz, M.G., Chain, P.S.G., Hauser, L.J., Hemp, J., *et al.* (2008) Genome of the Epsilonproteobacterial Chemolithoautotroph *Sulfurimonas denitrificans*. *Appl Environ Microbiol* **74**: 1145–1156.
- Sievert, S.M., Wieringa, E.B.A., Wirsén, C.O., and Taylor, C.D. (2007) Growth and mechanism of filamentous-sulfur formation by *Candidatus Arcobacter sulfidicus* in opposing oxygen-sulfide gradients. *Environ Microbiol* **9**: 271–276.
- Silva, J.C., Gorenstein, M.V., Li, G.-Z., Vissers, J.P.C., and Geromanos, S.J. (2006) Absolute Quantification of Proteins by LCMSE A Virtue of Parallel ms Acquisition. *Mol Cell Proteomics* **5**: 144–156.
- Sims, D., Sudbery, I., Ilott, N.E., Heger, A., and Ponting, C.P. (2014) Sequencing depth and coverage: key considerations in genomic analyses. *Nat Rev Genet* **15**: 121–132.
- Sogin, M.L., Morrison, H.G., Huber, J.A., Welch, D.M., Huse, S.M., Neal, P.R., *et al.* (2006) Microbial diversity in the deep sea and the underexplored “rare biosphere.” *Proc Natl Acad Sci* **103**: 12115–12120.
- Steudel, R. and Eckert, Bodo. (2003) Elemental sulfur and sulfur-rich compounds. 2., Berlin [u.a.]: Springer.
- Stokke, R., Dahle, H., Roalkvam, I., Wissuwa, J., Daae, F.L., Tooming-Klunderud, A., *et al.* (2015) Functional interactions among filamentous Epsilonproteobacteria and Bacteroidetes in a deep-sea hydrothermal vent biofilm. *Environ Microbiol* **17**: 4063–4077.
- Struyvé, M., Moons, M., and Tommassen, J. (1991) Carboxy-terminal phenylalanine is essential for the correct assembly of a bacterial outer membrane protein. *J Mol Biol* **218**: 141–148.
- Takai, K., Campbell, B.J., Cary, S.C., Suzuki, M., Oida, H., Nunoura, T., *et al.* (2005) Enzymatic and Genetic Characterization of Carbon and Energy Metabolisms by Deep-Sea Hydrothermal Chemolithoautotrophic Isolates of Epsilonproteobacteria. *Appl Environ Microbiol* **71**: 7310–7320.
- Takai, K., Suzuki, M., Nakagawa, S., Miyazaki, M., Suzuki, Y., Inagaki, F., and Horikoshi, K. (2006) *Sulfurimonas paralvinellae* sp. nov., a novel mesophilic, hydrogen- and sulfur-oxidizing chemolithoautotroph within the Epsilonproteobacteria isolated from a deep-sea hydrothermal vent polychaete nest, reclassification of *Thiomicrospira denitrificans* as *Sulfurimonas denitrificans* comb. nov. and emended description of the genus *Sulfurimonas*. *Int J Syst Evol Microbiol* **56**: 1725–1733.
- Tan Y.J., Tolstoy M., Waldhauser F., Wilcock W.S.D. (2016) Dynamics of a seafloor-spreading episode at the East Pacific Rise. *Nature* **540**: 261–266.
- Taylor, C.D. and Wirsén, C.O. (1997) Microbiology and Ecology of Filamentous Sulfur Formation. *Science* **277**: 1483–1485.
- Timmer-ten Hoor, A. (1975) A new type of thiosulphate oxidizing, nitrate reducing microorganism: *Thiomicrospira denitrificans* sp. Nov. *Neth J Sea Res* **9**: 344–350.

- Tivey, M. (2007) Generation of Seafloor Hydrothermal Vent Fluids and Associated Mineral Deposits. *Oceanography* **20**: 50–65.
- Tomassen, J. (2010) Assembly of outer-membrane proteins in bacteria and mitochondria. *Microbiology* **156**: 2587–2596.
- Torti, A., Lever, M.A., and Jørgensen, B.B. (2015) Origin, dynamics, and implications of extracellular DNA pools in marine sediments. *Mar Genomics* **24**: 185–196.
- Tuttle, J.H. and Jannasch, H.W. (1979) Microbial dark assimilation of CO₂ in the Cariaco Trench. *Limnol Oceanogr* **24**: 746–753.
- Tuttle, J.H., Wirsén, C.O., and Jannasch, H.W. (1983) Microbial activities in the emitted hydrothermal waters of the Galápagos rift vents. *Mar Biol* **73**: 293–299.
- Urich, T., Lanzén, A., Stokke, R., Pedersen, R.B., Bayer, C., Thorseth, I.H., *et al.* (2014) Microbial community structure and functioning in marine sediments associated with diffuse hydrothermal venting assessed by integrated meta-omics. *Environ Microbiol* **16**: 2699–2710.
- Van Assche, E., Van Puyvelde, S., Vanderleyden, J., and Steenackers, H.P. (2015) RNA-binding proteins involved in post-transcriptional regulation in bacteria. *Front Microbiol* **6**: <https://doi.org/10.3389/fmicb.2015.00141>.
- Vetriani, C., Tran, H.V., and Kerkhof, L.J. (2003) Fingerprinting Microbial Assemblages from the Oxic/Anoxic Chemocline of the Black Sea. *Appl Environ Microbiol* **69**: 6481–6488.
- Villanueva, L., Haveman, S.A., Summers, Z.M., and Lovley, D.R. (2008) Quantification of *Desulfovibrio vulgaris* Dissimilatory Sulfite Reductase Gene Expression during Electron Donor- and Electron Acceptor-Limited Growth. *Appl Environ Microbiol* **74**: 5850–5853.
- Vizcaíno, J.A., Csordas, A., del-Toro, N., Dianes, J.A., Griss, J., Lavidas, I., *et al.* (2016) 2016 update of the PRIDE database and its related tools. *Nucleic Acids Res* **44**: D447–456.
- Von Damm, K.L. (1995) Controls on the chemistry and temporal variability of seafloor hydrothermal fluids. *Wash DC Am Geophys Union Geophys Monogr Ser* **91**: 222–247.
- Von Damm, K.L., Edmond, J.M., Grant, B., Measures, C.I., Walden, B., and Weiss, R.F. (1985) Chemistry of submarine hydrothermal solutions at 21 °N, East Pacific Rise. *Geochim Cosmochim Acta* **49**: 2197–2220.
- W Harder and Dijkhuizen, and L. (1983) Physiological Responses to Nutrient Limitation. *Annu Rev Microbiol* **37**: 1–23.
- Waite, D.W., Vanwonterghem, I., Rinke, C., Parks, D.H., Zhang, Y., Takai, K., *et al.* (2017) Comparative Genomic Analysis of the Class Epsilonproteobacteria and Proposed Reclassification to Epsilonbacteraeota (phyl. nov.). *Front Microbiol* **8**: <https://doi.org/10.3389/fmicb.2017.00682>.
- Wang, Q., Garrity, G.M., Tiedje, J.M., and Cole, J.R. (2007) Naive Bayesian classifier for rapid assignment of rRNA sequences into the new bacterial taxonomy. *Appl Environ Microbiol* **73**: 5261–5267.
- Wang, S., Jiang, L., Hu, Q., Liu, X., Yang, S. and Shao, Z. (2020), Elemental sulfur reduction by a deep-sea hydrothermal vent *Campylobacterium Sulfurimonas* sp. NW10. *Environ Microbiol.* <https://doi.org/10.1111/1462-2920.15247>
- Weissgerber, T., Sylvester, M., Kröninger, L., and Dahl, C. (2014) A Comparative Quantitative Proteomic Study Identifies New Proteins Relevant for Sulfur Oxidation in the Purple Sulfur Bacterium *Allochromatium vinosum*. *Appl Environ Microbiol* **80**: 2279–2292.
- Widdel, F. and Bak, F. (1992) Gram-Negative Mesophilic Sulfate-Reducing Bacteria. In *The Prokaryotes: A Handbook on the Biology of Bacteria: Ecophysiology, Isolation, Identification, Applications*. Balows, A., Trüper, H.G., Dworkin, M., Harder, W., and Schleifer, K.-H. (eds). New York, NY: Springer, pp. 3352–3378.

- Wirsen, C.O., Sievert, S.M., Cavanaugh, C.M., Molyneux, S.J., Ahmad, A., Taylor, L.T., *et al.* (2002) Characterization of an Autotrophic Sulfide-Oxidizing Marine *Arcobacter* sp. That Produces Filamentous Sulfur. *Appl Environ Microbiol* **68**: 316–325.
- Woodruff, L.G. and Shanks, W.C. (1988) Sulfur isotope study of chimney minerals and vent fluids from 21°N, East Pacific Rise: Hydrothermal sulfur sources and disequilibrium sulfate reduction. *J Geophys Res Solid Earth* **93**: 4562–4572.
- Xie, W., Wang, F., Guo, L., Chen, Z., Sievert, S.M., Meng, J., *et al.* (2011) Comparative metagenomics of microbial communities inhabiting deep-sea hydrothermal vent chimneys with contrasting chemistries. *ISME J* **5**: 414–426.
- Yamamoto, M., Nakagawa, S., Shimamura, S., Takai, K., and Horikoshi, K. (2010) Molecular characterization of inorganic sulfur-compound metabolism in the deep-sea epsilonproteobacterium *Sulfurovum* sp. NBC37-1. *Environ Microbiol* **12**: 1144–1153.
- Yoshihara, E., Yoneyama, H., Ono, T., and Nakae, T. (1998) Identification of the Catalytic Triad of the Protein D2 Protease in *Pseudomonas aeruginosa*. *Biochem Biophys Res Commun* **247**: 142–145.
- Zhang, L., Zhang, C., Hu, C., Liu, H., and Qu, J. (2015) Denitrification of groundwater using a sulfur-oxidizing autotrophic denitrifying anaerobic fluidized-bed MBR: performance and bacterial community structure. *Appl Microbiol Biotechnol* **99**: 2815–2827.
- Zhang, Q., Meitzler, J.C., Huang, S., and Morishita, T. (2000) Sequence Polymorphism, Predicted Secondary Structures, and Surface-Exposed Conformational Epitopes of *Campylobacter* Major Outer Membrane Protein. *Infect Immun* **68**: 5679–5689.
- Zopfi, J., Ferdelman, T.G., and Fossing, H. (2004) Distribution and fate of sulfur intermediates—sulfite, tetrathionate, thiosulfate, and elemental sulfur—in marine sediments. *Geol Soc Am Spec Pap* **379**: 97–116.
- Zybailov, B., Mosley, A.L., Sardi, M.E., Coleman, M.K., Florens, L., and Washburn, M.P. (2006) Statistical Analysis of Membrane Proteome Expression Changes in *Saccharomyces cerevisiae*. *J Proteome Res* **5**: 2339–2347.

7 Appendix

Table of content for DVD

- 1. Raw Data Limitation, Hydrogen and Oxygen Chemostat samples:** The mass spectrometry proteomics data for thiosulfate limitation [TL 1-3], nitrate limitation [NL 1-3], thiosulfate and oxygen (TO 1-3) and hydrogen and nitrate (HN 7-9).
- 2. Supplement Table 1:** Metaproteome displayed with the Accession number, Database ID (subset DB), Gene function, Protein function, Organism, the molecular weight of the protein in kilo Dalton [kDa], average percent normalized spectral abundance factor [%NSAF] for soluble and membrane bound enriched proteins and the annotation. %NSAF are given as an average of the three technical replicates. The functional analysis was separated in different Tabs including the associated genes from the two Metagenomes LVP2 (LVP2 Gene) and LVP4 (LVP4 Gene).
- 3. Supplement Table 2:** Transcriptome and proteome of *Sulfurimonas denitrificans* displayed with the locus tag, NCBI protein ID number, length of the gene in base pairs [bp], the molecular weight of the protein in kilo Dalton [kDa], transcripts per million [TPM], percent normalized spectral abundance factor [%NSAF] and the annotation. Both TPM and %NSAF are given as an average of the biological replicates grown with cyclooctasulfur [S8] and thiosulfate [S₂O₃²⁻]. In addition, the p-values for both the transcripts and proteins are provided, with p-values <0.01 highlighted in light blue and p-values <0.05 highlighted in dark blue. Published in (Götz, Pjevac, *et al.*, 2018).
- 4. Supplement Table 3:** Proteomes of *Sulfurimonas denitrificans* displayed with Identified Proteins, NCBI protein ID number (Accession Number), the molecular weight of the protein in kilo Dalton [kDa] and average percent normalized spectral abundance factor [%NSAF]. %NSAF are given as an average of the biological replicates grown in chemostats under thiosulfate limitation [TL], nitrate limitation [NL], thiosulfate and oxygen (TO) and hydrogen and nitrate (HN).

R script Bubble Chart:

```
# TODO: This script is written to create a Bubble chart for Metaproteomic
data which was normalized (NSAF%) and sorted in an EXCEL spreadsheet prior
to the skript.

#
# Author: FGoetz
#####

installXLSXsupport("/usr/local/Cellar/perl/5.26.0/bin/perl")
    ### open/install perl for reading xls function to open excel files

library(gdata)    ### need Perl programm to read excel files

library(fields)
library(Rcpp)
library(ggplot2)
library(plotrix)
library(gplots)
library(graphics)

file<-file.choose(new=TRUE)
my_data<-read.xls(file)    ###saves the loaded data into an object

row_names<-as.vector(my_data[1])
Dataset_1<- as.vector(my_data[,2])
Dataset_2<-as.vector(my_data[,3])

radius_1 <- sqrt( Dataset_1/ pi )#to make dataset_1 and dataset_2, circle
area dependent, not radius
radius_2<- sqrt( Dataset_2/ pi )
radius_1 = rev(radius_1)
radius_2 = rev(radius_2)

if (max(radius_1)> max(radius_2)){          #calculate the max
value(calculated radius with values as area of the circle) of both Datasets
    MAX<-max(radius_1)
}else{
    MAX<-max(radius_2)
}

if (min(radius_1)< min(radius_2)){          #calculate the smallest value
(calculated radius with values as area of the circle) of both Datasets
    MIN<-min(radius_1)
}else{
    MIN<-min(radius_2)
}

if (mean(t(radius_1))< mean(t(radius_2))){          #calculate the smaller
mean value (calculated radius with values as area of the circle) of both
Datasets
    MEAN<-mean(t(radius_1))
}else{
    MEAN<-mean(t(radius_2))
}

y1<- ((MAX*2)*(nrow(my_data)))
```

```

Y<-seq(from=y1/nrow(my_data), to=as.numeric(y1), by=(y1/nrow(my_data))) #
y-axis
x<- ((MAX*2)*(nrow(my_data))) # x-axis

pdfFile=file.choose(new=TRUE); # define the pdf-name and saving location of
the plot

pdf(pdfFile,width=10,height=15) # pdf size

plot.new()# create the plot

frame()
par(mar=c(5,25,4,2),las=2,cex.axis=0.6,bty="n")
#Letter size for y-axis lables
plot((1:10),(1:10), type="n",xaxt="n", yaxt="n",xlab=NA,ylab=NA)

draw.circle(6,(MAX*4),MAX, border="black" , col="NA")
#to draw the histogram using the Maximum, Maximum/2 and the smaller
mean of both datasets.
draw.circle(6,(MAX*4),MEAN, border="black" , col="NA")
draw.circle(6,(MAX*4),MIN, border="black" , col="NA")
text(6,4, cex=0.7, labels=c(round((pi*(MAX^2)),5)))
#histogram values for the circle size showing the %NSAF factor
relation
text(6,3, cex=0.7, labels=c(round((pi*((MAX/2)^2)),5)))
text(6,2, cex=0.7, labels=c(round((pi*(MIN^2)),5)))

X_axis_Label<-c("LVP2","LVP4")

axis(1,at=c(2,4), labels=X_axis_Label)

counter = 1;
#calculate the distance to the next circle
distanceToNextVal = array(dim=c(1,length(radius_1),1),data = 0)
#draw the circles
for (j in c(1:length(radius_1))) {
  counter = counter + MAX;
  distanceToNextVal[j] = counter;

draw.circle(x=2,y=distanceToNextVal[j],radius=radius_1[j],border="NA" ,
col="blue")

draw.circle(x=4,y=distanceToNextVal[j],radius=radius_2[j],border="NA" ,
col="blue")
}
#apply labels
axis(side=2, at = distanceToNextVal, labels = rev(c(t(row_names))))
dev.off()#Finish the program

```

8 Appendix A: Eigenständigkeitserklärung

Hiermit erkläre ich, dass diese Arbeit bisher von mir weder an der Mathematisch-Naturwissenschaftlichen Fakultät der Universität Greifswald noch einer anderen wissenschaftlichen Einrichtung zum Zwecke der Promotion eingereicht wurde.

Ferner erkläre ich, dass ich diese Arbeit selbstständig verfasst und keine anderen als die darin angegebenen Hilfsmittel und Hilfen benutzt und keine Textabschnitte eines Dritten ohne Kennzeichnung übernommen habe.

21.12.2020

Datum



Unterschrift

Florian Götz: *Functional Analysis of Hydrothermal Vent Microbial Communities*, Dissertation zur Erlangung des akademischen Grades, doctor rerum naturalium (Dr. rer. nat.), © Dezember 2020

9 Appendix B: Curriculum Vitae

Personal Information

Florian Goetz

230 W Blackwell Street Rear 1, 07801 Dover, NJ, USA

Götzer Dorfstr. 5, OT Götz, 14550 Groß Kreutz, Germany

Education

04/2015 – Present	Dissertation , University of Greifswald, Institute of Pharmacy, Pharmaceutical Biotechnology, in cooperation with the Woods Hole Oceanographic Institute, MA, USA
04/2013 – 03/2015	Master of Science in Biotechnology , Brandenburg University of Technology, Senftenberg, Germany
09/2009 – 03/2013	Bachelor of Science in Biotechnology , Lausitz University of Applied Sciences, Senftenberg, Germany
2005 – 2009	Baccalaureate , European School Uccle1, Brussels, Belgium

Professional Experience

10/2020 – present	Associate Scientist , Department of Quality Control Microbiology, Bristol Myers Squibb, NJ, USA
08/2019 – 10/2020	QC Analyst , Department of Microbiology/ Validation Regeneron Pharmaceuticals, NY, USA
01/2019 – 08/2019	QC Microbiologist , Eurofins Scientific, NY, USA
01/2016 – 12/2018	Research Fellow/ PhD Candidate , Woods Hole Oceanographic Institution, MA, USA
04/2017 – 05/2017	Teaching Instructor , Massachusetts Maritime Academy MA, USA
04/2014 – 12/2014	Master Thesis , Woods Hole Oceanographic Institution
11/2014	Scientific expedition , “Dark Life” researching hydrothermal vents at the East Pacific Rise, Woods Hole Oceanographic Institution
08/2012 – 01/2013	Bachelor Thesis , Leibniz Institute for Baltic Sea Research, Warnemünde, Germany

09/2011 – 01/2012

Laboratory Trainee, Max Planck Institute for Marine Microbiology, Bremen, Germany

Language

German (native speaker)

English (fluent)

Spanish (basic)

French (basic)

List of Publications

Publications associated with this thesis

- I) Götz, F., Pjevac, P., Markert, S., McNichol, J., Becher, D., Schweder, T., et al. (2018) Transcriptomic and proteomic insight into the mechanism of cyclooctasulfur- versus thiosulfate-oxidation by the chemolithoautotroph *Sulfurimonas denitrificans*: S₈ metabolism in *Sulfurimonas denitrificans*. *Environ Microbiol.* **21**:244-258.

Author's contributions: FG prepared the culture medium and cultivation experiments, performed protein extraction and proteomic analyses, wrote a major part of the manuscript for the proteomic content, developed a new model for sulfur oxidation in Campylobacteria, designed most of the figures and tables.

Publications not discussed in this dissertation

- I) Götz, F., Longnecker, K., Soule, M.C.K., Becker, K.W., McNichol, J., Kujawinski, E.B., and Sievert, S.M. (2018) Targeted metabolomics reveals proline as a major osmolyte in the chemolithoautotroph *Sulfurimonas denitrificans*. *MicrobiologyOpen* **7**: e00586.
- II) Möller, L., Laas, P., Rogge, A., Goetz, F., Bahlo, R., Leipe, T., and Labrenz, M. (2019) *Sulfurimonas* subgroup GD17 cells accumulate polyphosphate under fluctuating redox conditions in the Baltic Sea: possible implications for their ecology. *ISME J* **13**: 482

21.12.2020

Date


Signature

10 Appendix D: Acknowledgement

First and foremost, I would like to thank my advisors Prof. Dr. Thomas Schweder and Dr. Stefan Sievert for their continuous support throughout my research project, accommodations in their laboratories and scientific discussions. Especially Stefan Sievert gave me the opportunity to work independently in his laboratory and encouraged me to do better and develop into an independent researcher. The welcoming and supportive environment in Cape Cod was exceptional and I quickly felt like a part of the Sievert family. Thank you very much Stefan, Christel, Lukas and Helen!

I would like to thank Dr. Stephanie Markert for introducing me to the world of Metaproteomics and data analysis tools! I would like to thank Dr. Jesse McNichol for being a good friend and colleague who always had good advice and supported me in my scientific endeavors. I would like to thank Dr. Petra Pjevac and Dr. Marc Mußmann for sharing their knowledge and findings to discuss and publish our elemental sulfur publication.

I am very grateful for my brother who always helped with IT problems along the way. He introduced me to R-coding, never asked for anything in return and was always there if I needed him. Without my brother, parents and wife, I would not have made it to this point and I am very grateful to all of them for pushing me to never give up.